

Journal of

ELECTROANALYTICAL CHEMISTRY

*International Journal Dealing with all Aspects
of Electroanalytical Chemistry,
Including Fundamental Electrochemistry*

EDITORIAL BOARD:

- J. O'M. BOCKRIS (Philadelphia, Pa.)
B. BREYER (Sydney)
G. CHARLOT (Paris)
B. E. CONWAY (Ottawa)
P. DELAHAY (Baton Rouge, La.)
A. N. FRUMKIN (Moscow)
L. GIERST (Brussels)
M. ISHIBASHI (Kyoto)
W. KEMULA (Warsaw)
H. L. KIES (Delft)
J. J. LINGANE (Cambridge, Mass.)
G. W. C. MILNER (Harwell)
J. E. PAGE (London)
R. PARSONS (Bristol)
C. N. REILLEY (Chapel Hill, N.C.)
G. SEMERANO (Padua)
M. VON STACKELBERG (Bonn)
I. TACHI (Kyoto)
P. ZUMAN (Prague)

E L S E V I E R

GENERAL INFORMATION

See also Suggestions and Instructions to Authors which will be sent free, on request to the Publishers.

Types of contributions

- (a) Original research work not previously published in other periodicals.
- (b) Reviews on recent developments in various fields.
- (c) Short communications.
- (d) Bibliographical notes and book reviews.

Languages

Papers will be published in English, French or German.

Submission of papers

Papers should be sent to one of the following Editors:

Professor J. O'M. BOCKRIS, John Harrison Laboratory of Chemistry,
University of Pennsylvania, Philadelphia 4, Pa., U.S.A.

Dr. R. PARSONS, Department of Chemistry,
The University, Bristol 8, England.

Professor C. N. REILLEY, Department of Chemistry,
University of North Carolina, Chapel Hill, N.C., U.S.A.

Authors should preferably submit two copies in double-spaced typing on pages of uniform size. Legends for figures should be typed on a separate page. The figures should be in a form suitable for reproduction, drawn in Indian ink on drawing paper or tracing paper, with lettering etc. in thin pencil. The sheets of drawing or tracing paper should preferably be of the same dimensions as those on which the article is typed. Photographs should be submitted as clear black and white prints on glossy paper.

All references should be given at the end of the paper. They should be numbered and the numbers should appear in the text at the appropriate places.

A summary of 50 to 200 words should be included.

Reprints

Twenty-five reprints will be supplied free of charge. Additional reprints can be ordered at quoted prices. They must be ordered on order forms which are sent together with the proofs.

Publication

The *Journal of Electroanalytical Chemistry* appears monthly and has six issues per volume and two volumes per year, each of approx. 500 pages.

Subscription price (post free): £ 10.15.0 or \$ 30.00 or Dfl. 108.00 per year; £ 5.7.6 or \$ 15.00 or Dfl. 54.00 per volume.

Additional cost for copies by air mail available on request.

For advertising rates apply to the publishers.

Subscriptions

Subscriptions should be sent to:

ELSEVIER PUBLISHING COMPANY, P.O. Box 211, Amsterdam, The Netherlands.

SUMMARIES OF PAPERS PUBLISHED IN
JOURNAL OF ELECTROANALYTICAL CHEMISTRY

Vol. 7, No. 4, April 1964

CHEMICAL KINETICS IN ELECTROCHEMICAL
PROCESSES

ELECTRON TRANSFER BETWEEN OR WITHIN MULTI-COMPONENT
SUB-SYSTEMS OF THE TYPE: $A_1 \rightleftharpoons A_2$, $A_2 \rightleftharpoons A_3$, $A_3 \rightleftharpoons A_1$

A general treatment is given for electrochemical processes involving (pseudo-) first order chemical reactions and semi-infinite planar diffusion. The physical implication of a derived general equation relating surface concentration and currents — which are time dependent functions — are discussed. The constants of the equation are evaluated for a generalized three-component sub-system, and the formulation of specific response functions is demonstrated for pre-kinetic, post-kinetic, both pre- and post-kinetic, and parallel-kinetic (catalytic) cases. Solutions of the equation are obtained for various specific systems and techniques, including chronopotentiometry, chronoamperometry, and a.c. chronopotentiometry. Also, a general expression for the phase angle (between current and potential) in a.c. methods involving only one pair of electroactive species is developed. Finally, the interpretation of experimental data is discussed and some methods (including the use of analog computers) which could be used to evaluate the constants of the equation for more complicated systems are mentioned.

J. W. ASHLEY, JR. AND C. N. REILLEY,

J. Electroanal. Chem., 7 (1964) 253-275.

THE CATALYTIC POLAROGRAPHIC CURRENT OF
A METAL COMPLEX

II. THE NICKEL(II)-*o*-PHENYLENEDIAMINE SYSTEM

The catalytic current observed as a pre-wave when Ni(II) is reduced polarographically in the presence of small quantities of *o*-phenylenediamine is studied as a function of Ni(II) ion and *o*-phenylenediamine concentration. The effect of pH, stirring, and mercury height on the pre-wave are described. The *i-t* curves of an individual drop and the effect of *o*-phenylenediamine concentration on the electrocapillary curve are discussed. On the basis of the experimental evidence, a mechanism which involves a rapid adsorption equilibrium between bulk and adsorbed *o*-phenylenediamine and a complexation reaction of Ni(II) with the adsorbed diamine is proposed. The complexation is thought to be the rate-determining step. A possible explanation as to why the adsorbed complex is more easily reduced than $\text{Ni}(\text{H}_2\text{O})_6^{2+}$ is proposed.

H. B. MARK, JR.,

J. Electroanal. Chem., 7 (1964) 276-287.

EFFECT OF DILUTE CHLORIDE ION ON PLATINUM ELECTRODES

Surface oxide formation in the presence of small concentrations of HCl has been studied in 2 N H₂SO₄ by anodic oxidation and cathodic stripping on bright platinum and molded platinum black-polytetrafluoroethylene electrodes. At the lowest concentrations, $< 10^{-3}$ M, the principal effect at potentials less than 1.4 V appears to result from halide ion surface adsorption which prevents formation of the amount of surface oxide ordinarily observed. On platinum-black, the adsorption effect is considerable and results in significant decrease in electrochemically determined surface area at 1.24 V, based on surface oxide formation. As the concentration of HCl is increased to 10^{-1} M, the sequence of surface oxide formation on bright platinum is changed and higher oxides (higher oxygen concentration at the surface) are not observed. Oxygen tends not to be held on the electrode surface. Chloride ion discharge potential is affected by current density and surface oxide formation on bright platinum electrodes.

J. S. MAYELL AND S. H. LANGER,

J. Electroanal. Chem., 7 (1964) 288-296.

THE ANODIC DISSOLUTION AND PASSIVATION OF SMOOTH PLATINUM

I. ANOMALOUS RESULTS FROM THE RADIOTRACER TECHNIQUE

Radioactive platinum was employed in a study of the electrochemical dissolution of smooth platinum and the amount of metal dissolving was determined by activity measurements. Correlation of the measurements of radioactivity with the coulometric measurements was found to be complicated by the presence of highly radioactive foreign atoms in the platinum. Methods of eliminating this complication are discussed.

T. DICKINSON, R. C. IRWIN AND W. F. K. WYNNE-JONES,

J. Electroanal. Chem., 7 (1964) 297-301.

VOLTAMMETRY OF NICKEL IN MOLTEN LITHIUM FLUORIDE-SODIUM FLUORIDE-POTASSIUM FLUORIDE

Results are presented on the rapid scan voltammetry and anodic stripping voltammetry of nickel in molten LiF-NaF-KF. The technique of anodic stripping voltammetry is promising as a means of determining trace quantities of nickel directly in the melt; a little as 1 p.p.m. can be detected. The half-wave potential for the reduction of Ni(II) \rightarrow Ni(0) occurs at approximately -0.2 V vs. the platinum quasi-reference electrode. Current-voltage curves were recorded at a pyrolytic graphite indicator electrode at voltage scan rates from 50 mV/min-10 V/min. At the faster scan rates, peak-shaped curves resulted which indicated that the transport process was mainly diffusion-controlled. A diffusion coefficient of $\sim 1 \cdot 10^{-6}$ cm²/sec at 500° was calculated. An activation energy of about 18 kcal/mole was calculated for the current-limiting process which corresponds to the reduction of Ni(II) to the metal.

D. L. MANNING,

J. Electroanal. Chem., 7 (1964) 302-306.

TRACE ANALYSIS BY ANODIC STRIPPING VOLTAMMETRY

II. THE METHOD OF MEDIUM EXCHANGE

The method of medium exchange, consisting of electrodeposition of an amalgam-forming metal or metals in the hanging mercury drop electrode, followed by a stripping process into a suitable, different medium, is described and its effectiveness in overcoming various sources of interference, common in complex materials, proved. Since the precision of results obtained through the introduction of this additional step into anodic stripping voltammetry methods is comparable to that obtained in regular anodic stripping determinations, the method affords a significant extension of the applicability of anodic stripping voltammetry to trace analysis.

M. ARIEL, U. EISNER AND S. GOTTESFELD,

J. Electroanal. Chem., 7 (1964) 307-314.

VOLTAMMETRIC DETERMINATION OF CARBON MONOXIDE AT GOLD ELECTRODES

A voltammetric method has been developed for the determination of dissolved carbon monoxide in 0.01 *F* sodium hydroxide solutions. Details of the activation process are discussed as well as effects of various supporting electrolytes. The peak current is diffusion-controlled and is directly proportional to the percentage by volume of carbon monoxide in gas mixtures used to saturate the electrolysis solution. In the concentration range of 10-100% by volume the method gives errors in accuracy of less than $\pm 2\%$.

J. L. ROBERTS, JR. AND D. T. SAWYER,

J. Electroanal. Chem., 7 (1964) 315-319.

LINEAR POTENTIOMETRIC TITRATIONS

A method for graphical representation of potentiometric titration curves is proposed. It permits determination of the end-point even if the conventional potentiometric curve, pH-volume, fails to define exactly an inflection point.

The limits and the possibilities of the method are discussed and some examples of practical applications are illustrated.

P. LANZA AND I. MAZZEI,

J. Electroanal. Chem., 7 (1964) 320-327.

THE POLAROGRAPHIC DIFFUSION COEFFICIENT OF
CADMIUM ION IN 0.1 M POTASSIUM CHLORIDE

The diffusion coefficient of cadmium ion in 0.1 M potassium chloride at 25° was determined by an absolute method. Straight calculations using the equation derived by Jost yielded values which were too high when compared to the infinite dilution value of 0.720×10^{-5} cm²/sec. A correction for initial mixing was made which yielded more reasonable values for *D*. The value of 0.700×10^{-5} cm²/sec which represents a weighted average of the diffusion coefficient values obtained in this and other investigations was selected as the best available value for the diffusion coefficient of cadmium ion in 0.1 M KCl at 25°.

D. J. MACERO AND C. L. RULFS,

J. Electroanal. Chem., 7 (1964) 328-331.

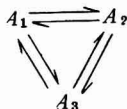
A SUBSTITUTION-INERT METAL COMPLEX AS AN
INDICATOR IN A.C. POLAROGRAPHIC TITRATIONS;
A NEW TYPE OF METAL INDICATOR

(Preliminary Note)

N. TANAKA AND H. OGINO,

J. Electroanal. Chem., 7 (1964) 332-334.

CHEMICAL KINETICS IN ELECTROCHEMICAL PROCESSES
ELECTRON TRANSFER BETWEEN OR WITHIN MULTI-COMPONENT
SUB-SYSTEMS OF THE TYPE:



J. W. ASHLEY, JR. AND CHARLES N. REILLEY

*Department of Chemistry, The University of North Carolina,
Chapel Hill, North Carolina (U.S.A.)*

(Received December 22nd, 1963)

Since the classical paper of WEISNER¹, a number of investigations concerning the role of chemical kinetics in electrochemical processes have been reported. The work of KOUTECKÝ AND BRDIČKA², in which the kinetic effects were added as source terms in the Fick's law differential equations, laid a rigorous foundation for future theoretical studies involving chemical kinetics in electrochemical processes. Subsequently, a large number of special cases have been treated by various investigators where emphasis was placed on a given technique — such as chronopotentiometry, chronoamperometry, a.c. polarography, polarography, etc. Much of this work has been reviewed recently. In this paper we wish to emphasize the general aspects of chemical kinetics, even to the point of subordinating the electrochemical techniques.

This approach serves to maintain generality and permits certain conclusions to be reached which are independent of the technique involved.

GENERAL APPROACH

When each of the pertinent processes in an electrochemical system can be described by one or more linear differential equations, the simultaneous solution of the entire set of equations yields a relationship between current and concentration which is linear. Examples of such processes include linear diffusion (for electrodes of any fixed geometry), chemical reactions involving only first-order (or pseudo-first-order) kinetics, surface adsorption involving only linear isotherms, and, of course, electron transfer in which current is proportional to flux at the electrode surface. Any process is linear when the microscopic *behaviors* of all molecules under consideration are mutually independent at each point in time and space. The "molecules under consideration" are those the concentration of which, at some point in space, vary with time. For example, in a linear diffusion process, a given molecule moves in a manner which does not depend on any concentration changes which might occur; its movement is characteristically a "random walk" process.

Most electrochemical techniques are based on observation of current and potential as function of time. Unfortunately, a non-linear relationship* exists among

$$\frac{i}{n\mathcal{F}\mathcal{A}k_e} = f_o C_o \exp\left[\frac{-\alpha n\mathcal{F}}{RT}(E - E^o)\right] - f_R C_R \exp\left[\frac{(1 - \alpha)n\mathcal{F}}{RT}(E - E^o)\right] \quad (1)$$

current, surface concentrations, and potential which severely complicates the mathematical treatment when attention is directed toward the potential. The treatment of data can be greatly simplified, then, by techniques which would permit direct observation of surface concentrations as functions of time and current. It would be a great boon to electrochemistry if some general techniques for directly measuring surface concentration were developed (*e.g.*, *via* attenuated total reflection). In a sense, many of the powerful techniques today are indirectly based on observing surface concentration. For example, in chronopotentiometry, the sharp change in potential which occurs at the transition time is used as a marker to indicate that the surface concentration of a species has reached zero. Because the surface concentration is then known at this one time, several experiments employing different current amplitudes allow evaluation of the system function, and hence the kinetic parameters. In this way, use of the non-linear potential relationship is circumvented. If, however, direct observation of surface concentration during the entire course of the experiment was possible, a single experiment may have sufficed (*i.e.*, current step with step reversal for post kinetics).

Similarly, in chronoamperometry and polarography, chemical kinetic parameters are usually measured by employing potentials such that the surface concentration is maintained at zero for certain species — the potential dependency being studied only to ascertain the potential region where this condition is fulfilled or to vary the components whose surface concentration is to be brought to zero. Because the surface concentration and current of the electroactive species are then known at all times during the experiment, only one experiment is necessary (*i.e.*, potential step with step reversal for post kinetics).

For certain techniques, such as a.c. polarography and a.c. chronopotentiometry, the actual surface concentration at any time is determined by the potential and current, so the mathematical complications of eqn. (1) cannot be avoided.

Considering a set of chemical species which are coupled only by first-order chemical reaction and/or electron transfer at the electrode surface, the following equation can be formulated for semi-infinite linear diffusion at a plane electrode (see Appendix):

$$\Delta\bar{C}_f = -D^{-1/2} \sum_g \bar{J}_g \sum_h K_{fgh} (p + \kappa_h)^{-1} \quad (2)$$

where— $\Delta\bar{C}_f$ is the change in surface concentration of component *f* from its initial value— \bar{J}_g is the flux of component *g* into the electrode and equals $i_g/n_g \mathcal{F}\mathcal{A} D^{1/2}$, i_g is the current (positive during reduction) due to the electrode reaction of component *g*, D is the diffusion constant (assumed the same for all species), n_g is the number of electrons per molecule lost by component *g* at the electrode surface (*i.e.*, the value of n_g is positive if *g* refers to an oxidized species, negative if *g* refers to a reduced species), h is a mathematical index, the K_{fgh} are constants involving only ratios of (pseudo-) first-order

* The symbol k_e is used here rather than the more usual symbol k_h because of extensive use of the subscript *h* for other purposes later.

reaction rate constants, the κ_h are constants depending on the magnitude of the reaction rate constants, and p is the Laplace transform variable (the bars over C and J refer to the Laplace transform taken with respect to time after the start of the experiment). The summation over g is taken over all components in the sub-system, and there is one value of h for each component in the sub-system.

Equation (2) illustrates the superposition principle by stating that the net response function, $\Delta\bar{C}_f$, is the sum of the individual *response functions*. Each individual response function is the product of the *excitation function*, \bar{J}_g/D^\dagger , and the particular *system function* applicable for that excitation. The elucidation of chemical kinetics by electrochemical means is based on the evaluation of the individual system functions, this end being achieved through measurement of the overall response that results from application of suitable excitations.

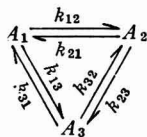
Equation (2) can be recast into another form which is sometimes useful:

$$\bar{J}_f = -D^\dagger \sum_g \Delta\bar{C}_g \sum_h K_{fgh} (p + \kappa_h)^\dagger \quad (3)$$

again illustrating the superposition principle. In this case the overall response function is \bar{J}_f , and the individual excitation functions are represented by $\Delta\bar{C}_g$. The constants, K_{fgh} and κ_h , have the same values in eqn. (3) as in eqn. (2).

Equations (2) and (3) serve to unify the treatment of electrochemical kinetics for various techniques and their applications will become apparent through the following discussions.

For purposes of illustration, we will consider sub-systems involving three components as denoted by the following scheme:



This sub-system permits solution for many of the (pseudo-) first-order chemical kinetic cases of interest; for situations involving more than three components, the rate-controlling processes usually necessitate consideration of not more than two slow chemical steps. This situation reflects itself in eqns. (2) and (3) by the fact that, for a particular set of experimental conditions, some of the terms in the inner summation are negligible compared to others.

For the sub-system given by eqn. (4), the values of K_{fgh} and κ_h are given in terms of the individual rate constants in Table I. The detailed derivation is given in the Appendix. The details are given here for this particular sub-system because it includes all the specific systems that have previously been presented individually in the literature. That is, simpler sub-systems can be obtained from eqn. (4) simply by setting appropriate rate constants equal to zero.

It is informative to note the physical significance of some of the parameters that appear in Table I. By employing the principle of microscopic reversibility (e.g., $k_{12}k_{23}k_{31} = k_{13}k_{32}k_{21}$) it can be seen that q_f (the coefficient of terms involving $\kappa_h = 0$) is simply the fraction of the sub-system which exists, at equilibrium, as component f . The parameters γ_f are the sums of cross-products of rate constants corresponding to

TABLE 1
VALUES OF SYSTEM CONSTANTS FOR THE THREE-COMPONENT SUB-SYSTEM

	$h = 1$	2	3
κ_h	0	$\sigma + \delta$	$\sigma - \delta$
K_{fjh}	q_f	$\frac{1}{2\delta} \sum_r (k_{fr} - q_r \kappa_3)$	$-\frac{1}{2\delta} \sum_r (k_{fr} - q_r \kappa_2)$
K_{fjh}	q_f	$-\frac{1}{2\delta} (k_{rf} - q_f \kappa_3)$	$\frac{1}{2\delta} (k_{rf} - q_f \kappa_2)$

In these expressions $r \neq f$.

$$2\sigma = k_{12} + k_{21} + k_{13} + k_{31} + k_{23} + k_{32}$$

$$\gamma_1 = k_{21}k_{31} + k_{32}k_{21} + k_{23}k_{31}$$

$$\gamma_2 = k_{12}k_{32} + k_{31}k_{12} + k_{13}k_{31}$$

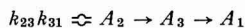
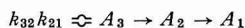
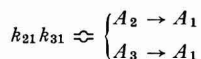
$$\gamma_3 = k_{13}k_{23} + k_{21}k_{13} + k_{12}k_{23}$$

$$\gamma = \gamma_1 + \gamma_2 + \gamma_3$$

$$q_f = \gamma_f/\gamma$$

$$\delta = |(\sigma^2 - \gamma)^{\frac{1}{2}}|$$

two-step paths for forming component f . For example, the three terms in γ_1 correspond to the double-step paths:



Noting that σ is half the sum of all the individual rate constants and that γ is the sum of all the cross-products for two-step paths, it can be seen that the two system constants κ_2 and κ_3 depend only on these two quantities — the value of κ_2 being between σ and 2σ and the value of κ_3 being between 0 and σ .

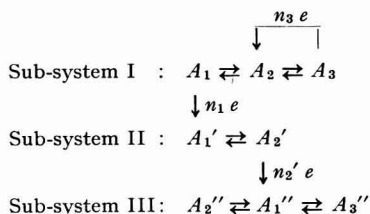
Reduction of the general three-component sub-system to a simpler one is demonstrated in Table 2, which corresponds to the general two-component sub-system. Table 2 is obtained from Table 1 by simply setting $k_{13} = k_{31} = k_{32} = k_{23} = 0$, thus completely eliminating component-3 from the sub-system.

Inspection of the model shows that the three-component sub-system treated here can be used to establish equations for any number of chemically independent sub-systems provided that each sub-system consists of no more than three chemically coupled species. Electron transfer at the electrode surface may, on the other hand, couple any two species whether they are in different sub-systems (*e.g.*, the pre- and post-kinetic case considered below) or in the same sub-system (*e.g.*, the parallel-

TABLE 2
VALUES OF SYSTEM CONSTANTS FOR THE TWO-COMPONENT SUB-SYSTEM

	$h = 1$	2
α_h	0	$k_{21} + k_{12}$
K_{11h}	$k_{21}/(k_{21} + k_{12})$	$k_{12}/(k_{21} + k_{12})$
K_{12h}	$k_{21}/(k_{21} + k_{12})$	$-k_{21}/(k_{21} + k_{12})$
K_{21h}	$k_{12}/(k_{21} + k_{12})$	$-k_{12}/(k_{21} + k_{12})$
K_{22h}	$k_{12}/(k_{21} + k_{12})$	$k_{21}/(k_{21} + k_{12})$

kinetic case considered below). For example, the constants given in Table 1 are sufficient for the description of a system such as:



where double arrows (\rightleftharpoons) denote chemical coupling (reactions occurring in solution) and single arrows (\rightarrow) denote electron-transfer reactions at the electrode surface. (The single arrow is not meant to imply irreversibility, but simply the net direction of the electron-transfer, *i.e.*, the notation $A_f \rightarrow A_r$ indicates the electrode reaction $A_f + n_f e \rightleftharpoons A_r$.)

FORMULATION OF RESPONSE FUNCTIONS FOR SPECIFIC SYSTEMS

The methods of formulating the response functions for several types of systems will now be demonstrated, using eqn. (2) and the appropriate Tables. The types of reaction mechanisms include pre-kinetic, post-kinetic, both pre- and post-kinetic, and parallel kinetic (catalytic) cases. In order to illustrate the principles without simultaneously introducing excessive bulkiness in the equations, chemical coupling between only two components is considered in these examples.

Pre-kinetics. Consider the system



in which the sub-system on the left-hand side of the electron-transfer reaction is the same as eqn. (4) when $k_{13} = k_{31} = k_{23} = k_{32} = 0$ as in Table 2. By eqn. (2), the response function is (noting that $J_2 = 0$ for this case),

$$\Delta \bar{C}_1 = - \frac{\bar{J}_1}{D^{\frac{1}{2}}} \left[\frac{K_{111}}{(p + \alpha_1)^{\frac{1}{2}}} + \frac{K_{112}}{(p + \alpha_2)^{\frac{1}{2}}} \right] \tag{6}$$

where the values of the four constants can be readily obtained from Table 2. Thus,

$$\Delta \bar{C}_1 = - \frac{\bar{J}_1}{D^{\frac{1}{2}}} \left[\frac{k_{21}}{(k_{12} + k_{21})p^{\frac{1}{2}}} + \frac{k_{12}}{(k_{12} + k_{21})(p + k_{12} + k_{21})^{\frac{1}{2}}} \right] \tag{7}$$

Post-kinetics. Consider the system



(The use of primes to denote quantities related to a sub-system following the electron-transfer reaction will be helpful in later discussions.) By eqn. (2), noting that $J_2' = 0$,

$$\Delta \bar{C}_1 = -\frac{\bar{J}_1'}{D^\ddagger} \left[\frac{K_{111}'}{(p + \kappa_1')^\ddagger} + \frac{K_{112}'}{(p + \kappa_2')^\ddagger} \right] \quad (9)$$

where the values of the four constants may be readily obtained from Table 2. If A_1' is the reduced species, then we also set $J_1 = -J_1'$ (to account for the negative value of n_1') and obtain

$$\Delta \bar{C}_1 = \frac{\bar{J}_1}{D^\ddagger} \left[\frac{k_{21}'}{(k_{12}' + k_{21}')p^\ddagger} + \frac{k_{13}'}{(k_{12}' + k_{21}') (p + k_{12}' + k_{21}')^\ddagger} \right] \quad (10)$$

Pre- and Post-kinetics. Consider the system



which is a combination of the two sub-systems treated above. Because the reactant sub-system and the product sub-system are coupled by electron transfer but not by chemical reaction, application of an excitation current yields a response in each sub-system. The response functions for the electroactive species, A_1 and A_1' , are given by eqns. (6) and (9), respectively. Thus, noting that $J_1 = -J_1'$, eqns. (7) and (10) are again applicable.

Parallel kinetics (catalytic). Consider the system:



By eqn. (2),

$$\Delta \bar{C}_2 = -\frac{\bar{J}_1}{D^\ddagger} \left[\frac{K_{211}}{(p + \kappa_1')^\ddagger} + \frac{K_{212}}{(p + \kappa_2')^\ddagger} \right] - \frac{\bar{J}_2}{D^\ddagger} \left[\frac{K_{221}}{(p + \kappa_1')^\ddagger} + \frac{K_{222}}{(p + \kappa_2')^\ddagger} \right] \quad (13)$$

and a similar equation for $\Delta \bar{C}_1$. By substituting the appropriate expressions from Table 2 for the six constants and setting $J_2 = -J_1$ (n_1 is negative if A_2 is the oxidized species), one obtains

$$\Delta \bar{C}_2 = -\frac{\bar{J}_2}{D^\ddagger (p + k_{12} + k_{21})^\ddagger} \quad (14)$$

and similarly,

$$\Delta \bar{C}_1 = \frac{\bar{J}_2}{D^\ddagger (p + k_{12} + k_{21})^\ddagger} \quad (15)$$

and

$$\begin{aligned} \Delta \bar{C}_2 = & -\frac{J_2}{D^{\frac{1}{2}}} \left[\frac{k_{12}}{(k_{12} + k_{21})p^{\frac{1}{2}}} + \frac{k_{21}}{(k_{12} + k_{21})(p + k_{12} + k_{21})^{\frac{1}{2}}} \right] \\ & -\frac{J_1}{D^{\frac{1}{2}}} \left[\frac{k_{12}}{(k_{12} + k_{21})p^{\frac{1}{2}}} - \frac{k_{12}}{(k_{12} + k_{21})(p + k_{12} + k_{21})^{\frac{1}{2}}} \right] \end{aligned} \quad (20)$$

The sum of eqns. (19) and (20) yields

$$\Delta \bar{C}_1 + \Delta \bar{C}_2 = - (J_2 + J_1) \frac{1}{D^{\frac{1}{2}} p^{\frac{1}{2}}} \quad (21)$$

Considering the simpler case in which the same number of electrons is involved in both reductions ($n = n_1 = n_2$) and the total current (and hence total flux) is constant, the inverse transformation of eqn. (21) gives

$$\Delta C_1 + \Delta C_2 = -\frac{2}{\pi^{\frac{1}{2}} D^{\frac{1}{2}}} (J_1 + J_2) t^{\frac{1}{2}} \quad (22)$$

Thus, at the second transition time, when $C_1 = C_2 = 0$,

$$C_1^* + C_2^* = \frac{2}{\pi^{\frac{1}{2}} D^{\frac{1}{2}}} (J_1 + J_2) \tau_2^{\frac{1}{2}} \quad (23)$$

Thus, the value of the second transition time is independent of chemical kinetic and equilibrium effects. However, when the numbers of electrons involved in the two reductions are unequal, the kinetic parameters will not completely disappear in the transition time expression. Such a relationship may be directly obtained, in Laplace form, by use of eqn. (3). The time-dependent solution is, however, more difficult to secure.

Post-kinetics. For the two-component case considered above (eqn. (8)), the transfer function is given by eqn. (10). Kinetic effects are most easily observed in such a system by first producing the electroactive component at the electrode surface, then reversing the current so as to remove this same component. While the excitation current function may be any one of an infinite variety (*e.g.*, current reversal with constant current, a negative ramp superimposed on a step, etc.), only current reversal with constant current will be considered here. Thus, the experiment is begun by applying a constant current, $i_1' = -I_1 n \mathcal{F} \mathcal{A}$, which is maintained until some arbitrary time, t_1 , at which the direction of the current is reversed, $i_1' = I_2 n \mathcal{F} \mathcal{A}$; (it is also assumed that t_1 is less than the transition time of the reactant component). Then, at some time after the current reversal, the surface concentration of A_1' reaches zero and a corresponding transition time, τ , is observed. For the current program stated above, the Laplace transformation of J_1' is given by:

$$J_1' = \frac{I_1}{p} - \frac{(I_1 + I_2)e^{-pt_1}}{p} \quad (24)$$

By substituting J_1' of eqn. (24) into eqn. (10) and taking the inverse Laplace transform of the result, one obtains

$$\Delta C_1' = \frac{I_1}{D^{\frac{1}{2}}} \left[\frac{2k_{21}'t^{\frac{1}{2}}}{\pi^{\frac{1}{2}}(k_{12}' + k_{21}')^{\frac{1}{2}}} + \frac{k_{12}'}{(k_{12}' + k_{21}')^{\frac{1}{2}}} \operatorname{erf} (k_{12}' + k_{21}')^{\frac{1}{2}}t^{\frac{1}{2}} \right] - \frac{(I_1 + I_2)}{D^{\frac{1}{2}}} \left[\frac{2k_{21}'(t - t_1)^{\frac{1}{2}}}{\pi^{\frac{1}{2}}(k_{12}' + k_{21}')^{\frac{1}{2}}} + \frac{k_{12}'}{(k_{12}' + k_{21}')^{\frac{1}{2}}} \operatorname{erf} (k_{12}' + k_{21}')^{\frac{1}{2}}(t - t_1)^{\frac{1}{2}} \right] \quad (25)$$

If the initial concentration of A_1' is zero, then the transition time is given by:

$$I_1 \left[\frac{2k_{21}'\tau^{\frac{1}{2}}}{\pi^{\frac{1}{2}}} + \frac{k_{12}'}{(k_{12}' + k_{21}')^{\frac{1}{2}}} \operatorname{erf} (k_{12}' + k_{21}')^{\frac{1}{2}}\tau^{\frac{1}{2}} \right] = (I_1 + I_2) \left[\frac{2k_{21}'(\tau - t_1)^{\frac{1}{2}}}{\pi^{\frac{1}{2}}} + \frac{k_{12}'}{(k_{12}' + k_{21}')^{\frac{1}{2}}} \operatorname{erf} (k_{12}' + k_{21}')^{\frac{1}{2}}(\tau - t_1)^{\frac{1}{2}} \right] \quad (26)$$

These results are in agreement with those of DRACKA⁴.

Parallel-kinetics. For the two-component case considered above (eqn. (12)) the response function for A_2 is given by eqn. (14). For a constant positive excitation current the inverse Laplace transformation of eqn. (14) yields

$$\Delta C_2 = - \frac{J_2}{D^{\frac{1}{2}}(k_{12} + k_{21})^{\frac{1}{2}}} \operatorname{erf} (k_{12} + k_{21})^{\frac{1}{2}}t^{\frac{1}{2}} \quad (27)$$

Thus, the transition time, τ , is given by

$$C_2^* = \frac{J_2}{D^{\frac{1}{2}}(k_{12} + k_{21})^{\frac{1}{2}}} \operatorname{erf} (k_{12} + k_{21})^{\frac{1}{2}}\tau^{\frac{1}{2}} \quad (28)$$

which, when $k_{21} = 0$, reduces to the expression obtained by DELAHAY, MATTAX AND BERZINS⁵.

Chronoamperometry

In this treatment it is assumed that, for each chronoamperometry experiment, a constant potential is initially applied and that the application of this potential creates and maintains a zero (or sufficiently close to zero) surface concentration for one or more specified components but does not directly (electrochemically) control the surface concentrations of other components. These assumptions are made in order to avoid the necessity of introducing, at this point, the non-linear relationships which follow from the use of eqn. (1).

Although eqns. (2) and (3) are equally as applicable for chronoamperometry as for chronopotentiometry, the inverse transformation of the Laplace solutions is often more difficult for chronoamperometry. Consider, for example, the following two systems which were treated above for chronopotentiometric conditions.

Parallel-kinetics. For the two-component system (eqn. (12)), the transfer function for A_2 is given by eqn. (14). In this case the surface concentration of A_2 is zero (after time zero). Thus, setting $\Delta C_2 = -C_2^*/p$ gives

$$J_2 = D^{\frac{1}{2}} \frac{C_2^*}{p} (p + k_{12} + k_{21})^{\frac{1}{2}} \quad (29)$$

The inverse Laplace transformation of eqn. (29) gives

$$J_2 = D^{\frac{1}{2}} C_2^* \left\{ \frac{1}{\pi^{\frac{1}{2}}t^{\frac{1}{2}}} \exp [-(k_{12} + k_{21})t] + (k_{12} + k_{21})^{\frac{1}{2}} \operatorname{erf} (k_{12} + k_{21})^{\frac{1}{2}}t^{\frac{1}{2}} \right\} \quad (30)$$

which, when $k_{21} = 0$, reduces to the results obtained by DELAHAY AND STIEHL⁶, POSPISIL⁷, and MILLER⁸.

Pre-kinetics. For the two-component sub-system considered above (eqn. (5)), the response function is given by eqn. (7). Thus, setting $\Delta\bar{C}_1 = -C_1^*/p$ gives

$$J_1 = \frac{D^{\frac{1}{2}} C_1^* (k_{12} + k_{21}) (p + k_{12} + k_{21})^{\frac{1}{2}}}{p^{\frac{1}{2}} [k_{21} (p + k_{12} + k_{21})^{\frac{1}{2}} + k_{12} p^{\frac{1}{2}}]} \quad (31)$$

Multiplying numerator and denominator by $[k_{21}(p + k_{12} + k_{21})^{\frac{1}{2}} - k_{12}p^{\frac{1}{2}}]$ yields a sum of three terms. Taking the inverse Laplace transform of each term individually gives the inverse Laplace transform of eqn. (31), which is, after rearrangement,

$$J_1 = \frac{D^{\frac{1}{2}} C_1^*}{(K - 1)} \left\{ \frac{Ke^{-kt} - 1}{\pi^{\frac{1}{2}} t^{\frac{1}{2}}} + K^2 \left(\frac{k}{K^2 - 1} \right)^{\frac{1}{2}} \exp \left(\frac{kt}{K^2 - 1} \right) \left[\operatorname{erf} K \left(\frac{kt}{K^2 - 1} \right)^{\frac{1}{2}} - \operatorname{erf} \left(\frac{kt}{K^2 - 1} \right)^{\frac{1}{2}} \right] \right\} \quad (32)$$

where $K = k_{12}/k_{21}$ and $k = k_{12} + k_{21}$.

Equation (32) is equivalent to the expression originally derived by KOUTECKÝ AND BRDIČKA⁹.

A.c. Chronopotentiometry

The mathematical treatment of this technique is considerably complicated by the necessity of introducing the potential function (eqn. (1)). However, so long as only current-surface concentration relationships are considered, the treatment of a.c. chronopotentiometry is only slightly more difficult than that of constant current chronopotentiometry, as will be seen below.

The excitation function employed in this technique consists of a sinusoidal current superimposed on a constant current and can, therefore, be expressed as the sum of these two independent parts. In general, because of the linear relationship between current and change in surface concentration exhibited by eqn. (2), the net change in surface concentration is equal to the sum of the surface concentration changes due to each individual component of the current. Thus, for example, if the total current is given by $i + \delta i$, the net surface concentration change may be expressed as $\Delta C + \delta C$, where ΔC results from i only and δC results from δi only. Thus, each contribution to the net surface concentration change may be calculated independently by eqn. (2). Therefore, in a.c. chronopotentiometry, the "d.c." components of surface concentration changes are calculated as in constant current chronopotentiometry and the problem is reduced to computing the a.c. components, which are independent of the d.c. current.

Applying eqn. (2), and restricting the treatment to a system involving only one pair of electroactive components leads to

$$\delta\bar{C}_O = - \frac{\delta\bar{J}}{D_O^{\frac{1}{2}}} \sum_h K_h (p + \kappa_h)^{-\frac{1}{2}} \quad (33)$$

$$\delta\bar{C}_R = + \frac{\delta\bar{J}}{D_R^{\frac{1}{2}}} \sum_m K_m (p + \kappa_m)^{-\frac{1}{2}} \quad (34)$$

where m has been used for h in eqn. (34) in order to indicate that the equation may be applied to two chemically independent sub-systems. Notice that parallel-kinetic cases are not really excluded by this formulation because the additional terms may be included in the sums by appropriate manipulation of the signs and values of K_h and K_m . Equations (33) and (34) are not restricted to sinusoidal currents although only sinusoidal fluctuations will be treated below.

When the current fluctuation is sinusoidal, *e.g.*,

$$\delta J = J_s \sin \omega t \quad (35)$$

where J_s is a constant, the solutions of eqns. (33) and (34) are, neglecting transient terms,

$$\delta C_O = (C_O)_s \sin \omega t + (C_O)_c \cos \omega t \quad (36)$$

$$\delta C_R = (C_R)_s \sin \omega t + (C_R)_c \cos \omega t \quad (37)$$

where

$$(C_O)_s = -\frac{J_s}{D_O^{1/2}} \sum_h K_h \left[\frac{(\omega^2 + \kappa_h^2)^{1/2} + \kappa_h}{2(\omega^2 + \kappa_h^2)} \right]^{1/2} \equiv \frac{X_s}{D_O^{1/2}} \quad (38)$$

$$(C_O)_c = \frac{J_s}{D_O^{1/2}} \sum_h K_h \left[\frac{(\omega^2 + \kappa_h^2)^{1/2} - \kappa_h}{2(\omega^2 + \kappa_h^2)} \right]^{1/2} \equiv \frac{X_c}{D_O^{1/2}} \quad (39)$$

$$(C_R)_s = \frac{J_s}{D_R^{1/2}} \sum_m K_m \left[\frac{(\omega^2 + \kappa_m^2)^{1/2} + \kappa_m}{2(\omega^2 + \kappa_m^2)} \right]^{1/2} \equiv \frac{R_s}{D_R^{1/2}} \quad (40)$$

$$(C_R)_c = -\frac{J_s}{D_R^{1/2}} \sum_m K_m \left[\frac{(\omega^2 + \kappa_m^2)^{1/2} - \kappa_m}{2(\omega^2 + \kappa_m^2)} \right]^{1/2} \equiv \frac{R_c}{D_R^{1/2}} \quad (41)$$

An expression for the potential may be obtained then by substituting $i + \delta i$ for the total current and $C_O + \delta C_O$ and $C_R + \delta C_R$ for the total surface concentrations of the oxidized and reduced species, respectively, into eqn. (1). However, because of the form of eqn. (1), a general solution for potential is not possible in closed form. On the other hand, the potential may be expressed as a three-dimensional Taylor series as shown below.

For convenience, eqn. (1) is written in the form

$$\frac{id}{n\mathcal{F}dke} = D_O^{1/2} C_O \exp(-\alpha) \frac{n\mathcal{F}}{RT} \Delta E - D_R^{1/2} C_R \exp(1-\alpha) \frac{n\mathcal{F}}{RT} \Delta E \quad (42)$$

where

$$\Delta E = E - E_3^r \quad (43)$$

$$E_3^r = E^\circ + \frac{RT}{n\mathcal{F}} \ln \left[\frac{f_O D_R^{1/2}}{f_R D_O^{1/2}} \right] \quad (44)$$

$$d = \frac{(D_R^\alpha D_O^{(1-\alpha)})^{1/2}}{f_R^\alpha f_O^{(1-\alpha)}} = \left(\frac{D_R^{1/2}}{f_R} \right)^\alpha \left(\frac{D_O^{1/2}}{f_O} \right)^{(1-\alpha)} \quad (45)$$

or, more concisely,

$$H = X e^{-\alpha\epsilon} - R e^{(1-\alpha)\epsilon} \quad (46)$$

where

$$H = \frac{Jd}{k_e} = \frac{i}{nF} \frac{d}{k_e} \quad (47)$$

$$X = D_O^{\frac{1}{2}} C_O \quad (48)$$

$$R = D_R^{\frac{1}{2}} C_R \quad (49)$$

$$\varepsilon = \frac{nF}{RT} \Delta E \quad (50)$$

Because ε is a function of H , X , and R , a three-dimensional Taylor expansion may be symbolized

$$\delta\varepsilon = \sum_{n=1}^{\infty} \frac{1}{n!} \left[(\delta H) \frac{\partial}{\partial H} + (\delta X) \frac{\partial}{\partial X} + (\delta R) \frac{\partial}{\partial R} \right]^n \varepsilon \quad (51)$$

where $\delta\varepsilon$ is the finite change in ε when H , X , and R are changed by δH , δX , and δR , respectively. The partial derivatives required by eqn. (51) may be readily computed from eqn. (46). A few of these derivatives are given in Table 3. Notice that $\delta\varepsilon$ is a function of ε , R , X , δR , δX , and δH .

TABLE 3
SOME COEFFICIENTS FOR TAYLOR EXPANSION

$\frac{\partial \varepsilon}{\partial H} = \frac{1}{H'}$	$\frac{\partial^2 \varepsilon}{\partial H^2} = -\frac{H''}{(H')^3}$
$\frac{\partial \varepsilon}{\partial X} = -\frac{e^{-\alpha\varepsilon}}{H'}$	$\frac{\partial^2 \varepsilon}{\partial X^2} = -\frac{(H'' + 2\alpha H')}{(H')^3} e^{-2\alpha\varepsilon}$
$\frac{\partial \varepsilon}{\partial R} = \frac{e^{(1-\alpha)\varepsilon}}{H'}$	$\frac{\partial^2 \varepsilon}{\partial R^2} = -\frac{[H'' - 2(1-\alpha)H']e^{2(1-\alpha)\varepsilon}}{(H')^3}$
	$\frac{\partial^2 \varepsilon}{\partial X \partial R} = \frac{[H'' - (1-2\alpha)H']e^{(1-2\alpha)\varepsilon}}{(H')^3}$
	$\frac{\partial^2 \varepsilon}{\partial X \partial H} = \frac{(H'' + \alpha H')e^{-\alpha\varepsilon}}{(H')^3}$
	$\frac{\partial^2 \varepsilon}{\partial R \partial H} = -\frac{[H'' - (1-\alpha)H']e^{(1-\alpha)\varepsilon}}{(H')^3}$

where

$$H = Xe^{-\alpha\varepsilon} - Re^{(1-\alpha)\varepsilon}$$

$$H' = \frac{\partial H}{\partial \varepsilon} = -\alpha Xe^{-\alpha\varepsilon} - (1-\alpha)Re^{(1-\alpha)\varepsilon}$$

$$H'' = \frac{\partial^2 H}{\partial \varepsilon^2} = \alpha^2 Xe^{-\alpha\varepsilon} - (1-\alpha)^2 Re^{(1-\alpha)\varepsilon}$$

For the a.c. chronopotentiometry case under consideration, ε , H , X , and R are the functions which would be applicable if only the "d.c." part of the excitation function were applied; δH , δX , and δR are the functions which would be applicable if only the sinusoidal part of the excitation function were applied; and $\delta\varepsilon$ represents the difference between the potentials obtained in these two hypothetical circumstances, that is, the change in potential which results from the sinusoidal current being superimposed on the constant current. Substitution of eqns. (35), (36), and (37) into eqn. (51) shows that $\delta\varepsilon$ is a sum of one frequency-independent term and harmonic sine and cosine terms (*i.e.*, a Fourier Series). The amplitude of each term depends on the "d.c." components of the potential, current, and both concentrations. Also, the amplitude of the n -th harmonic is itself a sum of contributions from finite differences of the orders n , $n + 2$, $n + 4$, . . . Thus, when the amplitudes of the oscillations are sufficiently small, contributions from the higher-order differences will be negligible. Under such conditions, the first harmonic (fundamental) of $\delta\varepsilon$ is given by

$$\delta_1\varepsilon = \left[\frac{H_s - X_s e^{-\alpha\varepsilon} + R_s e^{(1-\alpha)\varepsilon}}{H'} \right] \sin \omega t + \left[\frac{-X_c e^{-\alpha\varepsilon} + R_c e^{(1-\alpha)\varepsilon}}{H'} \right] \cos \omega t \quad (52)$$

where

$$H_s = \frac{J_s d}{k_e} \quad (52a)$$

Of great interest^{10,11} in electrochemical kinetic studies is the phase angle, ϕ , of this first harmonic which is given by

$$\text{ctn } \phi = \frac{H_s - X_s e^{-\alpha\varepsilon} + R_s e^{(1-\alpha)\varepsilon}}{-X_c e^{-\alpha\varepsilon} + R_c e^{(1-\alpha)\varepsilon}} \quad (53)$$

Thus, from eqns. (38), (39), (40), and (52a)

$$\text{ctn } \phi = - \frac{\frac{d}{k_e} e^{\alpha\varepsilon} + \sum_h K_h \left[\frac{(\omega^2 + \kappa_h^2)^{\frac{1}{2}} + \kappa_h}{2(\omega^2 + \kappa_h^2)} \right]^{\frac{1}{2}} + e^\varepsilon \sum_m K_m \left[\frac{(\omega^2 + \kappa_m^2)^{\frac{1}{2}} + \kappa_m}{2(\omega^2 + \kappa_m^2)} \right]^{\frac{1}{2}}}{\sum_h K_h \left[\frac{(\omega^2 + \kappa_h^2)^{\frac{1}{2}} - \kappa_h}{2(\omega^2 + \kappa_h^2)} \right]^{\frac{1}{2}} + e^\varepsilon \sum_m K_m \left[\frac{(\omega^2 + \kappa_m^2)^{\frac{1}{2}} - \kappa_m}{2(\omega^2 + \kappa_m^2)} \right]^{\frac{1}{2}}} \quad (54)$$

Notice that potential is the only time-dependent function in the phase-angle expression. This statement is true regardless of the time-dependence of the "d.c." current — which is not necessarily constant. Hence, the same expression (with opposite sign) is applicable for small amplitude a.c. chronoamperometry and a.c. polarography. The change in sign arises because in a.c. chronopotentiometry the potential response is measured relative to the excitation current, whereas in a.c. chronoamperometry and in a.c. polarography the quantities corresponding to excitation and response are reversed. The phase-angle equivalence of the a.c. techniques holds only for small amplitude oscillations where higher harmonics are negligible.

While expressions for higher harmonic a.c. chronopotentiometry can be derived on the basis of eqn. (52), the resulting equations appear to be too cumbersome to be useful when chemical kinetics is involved and so are not presented here.

Recently, SMITH *et al.*¹² have independently derived an expression for the phase angle, ϕ , in first-harmonic, small amplitude a.c. polarography involving (pseudo-)

first order chemical processes. Their equation, which was derived following MATSUDA's¹³ general treatment for a.c. polarography, is the same as our eqn. (54), which was, of course, derived from the viewpoint of a.c. chronopotentiometry.

GENERAL DISCUSSION

After becoming familiar with the application of eqn. (2) *via* the preceding specific examples, it is now beneficial to note some of its implication regarding the elucidation of chemical kinetics by electrochemical techniques. Clearly, the system constants (K_{fjh} and κ_h of eqn. (2)) are the parameters directly obtained through experimental measurement. That is, these quantities can be experimentally evaluated before postulating a specific reaction mechanism and even before determining their explicit dependence on the individual rate constants. In fact, chemical interpretations of the system constants are sometimes possible without resorting to the detailed calculations of the individual rate constants, just as is the case in homogeneous reaction kinetics. For example, in the sub-system $A_1 \rightleftharpoons A_2 \rightleftharpoons A_3$ it can be shown that κ_2 is approximately equal to the rate constant for the fastest individual step in the sub-system.

Implications of eqn. 2

Because the various κ_h 's occur as a sum with p in eqn. (2), the time-range over which experiments must be made in order to evaluate the κ_h 's is indicated. For example, in chronopotentiometry the current density must be such that the reciprocal of the transition time is in the order of magnitude of the κ_h 's which are to be determined. Similarly, in a.c. methods, frequencies in the order of magnitude of the κ_h 's must be used. Conversely, frequencies or reciprocal transition times corresponding to changes in the behavior of the system indicate the approximate values of the various κ_h 's. In chronoamperometry the overall experiment time is fixed by the values of the system constants; however, attention should be focused on time regions corresponding roughly to the values of the reciprocal κ_h 's.

Looking at the terms which occur in the inner summation (*i.e.*, the sum over h) of eqn. (2), it is readily seen (*cf.* Tables 1 and 2) that each term except the first contains a different piece of kinetic information. That is, experiments allowing the evaluation of only the first term will yield no kinetic information. However, the relative importance of the various terms in the sum can be altered by appropriate adjustments of the experimental conditions — such as changing the temperature, pH, etc. (*i.e.*, by altering the relative values of the individual pseudo-first order rate constants). Although a complete description of the kinetics requires the evaluation of each term, adequate partial descriptions may be formulated by experimental evaluation of some of the terms together with some chemical intuition.

Experimental evaluation of system constants for sub-systems containing only one electro-active component

(a) *Constant current chronopotentiometry.* For a single reducible component, eqn. (2) becomes

$$-\Delta\bar{C}_f = \frac{J_f}{D^{\frac{1}{2}}} \sum_h K_{fjh} (p + \kappa_h)^{-1} \quad (55)$$

For constant current chronopotentiometry $J_f = i/pnFA$, where i is the current

amplitude. Thus, the inverse Laplace transform of eqn. (55) gives, at the transition time,

$$C^* = \frac{i}{n\mathcal{F}\mathcal{A}D^{\frac{1}{2}}} \left[\frac{2\tau^{\frac{1}{2}}}{\pi^{\frac{1}{2}}} + \frac{1}{q_f} \sum_{h=2,3} \frac{K_{ffh}}{\kappa_h^{\frac{1}{2}}} \operatorname{erf}(\kappa_h\tau)^{\frac{1}{2}} \right] \quad (56)$$

In eqn. (56), K_{ff1} has been replaced by q_f , and $C^* = C_f^*/q_f = \sum_g C_g^*$ equals the total initial concentration of the sub-system. The system constants are perhaps most conveniently evaluated from experimental data by analyzing a plot of $i\tau^{\frac{1}{2}}$ vs. i . If the values of the various κ_h 's are sufficiently different, the shape of such a plot will be somewhat like that shown in Fig. 1. The curve will be nearly straight in regions

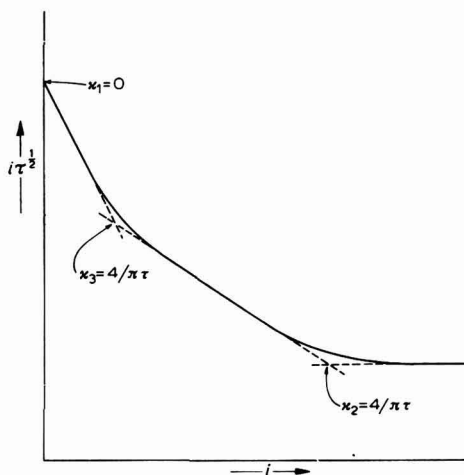


Fig. 1. Method for plotting chronopotentiometric data.

where all the values of $\kappa_h\tau$ differ somewhat from unity, being either greater or less. As shown in Fig. 1, the values of κ_h are nearly equal to the values of τ^{-1} at the intersections of these linear segments. The equation for each individual straight line segment is

$$i\tau^{\frac{1}{2}} = \frac{n\mathcal{F}\mathcal{A}D^{\frac{1}{2}}\pi^{\frac{1}{2}}q_fC^*}{2 \sum_{m'} K_{ffm'}} - \frac{\pi^{\frac{1}{2}} \sum_m K_{ffm}|\kappa_m^{\frac{1}{2}}}{2 \sum_{m'} K_{ffm'}} \quad (57)$$

where the subscript h has been replaced by m' when $\kappa_h\tau$ is less than unity or by m when $\kappa_h\tau$ is greater than unity. Hence, the values of the system constants can be obtained from the slopes and intercepts of the various linear segments.

(b) *Chronoamperometry*. Chronopotentiometric methods suffer the disadvantage that only one piece of information (*i.e.*, only one pair of values for transition time and current amplitude) is obtained from each experiment. Thus, many experiments are required to obtain enough data to evaluate the kinetic parameters. In chronoamperometry, however, the measured variable, current, is a linear function, so the entire chronoamperogram can be described by linear equations (*i.e.*, eqn. (2)). Also,

a single chronoamperometric experiment automatically covers the time ranges appropriate to the determination of kinetic constants.

Perhaps the most general (and mathematically simplest) method for analyzing chronoamperometric data follows from a proposal by WIJNEN¹⁴, who suggested comparing the Laplace transformations of experimental chronoamperograms with the theoretical Laplace transform expression for the proposed mechanism. For chronoamperometry involving reduction of only one component eqn. (2) becomes

$$- \Delta \bar{C}_f = \frac{C_f^*}{p} = \frac{\bar{i}_f}{n \mathcal{F} \mathcal{A} D^{\frac{1}{2}}} \sum_h K_{ffh} (p + \kappa_h)^{-\frac{1}{2}} \quad (58)$$

where \bar{i}_f is the Laplace transform of the experimental chronoamperogram. By substituting C^* for C_f^*/q_f eqn. (58) can be cast into the form

$$(p^{\frac{1}{2}} \bar{i}_f)^{-1} = (n \mathcal{F} \mathcal{A} D^{\frac{1}{2}} C^*)^{-1} \sum_h \frac{K_{ffh} p^{\frac{1}{2}}}{q_f (p + \kappa_h)^{\frac{1}{2}}} \quad (59)$$

Thus, a plot of $(p^{\frac{1}{2}} \bar{i}_f)^{-1}$ vs. $p^{\frac{1}{2}}$ contains a series of linear portions as indicated in Fig. 2. The intersections of these linear portions occur in the vicinities of $p = \kappa_n$, and the K_{ffh} 's can be evaluated from the slopes of the segments. An alternate plot would be

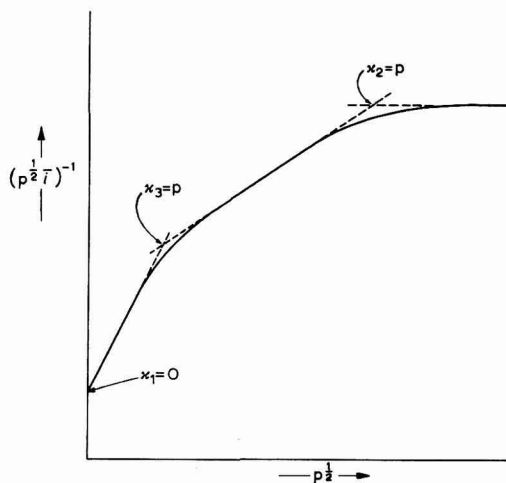


Fig. 2. Method for plotting chronopotentiometric data.

$(p \bar{i}_f)^{-1}$ vs. $p^{-\frac{1}{2}}$, which also yields a series of linear segments from which the system constants can be evaluated. In this latter procedure, the values of $p \bar{i}_f$ could be obtained by differentiating the chronoamperogram before taking the Laplace transform.

(c) *Other controlled-potential techniques.* For a more sophisticated treatment of chronoamperometry at constant potential, it is noted that when potential is maintained constant eqn. (1) is readily amenable to Laplace transformation. Thus, using

the notation of eqn. (50), the Laplace transform of eqn. (1) is, for constant potential,

$$J_o \frac{d}{k_e} = D_o^{\frac{1}{2}} \bar{C}_O e^{-\alpha e} - D_R^{\frac{1}{2}} \bar{C}_R e^{(1-\alpha)e} \quad (60)$$

From eqn. (2), the Laplace transforms of the concentration of the oxidized and reduced species are:

$$\bar{C}_O = \frac{C_o^*}{p} - \frac{J_o}{D_o^{\frac{1}{2}}} \sum_h K_h (p + \kappa_h)^{-\frac{1}{2}} \quad (61)$$

$$\bar{C}_R = \frac{C_R^*}{p} + \frac{J_o}{D_R^{\frac{1}{2}}} \sum_m K_m (p + \kappa_m)^{-\frac{1}{2}} \quad (62)$$

which, upon substitution into eqn. (60), yield

$$\frac{nFA}{ip} = \frac{\frac{d}{k_e} e^{\alpha e} + \sum_h K_h (p + \kappa_h)^{-\frac{1}{2}} - e^e \sum_m K_m (p + \kappa_m)^{-\frac{1}{2}}}{D_o^{\frac{1}{2}} C_o^* - D_R^{\frac{1}{2}} C_R^* e^e} \quad (63)$$

which, of course, reduces to eqn. (59) when the potential is sufficiently negative.

Equation (1) becomes linear in current and concentration whenever potential is expressed as an explicit function of time only, thus, in principle, allowing its Laplace transformation to be taken. Hence, other controlled-potential techniques such as linear potential scan voltammetry can be treated, in the Laplace plane, by the use of eqn. (2) and the Laplace transformations of both eqn. (1) and the experimental current-time data. While these Laplace expressions are rather involved, they are, no doubt, considerably less complicated than their inverse Laplace transforms.

It is important to note that eqns. (56), (59), and (63) are not restricted to any one specific reaction mechanism. Thus, the forms of these equations can be used to evaluate the system constants for an undescribed mechanism and *then* the system constants can be interpreted in terms of a specific mechanism. Obviously, the number of terms and values (and variations with experimental conditions) of the system constants which are experimentally accessible can give some insight into the complexity of the mechanism and can indicate some approximations which are permissible in the formulation of a proposed reaction mechanism.

Interpretation of system constants

The conversion of experimental system constants into individual rate constants by direct calculation is rather difficult for sub-systems involving more than two components. Evidently, iterative computations which can be easily performed by a digital computer provide the most useful approach in such cases.

In connection with these calculations it is quite useful to note that the relationships between the individual rate constants and the system constants in electrochemistry are exactly the same as the relationships used in the treatment of first-order homogeneous reaction kinetics. The equation for the latter, which resembles the form of eqn. (2), is

$$A\bar{C}_f = \sum_g (AC_g)^* \sum_h K_{fgh} (p + \kappa_h)^{-1} \quad (64)$$

where ΔC_f is the concentration of component f measured relative to the initial equilibrium concentration of component f before excitation. The excitation is an impulsive change in the concentration of component g by the amount $(\Delta C_g)^*$. The constants K_{fgh} and κ_h bear exactly the same relationship to the individual rate constants in eqn. (64) as they do in eqn. (2). Hence, the cumbersome mathematics involved in deriving these relationships may sometimes be avoided by referring to treatments of homogeneous reaction kinetics. Also, similar relationships are used in the calculation of the fundamental frequencies in the vibration of polyatomic molecules, electronic networks, and servo-mechanisms and in quantum-mechanical calculations of electronic energies of molecules.

Because of the identity of the relations between system constants and individual rate constants in electrochemistry and homogeneous reaction kinetics, the system constants can be evaluated for complicated systems by the use of an electronic analog computer designed according to the coupled rate equations describing the reaction mechanism. By exciting the analog computer with an impulsive signal, the values of the system constants can be evaluated by fitting the response to the inverse transformation of eqn. (64), which is

$$\Delta C_f = \sum_g \Delta C_g^* \sum_h K_{fgh} e^{-\kappa_h t} \quad (65)$$

The values of the system constants thus secured can be compared with the electrochemically obtained system constants and the values of the individual rate constants (of the analog computer) varied until the two sets of system constants match. A particular advantage of this method is that the sensitivity of each system constant to each individual rate constant (and hence *vice-versa*) is directly indicated.

Another analog system which involves the same system constants is a system of coupled harmonic oscillators. In this case, the analogy to eqn. (2) is

$$\Delta \bar{C}_f = \sum_g \bar{y}_g \sum_h K_{fgh} (p^2 + \kappa_h)^{-1} \quad (66)$$

where y_g corresponds to the sinusoidal force acting on oscillator g and ΔC_f is the displacement from equilibrium of oscillator f due to the excitation forces. Equation (66) results when the set of relations

$$\frac{d^2 C_f}{dt^2} = \sum_g k_{gf} C_g + y_f \quad (67)$$

are treated in a manner similar to that given in the appendix. As a method for determining system constants from first-order rate constants, an analog computer based on the coupled system of sinusoidally excited harmonic oscillators offers the advantage that resonance occurs whenever the excitation frequency is proportional to the square root of one of the κ_h 's. Hence, values of the system constants can be obtained by observing the resonance frequencies and the rate of amplitude build-up of the response signals at the resonance frequencies, the latter yielding the values of K_{fgh} 's.

APPENDIX

Derivation of eqns. (2) and (3)

Consider a reaction scheme involving N components where each component A_f

is coupled with each other component A_r by a (pseudo-) first-order chemical reaction. For a chemical process involving non-zero concentration gradients in an unstirred solution, the rate of change in the concentration of A_f is the sum of contributions from diffusion (Fick's second law) and from chemical reaction (reaction kinetics). Thus, for a plane electrode (non-zero concentration gradients in only one dimension) the rate of change in concentration, C_f , of A_f is given by

$$\frac{\partial C_f}{\partial t} = D_f \frac{\partial^2 C_f}{\partial x^2} - \sum_r k_{fr} C_f + \sum_r k_{rf} C_r \quad (r \neq f) \quad (1A)$$

where D_f is the diffusion constant of A_f , and k_{fr} is the (pseudo-) first-order rate constant for the chemical reaction $A_f \rightarrow A_r$. Assuming for simplicity that all the diffusion constants are equal, eqn. (1A), which represents one equation for each of the N components, may be cast into the more convenient form

$$\mathcal{D} C_f - \sum_g k_{gf} C_g = 0 \quad (2A)$$

where

$$\mathcal{D} \equiv \frac{\partial}{\partial t} - D \frac{\partial^2}{\partial x^2} \quad (3A)$$

and

$$k_{ff} \equiv - \sum_r k_{fr} \quad (r \neq f) \quad (4A)$$

In eqn. (2A) the summation is taken over all N components.

Noting that concentration is a function of both distance and time, $C_f = C_f(x, t)$, the initial and boundary conditions corresponding to initial homogeneity in solution, semi-infinite linear diffusion, and a plane electrode, are

$$C_f(x, 0) = C_f^* \quad (5A)$$

$$C_f(\infty, t) = C_f^* \quad (6A)$$

and

$$\frac{\partial C_f}{\partial x}(0, t) = - \frac{J_f}{D} = - \frac{i_f}{n_f F A D} \quad (7A)$$

where C_f^* is the initial concentration of A_f , J_f is the flux of A_f into the electrode from solution, i_f is the current (positive during reduction) due to the electrode reaction involving A_f , and n_f is the number of electrons per molecule transferred from the electrode to A_f (*i.e.*, the value of n_f is negative when A_f is the reduced species). It is important to notice that the latter boundary condition is not specific because current is left as a general function of time.

The above system of partial differential equations is perhaps most conveniently handled by first taking N linear combinations of the N equations represented by eqn. (2A), *i.e.*,

$$\sum_f a_{fh} [\mathcal{D} C_f - \sum_g k_{gf} C_g] = 0 \quad (8A)$$

with the values of the coefficients a_{fh} being such that

$$\mathcal{D} \varphi_h + \kappa_h \varphi_h = 0 \quad (9A)$$

where

$$\varphi_h \equiv \sum_f a_{fh} C_f \quad (10A)$$

and where the κ_h are constants. Evidently, linear combinations satisfying eqn. (9A) are always possible for stoichiometric reactions. It is instructive to notice that one satisfactory combination is simply the sum of eqn. (2A). In this case, each coefficient a_{fh} is unity and κ_h is zero. Also, because only the relative values of the a_{fh} are important, the values of a_{fh} may be arbitrarily selected for one value of f . The evaluation of the constants is discussed and illustrated below.

Equation (9A) can be cast into another useful form by the transformation of variables

$$\Phi_h \equiv \varphi_h e^{\kappa_h t} \quad (11A)$$

which gives

$$\partial \Phi_h = 0 \quad (12A)$$

or, by eqn. (3A),

$$\frac{\partial \Phi_h}{\partial t} = D \frac{\partial^2 \Phi_h}{\partial x^2} \quad (13A)$$

Notice that eqn. (13A) has the form that would obtain if Φ_h corresponded to the concentration of a single species and no chemical reactions were involved. Thus, taking the Laplace transform (with respect to time) of eqn. (13A) and inserting the initial and boundary conditions [in terms of Φ_h^* and $(\partial \Phi_h / \partial x)(0, t)$] yields

$$\overline{(\Phi_h - \Phi_h^*)} (0, p) = \frac{D^{\frac{1}{2}}}{p^{\frac{1}{2}}} \left(\frac{\partial \overline{\Phi_h}}{\partial x} \right) (0, p) \quad (14A)$$

where $\overline{F}(x, p)$ denotes the Laplace transform of $F(x, t)$.

Inserting eqn. (11A) gives

$$\overline{(\varphi_h - \varphi_h^*)} (0, p - \kappa_h) = \frac{D^{\frac{1}{2}}}{p^{\frac{1}{2}}} \left(\frac{\partial \overline{\varphi_h}}{\partial x} \right) (0, p - \kappa_h) \quad (15A)$$

Upon replacing p by $p + \kappa_h$ (which is equivalent to multiplying both sides of the inverse Laplace transform by $e^{-\kappa_h t}$) eqn. (15A) becomes

$$\Delta \overline{\varphi_h} = \overline{(\varphi_h - \varphi_h^*)} = \frac{D^{\frac{1}{2}}}{(p + \kappa_h)^{\frac{1}{2}}} \left(\frac{\partial \overline{\varphi_h}}{\partial x} \right) \quad (16A)$$

where it is to be understood that eqn. (16A) and following equations are applicable at the electrode surface and that the Laplace variable is p . By inserting linear combinations of eqn. (7A) for $(\partial \varphi_h / \partial x)$,

$$\Delta \overline{\varphi_h} = - \sum_g \frac{a_{gh} \overline{J}_g}{D^{\frac{1}{2}} (p + \kappa_h)^{\frac{1}{2}}} \quad (17A)$$

Although eqn. (17A) represents the solutions to the original equations, it is still necessary to express the results in terms of the individual surface concentrations of the chemical species rather than linear combinations of these. Because each φ_h is a

linear combination of all the C_f each C_f may be expressed as a linear combination of the φ_h . Thus,

$$\Delta \bar{C}_f = \sum_h b_{hf} \Delta \bar{\varphi}_h \tag{18A}$$

Hence, by inserting eqn. (17A) into eqn. (18A) and rearranging, one obtains

$$\Delta \bar{C}_f = - D^{-1} \sum_g \bar{J}_g \sum_h K_{fgh} (p + \kappa_h)^{-1} \tag{19A}$$

where $K_{fgh} = a_{gh} b_{hf}$.

Similarly, inversion of eqn. 17A gives

$$\bar{J}_f = - D^{\dagger} \sum_h b_{hf} \Delta \bar{\varphi}_h \tag{20A}$$

Thus, substituting

$$\Delta \bar{\varphi}_h = \sum_g a_{gh} \Delta \bar{C}_g \tag{21A}$$

and rearranging yields

$$\bar{J}_f = - D^{\dagger} \sum_g \Delta \bar{C}_g \sum_h K_{fgh} (p + \kappa_h)^{\dagger} \tag{22A}$$

where $K_{fgh} = a_{gh} b_{hf}$, as before. Equations (19A) and (22A) are eqns. (2) and (3), respectively, of the text.

Evaluation of system constants, κ_h and K_{fgh}

Equation (9A) requires the identity,

$$\kappa_h \varphi_h \equiv - \sum_f a_{fh} \sum_g k_{gf} C_g \tag{23A}$$

Substituting eqn. (10A) for φ_h gives, after rearrangement,

$$\sum_g \kappa_h a_{gh} C_g \equiv - \sum_g \sum_f a_{fh} k_{gf} C_g \tag{24A}$$

Equating coefficients of the C_g yields

$$\kappa_h a_{gh} = - \sum_f a_{fh} k_{gf} \tag{25A}$$

By introducing the Kronecker delta, δ_{gf} , which is unity when $g = f$, and zero when $g \neq f$, eqn. (25A) can be cast into the more useful form

$$\sum_f (\kappa_h \delta_{gf} + k_{gf}) a_{fh} = 0 \tag{26A}$$

Equation (26A) represents a set of N equations (one for each g) from which the values of κ_h and the relative values of the a_{fh} can be determined. Non-trivial solutions of eqn. (16A) for the a_{fh} require the relationship expressed by the secular equation (given here in shorthand determinant notation)

$$|(\kappa_h \delta_{gf} + k_{gf})| = 0 \tag{27A}$$

which can be solved for N values of κ_h .

Because the value of a_{fh} is arbitrary for one value of f , any $N - 1$ of the N equations represented by eqn. (26A) can be used to determine the values of the remaining a_{fh} in terms of κ_h . The values of b_{hf} can be determined by solving the N equations represented by eqn. (10A) for C_f in terms of φ_h and comparing the coefficients with those of eqn. (18A).

System constants of three-component sub-system

For the three-component sub-system,



eqn. (27A) becomes

$$\begin{vmatrix} \kappa_h + k_{11} & k_{12} & k_{13} \\ k_{21} & \kappa_h + k_{22} & k_{23} \\ k_{31} & k_{32} & \kappa_h + k_{33} \end{vmatrix} = 0 \quad (29A)$$

where $k_{11} = -(k_{12} + k_{13})$, $k_{22} = -(k_{21} + k_{23})$, and $k_{33} = -(k_{31} + k_{32})$ as indicated by eqn. (4A). Evaluating this determinant gives the cubic equation

$$\kappa_h^3 + 2\sigma\kappa_h^2 + \gamma\kappa_h = 0 \quad (30A)$$

where σ and γ are defined in Table I. The three solutions of eqn. (30A) are

$$\kappa_1 = 0 \quad (31A)$$

$$\kappa_2 = \sigma + (\sigma^2 - \gamma)^{\dagger} \quad (32A)$$

$$\kappa_3 = \sigma - (\sigma^2 - \gamma)^{\dagger} \quad (33A)$$

as given in Table I.

By arbitrarily selecting a_{3h} equal to unity, eqn. (26A) can be written

$$(\kappa_h + k_{11})a_{1h} + k_{12}a_{2h} = -k_{13} \quad (34A)$$

$$k_{21}a_{1h} + (\kappa_h + k_{22})a_{2h} = -k_{23} \quad (35A)$$

$$k_{31}a_{2h} + k_{32}a_{2h} = -(\kappa_h + k_{33}) \quad (36A)$$

Solving eqns. (34A) and (36A) for a_{1h} , and then eqns. (35A) and (36A) for a_{2h} , yields

$$a_{1h} = \frac{\gamma_2 - k_{12}\kappa_h}{\gamma_2 - k_{32}\kappa_h} \quad (37A)$$

$$a_{2h} = \frac{\gamma_1 - k_{21}\kappa_h}{\gamma_1 - k_{31}\kappa_h} \quad (38A)$$

$$a_{3h} = 1 \quad (39A)$$

In matrix form the three equations represented by eqn. (10A) are,

$$\begin{bmatrix} 1 & 1 & 1 \\ a_{12} & a_{22} & 1 \\ a_{13} & a_{23} & 1 \end{bmatrix} \begin{bmatrix} C_1 \\ C_2 \\ C_3 \end{bmatrix} = \begin{bmatrix} \varphi_1 \\ \varphi_2 \\ \varphi_3 \end{bmatrix} \quad (40A)$$

where the a_{3h} and a_{f1} have been replaced by unity. (Eqns. (37A) and (38A) show that a_{fh} is unity when $\kappa_h = 0$, which, by eqn. (31A), is the case for $h = 1$.) Thus, the solution for C_1 is

$$C_1 = \frac{(a_{22} - a_{23})\varphi_1 + (a_{23} - 1)\varphi_2 + (1 - a_{22})\varphi_3}{(a_{23} - 1)(a_{12} - 1) - (a_{22} - 1)(a_{13} - 1)} \quad (41A)$$

Hence, the values of b_{hf} are

$$b_{11} = \frac{a_{22} - a_{23}}{(a_{23} - 1)(a_{12} - 1) - (a_{22} - 1)(a_{13} - 1)} \quad (42A)$$

$$b_{21} = \frac{a_{23} - 1}{(a_{23} - 1)(a_{12} - 1) - (a_{22} - 1)(a_{13} - 1)} \quad (43A)$$

$$b_{31} = \frac{1 - a_{22}}{(a_{23} - 1)(a_{12} - 1) - (a_{22} - 1)(a_{13} - 1)} \quad (44A)$$

Using eqns. (31A), (32A), (33A), (37A), (38A), (39A), (42A), (43A), and (44A), values of $K_{fgh} = a_{gh}b_{hf}$ have been computed for the various combinations of $f = 1$; $g = 1, 2, 3$; and $h = 1, 2, 3$. The results of these laborious algebraic manipulations are given in Table 1. Because of the symmetry of the sub-system only the expressions corresponding to $f = 1$ were evaluated; expressions for $f = 2$ and 3 were then readily obtained by appropriate interchange of subscripts.

This research was supported by the Advanced Research Projects Agency, Contract No. SD-100.

SUMMARY

A general treatment is given for electrochemical processes involving (pseudo-) first-order chemical reactions and semi-infinite planar diffusion. The physical implication of a derived general equation relating surface concentration and currents — which are time dependent functions — are discussed. The constants of the equation are evaluated for a generalized three-component sub-system, and the formulation of specific response functions is demonstrated for pre-kinetic, post-kinetic, both pre- and post-kinetic, and parallel-kinetic (catalytic) cases. Solutions of the equation are obtained for various specific systems and techniques, including chronopotentiometry, chronoamperometry, and a.c. chronopotentiometry. Also, a general expression for the phase angle (between current and potential) in a.c. methods involving only one pair of electroactive species is developed. Finally, the interpretation of experimental data is discussed and some methods (including the use of analog computers) which could be used to evaluate the constants of the equation for more complicated systems are mentioned.

REFERENCES

- 1 K. WEISNER, *Z. Elektrochem.*, 49 (1943) 164.
- 2 J. KOUTECKÝ AND R. BRDIČKA, *Collection Czech. Chem. Commun.*, 12 (1947) 337.
- 3 P. DELAHAY AND T. BERZINS, *J. Am. Chem. Soc.*, 75 (1953) 2486.
- 4 O. DRACKA, *Collection Czech. Chem. Commun.*, 25 (1960) 338.
- 5 P. DELAHAY, C. C. MATTAX AND T. BERZINS, *J. Am. Chem. Soc.*, 76 (1954) 5319.
- 6 P. DELAHAY AND G. L. STIEHL, *J. Am. Chem. Soc.*, 74 (1952) 3500.
- 7 Z. POSPISIL, *Collection Czech. Chem. Commun.*, 18 (1953) 337.
- 8 S. L. MILLER, *J. Am. Chem. Soc.*, 74 (1952) 4130.
- 9 J. KOUTECKÝ AND R. BRDIČKA, *Collection Czech. Chem. Commun.*, 12 (1947) 337.
- 10 D. E. SMITH, *Anal. Chem.*, 35 (1963) 602.
- 11 D. E. SMITH, *Anal. Chem.*, 35 (1963) 610.
- 12 H. L. HUNG, J. R. DELMASTRO AND D. E. SMITH, *J. Electroanal. Chem.*, 7 (1964) 1.
- 13 H. MATSUDA, *Z. Elektrochem.*, 62 (1958) 977.
- 14 M. D. WIJNEN, *Rec. Trav. Chim.*, 79 (1960) 1203.

THE CATALYTIC POLAROGRAPHIC CURRENT OF A METAL COMPLEX

II. THE NICKEL(II)-*o*-PHENYLENEDIAMINE SYSTEM

HARRY B. MARK, Jr.

Department of Chemistry, The University of Michigan, Ann Arbor, Michigan (U.S.A.)

(Received January 3rd, 1964)

INTRODUCTION

The polarographic reduction of Ni(II), in aqueous solutions containing small quantities of pyridine^{1,2} as well as other organic amines^{2,3} and in acetonitrile containing chloride ion⁴, has previously been reported to exhibit a catalytic wave before the main free-metal ion wave. This pre-wave is thought to represent the reduction of Ni(II) which is complexed with the organic amine¹ or the chloride ion⁴. Because of the great sensitivity of a catalytic polarographic wave, the Ni(II)-complex catalytic pre-wave has been used successfully for the determination of small quantities of pyridine², ethylenediamine⁵, and *o*-phenylenediamine³. Although it was postulated that the mechanism of this catalytic wave probably involved (i) the ability of the ligand to form a complex, (ii) adsorption of the ligand on the mercury surface, (iii) the ability of the ligand to act as a bridge which facilitates the electron transfer, and (iv) various competitive effects of protonation on certain of these processes^{1,2}, no conclusive experimental evidence has been previously found to substantiate such a mechanism.

An extensive investigation of the properties of the catalytic pre-wave observed when Ni(II) was reduced in the presence of *o*-phenylenediamine was undertaken in an effort to determine the details of the mechanism involved. This aromatic diamine was chosen because it gave the most well-defined pre-wave of any other substance studied^{2,3}. The $E_{\frac{1}{2}}$ of this wave is approximately 0.30 V more positive than the Ni(H₂O)₆²⁺ background wave and the catalytic enhancement of the wave is quite large². This paper describes the experimental results of this study which indicate that the pre-wave current is limited by two factors: (i) the surface concentration of adsorbed *o*-phenylenediamine, and (ii) the rate of complexation of the free Ni(II) with the adsorbed diamine.

EXPERIMENTAL

Apparatus

The dropping mercury electrode (D.M.E.) used in these experiments had a drop time of 3.10 sec at a height of 62.8 cm of mercury in 0.1 M KCl with no applied potential. Under these conditions the outflow of mercury was 2.25 mg/sec. A saturated calomel electrode (S.C.E.) was used as the reference electrode, and its electrical

contact with the sample solution in the polarograph cell was made through an agar-agar KCl bridge.

The polarograms were obtained with a Leeds and Northrup type-E Electrochemograph with no damping. The ultra violet and visible spectral data were obtained with a Beckman Model-DB recording spectrophotometer using matched 1-cm silica cells. The current-time curves during the life-time of an individual drop were measured by recording, with a Tektronix Model-502 oscilloscope, the potential drop across a small resistor, $200 \Omega \pm 0.1\%$, placed in series with the polarograph cell. A constant potential, corresponding to the potential of the peak pre-wave limiting current was applied to the series combination using the Electrochemograph as the potential source.

Reagents

The *o*-phenylenediamine was purified by recrystallization from concentrated hydrochloric acid⁶. Because of their susceptibility to air oxidation, stock solutions were prepared, just prior to taking measurements, with air-free deionized water. All other solutions were prepared with reagent-grade chemicals and deionized water.

Procedure

In order to minimize the magnitude of the air oxidation of the *o*-phenylenediamine, the sample solutions to be measured were actually prepared in the polarograph cell under a nitrogen atmosphere. The stock *o*-phenylenediamine solution was added in known volume, by means of a 5-ml microburette, to 40 ml of an air-free Ni(II)-supporting electrolyte solution, and the resulting solutions were measured. All polarograms in this paper are drawn as the maximum current attained during drop life. All solutions were de-aerated with nitrogen gas purified according to standard practice⁷. Ca^{2+} ion was added as a maximum suppressor^{2,8,9} for the $\text{Ni}(\text{H}_2\text{O})_6^{2+}$ background wave. Its presence did not affect the limiting current of the pre-wave but did increase its definition by decreasing the rate of rise of the foot of the background wave.

A few polarographic experiments were performed with a stirred sample solution. The stirring was accomplished by means of a variable speed magnetic stirrer. All experiments were performed at room temperature, $25^\circ \pm 0.5$.

RESULTS AND DISCUSSION

The variation of the characteristics of the catalytic pre-wave as a function of concentration of both *o*-phenylenediamine and Ni(II) concentration, stirring of the sample solution, height of the mercury column, and pH were studied to establish the mechanism of the process. The characteristics of the current-time curves for individual drops were also determined. The spectra of the Ni(II)-*o*-phenylenediamine system was investigated as a function of pH and *o*-phenylenediamine concentration to determine if a complex is formed in the bulk solution. The electrocapillary curves were measured as a function of *o*-phenylenediamine concentration to determine if this species is absorbed on the electrode surface.

Effects of Ni(II) and *o*-phenylenediamine concentration

The effect of *o*-phenylenediamine concentration over a range $0-10^{-3} M$ on the

polarograms of $5 \times 10^{-4} M$ $\text{Ni}(\text{Ac})_2$, $1 \times 10^{-3} M$ $\text{Ca}(\text{Ac})_2$ and $1.00 M$ KAc solutions are shown in Fig. 1. The pH of the solutions was 6.8 ± 0.1 . Note that the pre-wave actually reaches a peak current value rather than a limiting plateau. This current peak occurs at about $-0.86 \text{ V vs. S.C.E.}$ This peaking of the current could be the result

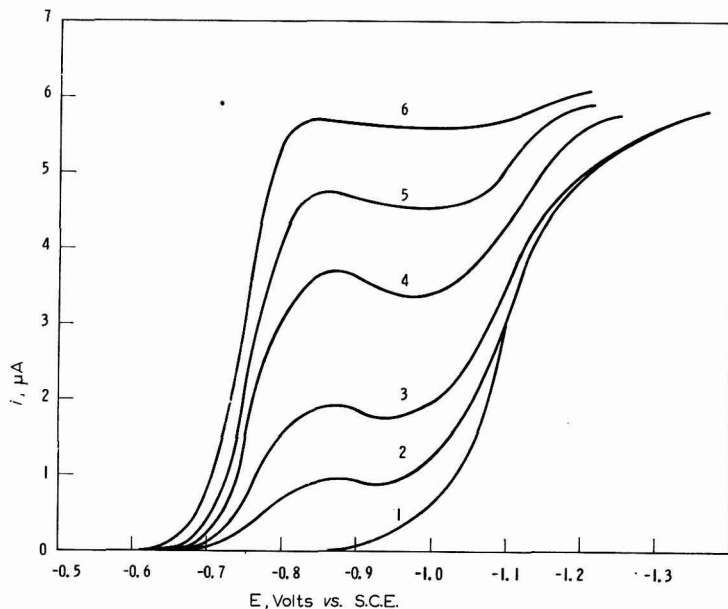


Fig. 1. Effect of concn. of *o*-phenylenediamine on the polarograms of $\text{Ni}(\text{II})$. $[\text{Ni}^{2+}] = 5 \times 10^{-4} M$, $[\text{Ca}^{2+}] = 1 \times 10^{-3} M$, $[\text{KAc}] = 1.0 M$, $\text{pH} = 6.8 \pm 0.1$. [*o*-pda]: curve 1, $0 M$; curve 2, $0.35 \times 10^{-4} M$; curve 3, $0.81 \times 10^{-4} M$; curve 4, $2.20 \times 10^{-4} M$; curve 5, $4.4 \times 10^{-4} M$; curve 6, $11.6 \times 10^{-4} M$.

of a slight polarographic maximum, or it could indicate that the electrode mechanism involves some adsorbed species which is partially desorbed at potentials more negative than $-0.8 \text{ V vs. S.C.E.}$ The catalytic hydrogen waves of some organic sulphydryl compounds^{10,11} and amines¹² exhibit peaks which have been attributed to a mechanism involving an adsorbed species¹²⁻¹⁴.

The theoretical treatment of MAĪRANOVSKIĪ^{14a} predicts that catalytic reactions involving adsorbed species will exhibit a peak current.

The height of the pre-wave, measured at the current peak, i_p , is shown in Fig. 2 as a function of the concentration of *o*-phenylenediamine for $\text{Ni}(\text{II})$ solutions of 5 different concentrations. The peak current does not vary linearly with concentration of the diamine, which is typical of catalytic waves¹⁴. Although the *o*-phenylenediamine concentration has a very large effect on i_p up to a concentration of about $4 \times 10^{-4} M$, further increase does not greatly affect i_p .

Figure 3 shows plots of i_p vs. $\text{Ni}(\text{II})$ concentration for four different constant concentrations of *o*-phenylenediamine. As expected for a catalytic wave, i_p increases with increasing $\text{Ni}(\text{II})$ ion concentration¹⁴. It is interesting to note that i_p is almost linear with $[\text{Ni}^{2+}]$ over the range of 0 to $8 \times 10^{-3} M$ $[\text{Ni}^{2+}]$. A similar plot for the $\text{Ni}(\text{II})$ -pyridine pre-wave was considerably less linear².

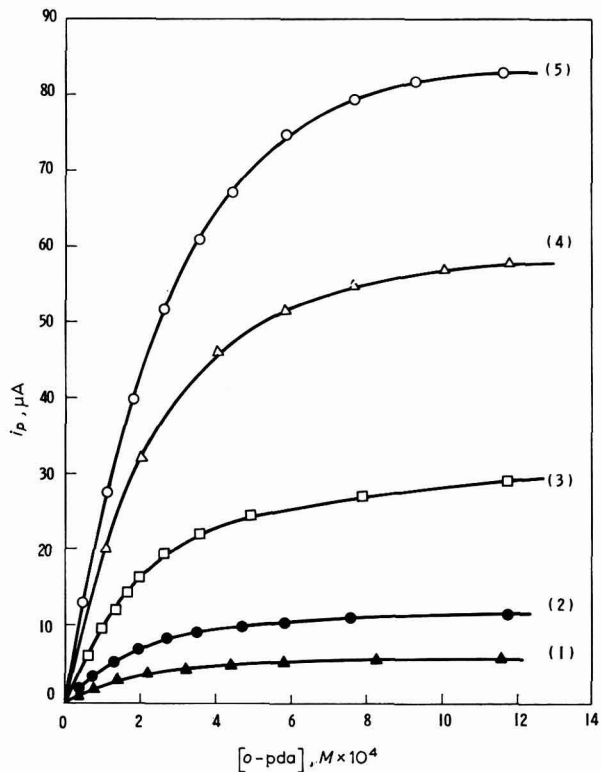


Fig. 2. Variation of peak pre-wave height, i_p , with concn. of o -phenylenediamine, $\text{pH} = 6.8 \pm 0.1$. $[\text{Ni}^{2+}]$: curve 1, $0.5 \times 10^{-3} M$; curve 2, $1.0 \times 10^{-3} M$; curve 3, $2.5 \times 10^{-3} M$; curve 4, $5.0 \times 10^{-3} M$; curve 5, $7.5 \times 10^{-3} M$.

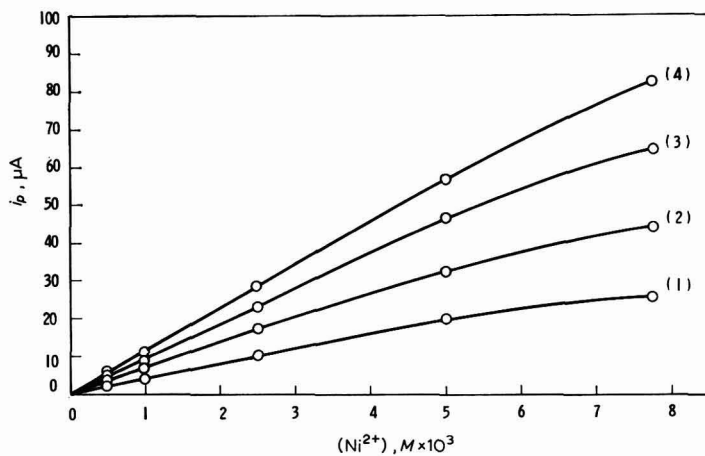


Fig. 3. Variation of peak pre-wave height, i_p , with concn. of $\text{Ni}(\text{II})$, $\text{pH} = 6.8 \pm 0.1$. $[o\text{-pda}]$: curve 1, $1.0 \times 10^{-4} M$; curve 2, $2.0 \times 10^{-4} M$; curve 3, $4.0 \times 10^{-4} M$; curve 4, $10.0 \times 10^{-4} M$.

Effect of o-phenylenediamine on the electrocapillary curve

The electrocapillary curves of the D.M.E. in 1.0 M KAc solution, and 1.0 M KAc solution which is 0.2 M in *o*-phenylenediamine, are given by curves A and B respectively of Fig. 4. The presence of *o*-phenylenediamine in the solution decreases the drop time of the D.M.E. to an appreciable extent as potentials approach the region

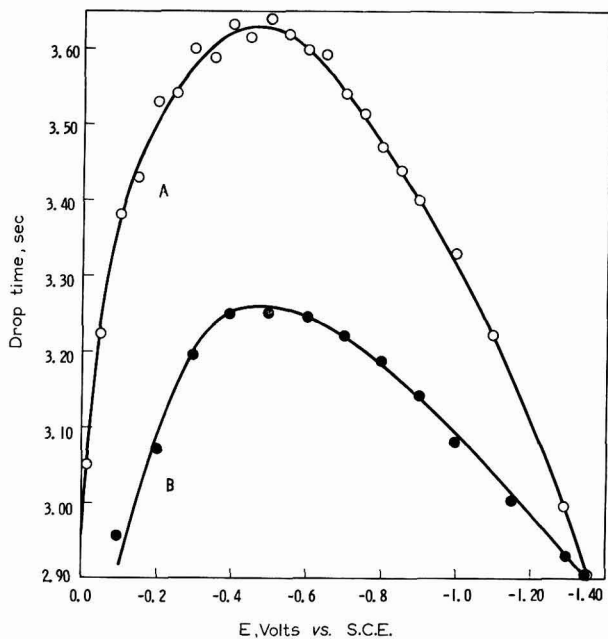


Fig. 4. Electrocapillary curve of *o*-phenylenediamine in 1.0 M KAc, pH = 6.8 ± 0.1 : curve A, without *o*-phenylenediamine; curve B, with 0.2 M *o*-phenylenediamine.

of the electrocapillary maximum and this effect decreases at potentials remote from it. This phenomenon is a typical effect resulting from the adsorption of a neutral species on the electrode surface. Such specific adsorption lowers the interfacial tension (proportional to drop time)^{18,19}. Complete desorption of *o*-phenylenediamine at potentials more negative than that of the electrocapillary maximum occurs at -1.35 V vs. S.C.E. where curves A and B coincide.

The $i-t$ curves and effect of drop time

The current-time curves of individual drops obtained at the potential of the peak current and the effect of drop time (height of the mercury column) were investigated to determine if the electrode process was diffusion- or kinetic-controlled.

Curve A of Fig. 5 shows a typical $i-t$ wave obtained for a solution which was 2.3×10^{-4} M in *o*-phenylenediamine, 7.5×10^{-3} M in Ni(Ac)₂, 1.5×10^{-3} M in Ca(Ac)₂, and 1.0 M in KAc. The slope of the log i -log t plot of the data of curve A had a value of 0.61 as shown by curve B. This value is very close to the value of 0.67 expected for a pure kinetic-controlled electrode mechanism¹⁹ ($i \approx t^{2/3}$) and well beyond the

value of 0.167 expected for a diffusion-controlled mechanism ($i \approx t^{1/6}$), as predicted by the Ilkovič equation^{21,22}.

It was found that the height of the pre-wave was totally independent of the height of the mercury column (varied from 24–85 cm) up to concentration of $1 \times 10^{-4} M$ *o*-phenylenediamine (for all $[\text{Ni}^{2+}]$ concentrations studied). In this concentration range, the height of the pre-wave was only a small fraction, $\sim 25\%$ or less, of the total Ni(II) ion limiting current. The limiting current of a pure kinetic-controlled process is generally independent of height of the mercury column²⁰. As the concentration of *o*-phenylenediamine is increased and the pre-wave becomes a more appreciable portion of the total limiting current of Ni(II) species, the wave height begins to

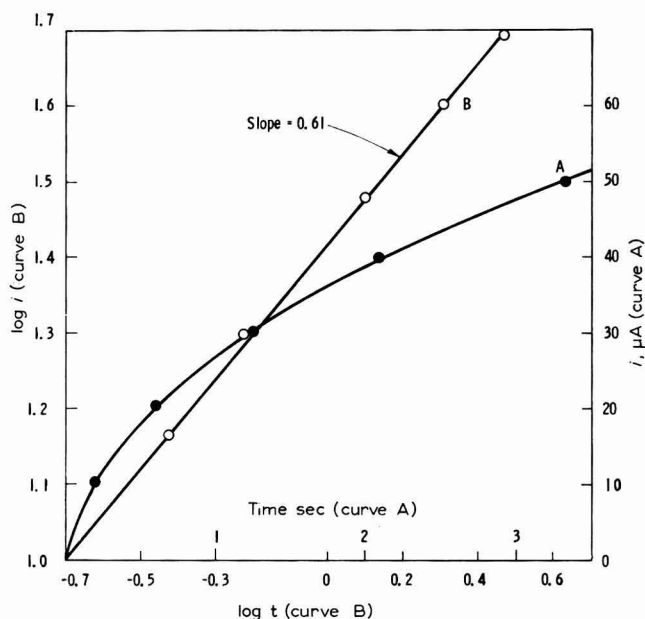


Fig. 5. Current-time curve of an individual drop. Applied potential = -0.87 V vs. S.C.E., $[\text{Ni}^{2+}] = 7.5 \times 10^{-3} M$, $[\text{Ca}^{2+}] = 15.0 \times 10^{-3} M$, $[\text{KAc}] = 1.0 M$, $[o\text{-pda}] = 2.3 \times 10^{-4} M$, pH = 6.8: curve A, $i-t$ plot; curve B, $\log i-\log t$ plot (slope = 0.61).

vary with the height of the column, indicating that the process now has an appreciable contribution from a diffusion-controlled reaction. At large *o*-phenylenediamine concentrations, i_p was found to be proportional to the square root of column height as expected for a diffusion-controlled mechanism²⁰.

Effect of stirring

Some Ni(II) solutions containing various amounts of *o*-phenylenediamine were stirred at a rate that was found to increase a Cd^{2+} diffusion plateau threefold (stirring was not vigorous enough to appreciably affect the drop time). It was found that the pre-wave current in the region, $0-0.5 \times 10^{-4} M$ *o*-phenylenediamine, was essentially independent of stirring (only a 2–5% increase in i_p was observed in this region). As the concentration of *o*-phenylenediamine increased, the percentage increase in i_p

was proportional to [*o*-phenylenediamine]. It should be noted that this stirring rate increased the $\text{Ni}(\text{H}_2\text{O})_6^{2+}$ background wave about threefold in all cases. Thus, it appears that the magnitude of the current of the electrode mechanism of the pre-wave is controlled by some process, in the *o*-phenylenediamine concentration range between 0 and $\sim 1 \times 10^{-4} M$, which does *not* involve the formation of a concentration gradient of some reactive species in the vicinity of the electrode.

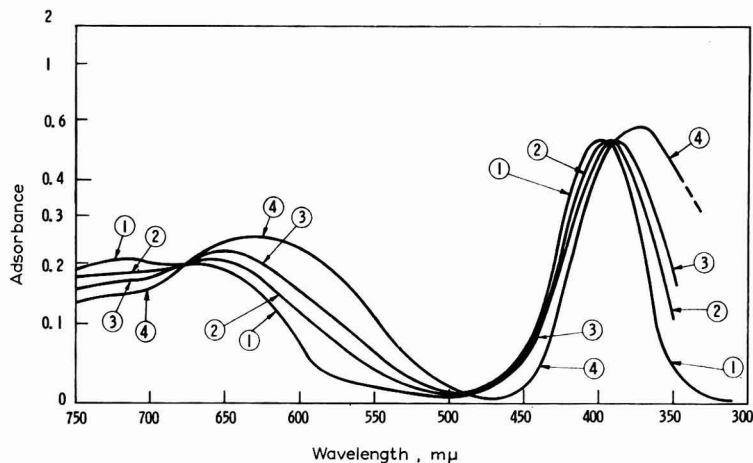


Fig. 6. Ultra-violet and visible adsorption spectra of $0.1 M \text{Ni}(\text{Ac})_2$ and $0.2 M \text{Ca}(\text{Ac})_2$ in $1.0 M \text{KAc}$ in the presence of *o*-phenylenediamine, $\text{pH} = 6.8 \pm 0.1$ [*o*-pda]: curve 1, 0; curve 2, $0.025 M$; curve 3, $0.050 M$; curve 4, $0.10 M$.

Spectral studies and pH effects

The visible and ultraviolet spectra of $0.1 M \text{Ni}(\text{Ac})_2$, $0.2 M \text{Ca}(\text{Ac})_2$ and $1.0 M \text{KAc}$ solutions ($\text{pH} = 6.8$) containing various amounts of *o*-phenylenediamine (from 0– $0.1 M$) were measured to determine if a complex of $\text{Ni}(\text{II})$ and *o*-phenylenediamine was formed. Figure 6 shows that there is a definite change in the adsorption spectra

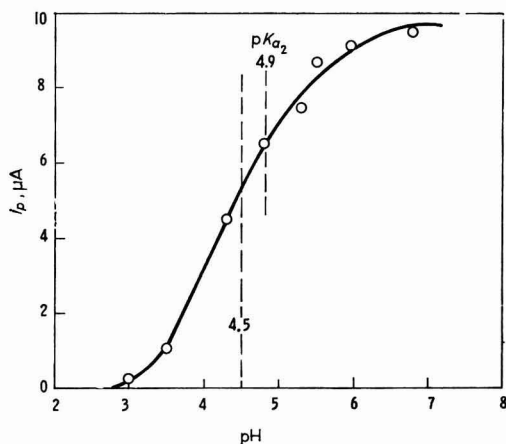
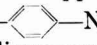


Fig. 7. Variation of peak pre-wave height, i_p , with pH. $[\text{Ni}^{2+}] = 2.5 \times 10^{-4} M$, $[\text{Ca}^{2+}] = 5.0 \times 10^{-3} M$, [*o*-pda] = $7.6 \times 10^{-5} M$.

of the Ni(II) ion as the concentration of *o*-phenylenediamine increases, which indicates that a complex does form under these conditions. A similar change in the spectrum would be expected if a small amount ($\sim 1\%$) of a tetrahedral Ni(II) complex was formed in the solution^{23,24}. The molar extinction coefficient of a tetrahedral complex would be expected to be of the order of 100 times that of the octahedral Ni(H₂O)₆²⁺ complex²⁴. A detailed study of this complex formation was not possible under the conditions of this investigation, because a precipitate was observed to form at ratios of [*o*-phenylenediamine]: [Ni(II)] greater than 2:1.

If the assumption that only a small fraction of the Ni(II) forms a tetrahedral complex even when the ratio of [Ni]:[*o*-phenylenediamine] is 1:1 is true, the stability constant of this complex must be quite small. Evidence to support this conclusion was obtained by studying the effect of pH on both i_p and the adsorption spectrum of the Ni(II)-*o*-phenylenediamine system.

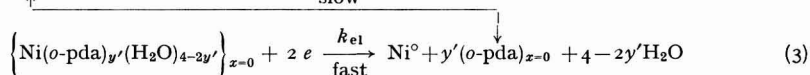
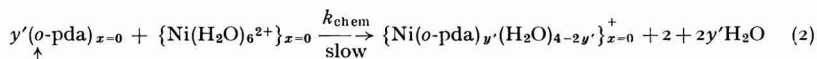
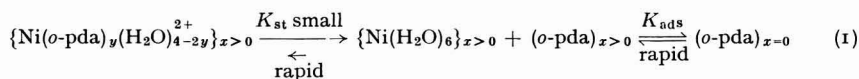
The pH of solutions containing $2.5 \times 10^{-3} M$ Ni(Ac)₂, $5.0 \times 10^{-3} M$ Ca(Ac)₂ and $7.6 \times 10^{-5} M$ *o*-phenylenediamine was varied from 6.80 to 3.00 by varying the ratio of potassium acetate to acetic acid in the supporting electrolyte. The total acetate concentration was kept constant at 1.0 *M* in all solutions. The results are shown in Fig. 7. It appears likely that the mono-protonate form of *o*-phenylenediamine, H₃N⁺--NH₂, does not take part in the catalytic mechanism, because the pre-wave disappears as the pH becomes less than the pK_{a_2} of the mono-protonated species ($pK_{a_2} = 4.9^{6,25,26}$). This suggests that a complex must be involved in some step in the catalytic process. The fact that the mid-point of the i_p -pH curve of Fig. 7 occurs at pH 4.5 rather than pH 4.9 also suggests that a weak complex is involved in the mechanism.

Qualitatively, it was also observed that the spectra of 0.1 *M* Ni(Ac)₂ and 0.1 *M* *o*-phenylenediamine solutions shifted from that corresponding to curve 4 of Fig. 6 to spectra more closely resembling curve 1 (Ni(II) only at pH = 6.8) as the pH was varied from 6.8 to 3.0 (ratio, acetic acid: potassium acetate concentration, varied; total acetate ion = 1.0 *M*). This supports the electrochemical inference that the tetrahedral complex is not very stable and is easily dissociated by lowering the pH.

CONCLUSIONS

The results of the investigation of the $i-t$ curves of an individual drop and the effect of height of the mercury column on i_p under conditions where the pre-wave is small compared to the Ni(H₂O)₆²⁺ background wave, clearly indicate that the mechanism of the catalytic wave involves a chemical reaction which precedes the electron transfer step. The rate of this reaction controls the magnitude of the catalytic wave. The lack of any effect of stirring of the solution indicates also that the limiting process does *not* involve any reaction which results in depletion of the concentration of a species (resulting in concentration gradient) in the vicinity of the electrode. The electrocapillary measurements show definite adsorption of *o*-phenylenediamine and suggest that the limiting current is also a function of the surface coverage of *o*-phenylenediamine. These properties of the pre-wave (observed when pre-wave \ll Ni(H₂O)₆²⁺ wave) suggest that the mechanism involves a very rapid adsorption equilibrium of *o*-phenylenediamine which controls the effective (or reactive) surface area of the electrode. If the equilibrium between the bulk concentration of *o*-phenylenediamine and the surface concentration excess were sufficiently rapid, stirring

of the solution would have no appreciable effect on the surface excess Γ . This evidence also implies that the adsorbed *o*-phenylenediamine reacts with $\text{Ni}(\text{H}_2\text{O})_6^{2+}$ to form a complex at the surface prior to electron transfer. This complexation reaction is probably relatively slow as the limiting current is kinetic-controlled. Stirring has no appreciable effect on the rate of complexation as, under these conditions, there is a large excess of $\text{Ni}(\text{H}_2\text{O})_6^{2+}$ ions available at the electrode surface. Stirring effects on the pre-wave would only become appreciable under conditions where the pre-wave is an appreciable portion of the total Ni(II) limiting wave. The concentration of $\text{Ni}(\text{H}_2\text{O})_6^{2+}$ at the surface, under these conditions, has undergone considerable depletion. It should be noted that the lack of stirring effects also suggest that the stability constant of the Ni(II)-*o*-phenylenediamine complex in the bulk of the solution must be very small, as was postulated from the spectral data. The reaction mechanism of the catalytic wave can probably be represented by the following sequence (*o*-pda refers to *o*-phenylenediamine):



where the subscripted x represents the linear distance from the electrode surface, K_{st} the effective stability constant of the Ni(II)-*o*-pda complex in the bulk of solution, K_{ads} the *o*-pda adsorption equilibrium constant, and k_{chem} and k_{el} the rate constants of reactions (2) and (3) respectively. Reaction (1) represents the rapid competitive equilibrium that is stabilized between the Ni(II) complex and the *o*-phenylenediamine in the bulk of the solution (shifted far toward free ligand) and that between the bulk and adsorbed *o*-phenylenediamine. As experimental evidence indicates that the adsorption equilibrium is rapidly established, *o*-phenylenediamine is probably a weakly adsorbed species^{16,18,27}. The cyclic regeneration of the *adsorbed* ligand in the sequence of reactions (2) and (3) accounts for the catalytic enhancement; the rate must be finite in order that a limiting current is attained.

If it is assumed that the layer of adsorbed *o*-phenylenediamine is a mono-layer, the adsorption of the system can be described by a *Langmuir isotherm*¹⁸.

$$\Gamma = \frac{C\Gamma_m}{a + C} \quad (4)$$

where Γ_m is the maximum surface excess concentration of *o*-phenylenediamine that can be attained, C the bulk concentration of *o*-phenylenediamine, and a a constant for the particular adsorbate. Also, if the assumption that the active surface area of the electrode is actually that covered with adsorbed *o*-phenylenediamine, is correct, the limiting current, i_p , of the pre-wave should be proportional to the surface

coverage, and a plot of C/i_p vs. C should be linear²⁸. Such a plot was found to be linear, as shown in Fig. 8.

Although this study has indicated the sequence of reactions that are probably involved in the mechanism of the catalytic pre-wave, it has not provided any conclusive evidence as to the exact nature of the Ni(II)-*o*-phenylenediamine complex involved. Nor does it explain why this complex is reduced at potentials considerably more positive than the hexaquo complex. Such behavior is difficult to understand as the effective stability constant of the Ni(II)-*o*-phenylenediamine complex must be slightly larger than that of the Ni(H₂O)₆²⁺ complex under the conditions used. The fact that the spectrum of the Ni(II)-*o*-phenylenediamine system (Fig. 6) hints that a tetrahedral Ni(II) complex might be forming, leads to the speculation that

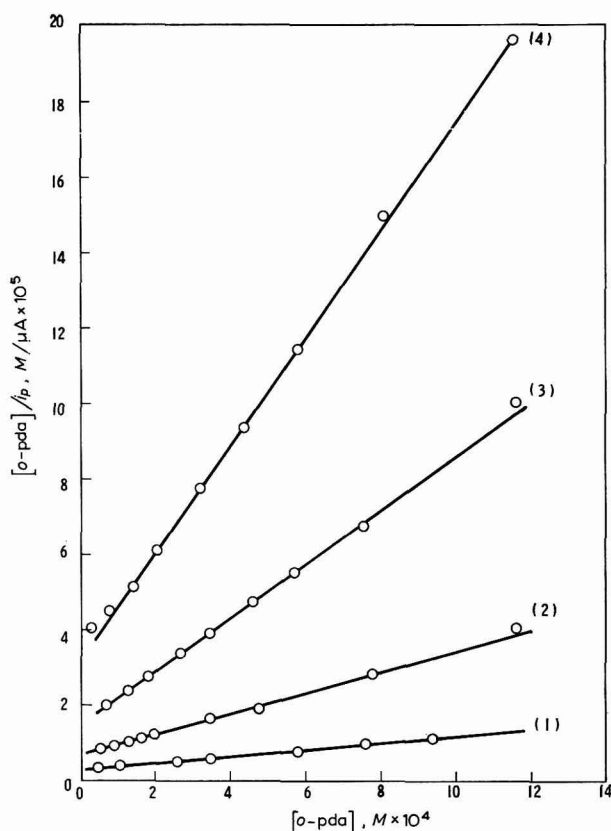


Fig. 8. Langmuir adsorption isotherm plots. [Ni²⁺]: curve 1, $7.5 \times 10^{-3} M$; curve 2, $2.5 \times 10^{-3} M$; curve 3, $1.0 \times 10^{-3} M$; curve 4, $0.5 \times 10^{-3} M$.

Ni(II) in a tetrahedral configuration might be more easily reduced than in the octahedral configuration. Simply, the orbital configuration of the tetrahedral complex might be more closely analogous to that of the activated reduction intermediate (or reduction product) than that of the octahedral complex, which would lower the

activation energy of the reaction. ANSON²⁹ has proposed a similar explanation of the effect of Br⁻ ions which facilitate the electro-oxidation of Co(II) complexes. He suggested that the presence of Br⁻ perturbed the ligand field of CoY complexes near the electrode. The fact that Cl⁻ ions also shift the Ni(II) reduction potential to more positive values in aqueous solution³⁰⁻³³ also supports this idea. There is some evidence^{33,34} that the NiCl₄²⁻ ion is the electroactive species (in their study of the Ni(II)-Cl⁻ system in acetonitrile; NELSON AND IWAMOTO⁴ suggested that actually four complexes are reduced at more positive potentials: NiCl⁺, NiCl₂, NiCl₃⁻, and NiCl₃²⁻). In this reaction, it is, therefore, interesting that GRUEN AND MCBETH³⁵ have prepared NiCl₄²⁻ in a fused NiCl₂-LiCl system and have shown that this complex is tetrahedral^{24,35}. Further study of the tetrahedral Ni(II) complexes is in progress.

ACKNOWLEDGEMENT

Acknowledgement is made to the donors of the Petroleum Research Fund, administered by the American Chemical Society, for partial support of this research.

SUMMARY

The catalytic current observed as a pre-wave when Ni(II) is reduced polarographically in the presence of small quantities of *o*-phenylenediamine is studied as a function of Ni(II) ion and *o*-phenylenediamine concentration. The effect of pH, stirring, and mercury height on the pre-wave are described. The *i-t* curves of an individual drop and the effect of *o*-phenylenediamine concentration on the electrocapillary curve are discussed. On the basis of the experimental evidence, a mechanism which involves a rapid adsorption equilibrium between bulk and adsorbed *o*-phenylenediamine and a complexation reaction of Ni(II) with the adsorbed diamine is proposed. The complexation reaction is thought to be the rate-determining step. A possible explanation as to why the adsorbed complex is more easily reduced than Ni(H₂O)₆²⁺ is proposed.

REFERENCES

- 1 H. B. MARK, JR. AND C. N. REILLEY, *J. Electroanal. Chem.*, 4 (1962) 189.
- 2 H. B. MARK, JR. AND C. N. REILLEY, *Anal. Chem.*, 35 (1963) 195.
- 3 H. B. MARK, JR., *Anal. Chem.*, in press.
- 4 I. V. NELSON AND R. T. IWAMOTO, *J. Electroanal. Chem.*, 6 (1963) 234.
- 5 H. B. MARK, JR. AND C. N. REILLEY, Combined Meeting of the South-east and South-west Sections, ACS, New Orleans, La., December, 1961.
- 6 H. V. LEE AND R. N. ADAMS, *Anal. Chem.*, 34 (1962) 1587.
- 7 L. MEITES, *Polarographic Techniques*, Interscience Publishers, Inc., New York, 1955, pp. 32-34.
- 8 N. V. EMELIANOVA AND J. HEYROVSKÝ, *Trans. Faraday Soc.*, 24 (1928) 257.
- 9 D. KYRIACOU, *Anal. Chem.*, 32 (1960) 1893.
- 10 R. BRDIČKA, *Collection Czech. Chem. Commun.*, 8 (1936) 366.
- 11 I. M. KOLTHOFF AND J. J. LINGANE, *Polarography*, Vol. 2, Interscience Publishers, Inc., New York, 2nd ed., 1952, Chapter 46.
- 12 H. B. MARK, JR. AND H. G. SCHWARTZ, JR., *J. Electroanal. Chem.*, 6 (1963) 443.
- 13 R. BRDIČKA, *Collection Czech. Chem. Commun.*, 5 (1933) 148; W. BREZINA, *Advan. Polarog. Intern. Congr.*, 2nd ed. Cambridge, England, 3 (1959) 933, published 1960.
- 14 L. MEITES, *Polarographic Techniques*, Interscience Publishers, Inc., New York, 1955, pp. 78-82.
- 14a S. G. MAĪRANOVSKIĪ, *J. Electroanal. Chem.*, 6 (1963) 77; C.I.T.C.E. Meeting, Moscow, 1963.
- 15 M. GOUY, *Ann. Chim. Phys.*, 8 (1906) 291.
- 16 R. PARSONS, *Advances in Electrochemistry and Electrochemical Engineering*, Vol. 1, edited by P. DELAHAY, Interscience Publishers, Inc., New York, 1961, Chapter I.

- 17 B. BREITER AND P. DELAHAY, *J. Am. Chem. Soc.*, 81 (1959) 2938
- 18 C. N. REILLEY AND W. STUMM, *Progress in Polarography*, Vol. 1, edited by P. ZUMAN AND I. M. KOLTHOFF, Interscience Publishers, Inc., London, 1962, Chapter V.
- 19 J. A. V. BUTLER, *Electrical Phenomena at Interfaces*, Methuen, London, 1951.
- 20 I. M. KOLTHOFF AND J. J. LINGANE, *Polarography*, Vol. 1, Interscience Publishers, Inc., New York, 2nd ed., 1952, Chapter XV.
- 21 D. ILKOVIČ, *Collection Czech. Chem. Commun.*, 6 (1934) 498.
- 22 P. DELAHAY, *New Instrumental Methods in Electrochemistry*, Interscience Publishers, Inc., New York, 1954, pp. 63-66.
- 23 T. M. DUNN, private communication, 1963.
- 24 W. MANCH AND W. C. FERNELIUS, *J. Chem. Educ.*, 38 (1961) 192.
- 25 R. E. PARKER AND R. N. ADAMS, *Anal. Chem.*, 28 (1956) 828.
- 26 J. M. VANDENBELT, C. HENRICH AND S. G. VANDEN BERG, *Anal. Chem.*, 26 (1954) 726.
- 27 R. W. SCHMID AND C. N. REILLEY, *J. Am. Chem. Soc.*, 80 (1956) 2087.
- 28 S. GLASSTONE, *Textbook of Physical Chemistry*, Van Nostrand Co., Inc., New York, 2nd ed., 1946, pp. 1198-1200.
- 29 F. C. ANSON, *J. Electrochem. Soc.*, 110 (1963) 436.
- 30 M. PAVLÍK, *Collection Czech. Chem. Commun.*, 3 (1931) 223.
- 31 N. YA. KHOPIN, *Zh. Analit. Chem.*, 2 (1947) 55.
- 32 G. F. REYNOLDS, H. I. SHALGOSKY AND T. J. WEBER, *Anal. Chim. Acta*, 8 (1953) 567.
- 33 A. A. VLČEK, *Z. Elektrochem.*, 61 (1957) 1014.
- 34 N. TANAKA, R. TAMAMUSHI AND M. KODAMA, *Bull. Chem. Soc., Japan*, 33 (1960) 14.
- 35 D. M. GRUEN AND R. L. MCBETH, *J. Phys. Chem.*, 63 (1959) 393.

J. Electroanal. Chem., 7 (1964) 276-287

EFFECT OF DILUTE CHLORIDE ION ON PLATINUM ELECTRODES

JASPAL S. MAYELL AND STANLEY H. LANGER

*Central Research Division, American Cyanamid Company,
Stamford, Connecticut (U.S.A.)*

(Received December 21st, 1963)

The importance of oxide films on platinum electrodes is presently recognized although not yet completely understood. MÜLLER¹ first reported additional complications in the behavior of platinum electrodes due to the presence of halide ions. This has been the subject of many subsequent investigations. GLASSTONE AND HICKLING² reviewed the literature on halide ion effects with platinum electrodes in 1934 and investigated additional phenomena associated with variations in current density at these electrodes. More recently, LLOPIS AND VÁZQUEZ³, LLOPIS AND SANCHO⁴, and PETERS AND LINGANE⁵ have presented excellent reviews on discharge of halide ions at platinum electrodes in connection with their own work on halide ion interaction with the electrodes. Furthermore, ANSON AND LINGANE⁶ and BREITER AND WEININGER⁷ have discussed and studied the dissolution of platinum surface oxides in acidic chloride solutions.

The present work was undertaken to investigate the effect of the presence of dilute chloride ion on surface-film formation in sulfuric acid and to compare results with our previous study of platinum surface oxide formation⁸. The presence of halide ions can complicate electrochemical procedures and reactions, (*e.g.*, HARRAR's study of controlled potential coulometric analysis of H₂O₂)⁹ and it seems that additional quantitative coulometric data would be of value in interpreting and anticipating the effect of halide ion on working platinum electrodes. We have included molded platinum-black electrodes in our study because they serve as a reasonably stable model for conventional platinized platinum electrodes and because of the growth of their importance in fuel cell¹⁰ and other applications¹¹. The literature reviews in references 2-8 may be considered to be introductory to the work described here.

EXPERIMENTAL

Almost all of the equipment used was that described previously⁸. Experiments were performed at $25.00^\circ \pm 0.05^\circ$ in a water bath. A conventional H-type electrolysis cell was used. The cathode and anode compartments were separated by a sintered-glass disc 3 cm in diameter. The auxiliary platinum sheet electrode was 4 cm². The isolating hydrogen reference electrode arrangement is shown in Fig. 1.

The hydrogen reference electrode was constructed from molded polytetrafluoroethylene-platinum black on platinum screen⁸. Hydrogen gas was bubbled over the

electrode in a solution of aqueous $2\text{ N H}_2\text{SO}_4$ which was isolated from the main body of the solution by a Vycor tube and bulb (#7900 and #7930, Corning Glass Works, Corning, New York). Nitrogen was bubbled continuously in both compartments (Fig. 1) through sintered-glass discs, in order to remove any hydrogen leaking

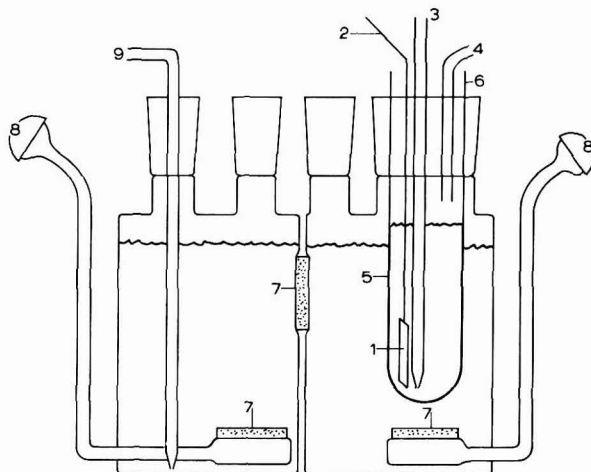


Fig. 1. Hydrogen reference electrode assembly: 1, molded platinum black electrode; 2, platinum wire; 3, hydrogen inlet; 4, hydrogen outlet; 5, Vycor No. 7930; 6, Vycor No. 7900; 7, sintered-glass discs; 8, nitrogen inlets; 9, capillary bridge to electrolysis cell.

through the Vycor tube or migrating through the sintered-glass filter, or any gases entering from the working compartment of the electrolysis cell through the capillary.

The electrode surface was observed with the aid of a mirror⁸.

The preparations of smooth shielded platinum¹² and molded platinum-black electrodes have been described⁸. For the molded platinum-black electrode, a shielded polychlorotrifluoroethylene electrode holder⁸ was used which permitted easy interchange of electrodes having reproducible geometrical area exposed to the solution. The shielded electrodes have the advantage of insuring uniform electric fields.

Reagents were all of analytical grade. Platinum was obtained from Engelhard Industries.

PROCEDURE

The electrodes studied were oxidized to pre-determined potentials at constant current in the presence of various concentrations of chloride ions in $2\text{ N H}_2\text{SO}_4$. The oxidized electrode was kept at open circuit voltage for 3 min and then reduced at constant current.

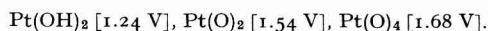
The solutions were de-aerated with nitrogen to remove oxygen and a nitrogen atmosphere was maintained while performing oxidation and reduction.

During reduction, the potential of the oxidized electrode was recorded with respect to time as is done in chronopotentiometry. Any oxygen or chlorine, if evolved during oxidation, was removed and the solution de-aerated with nitrogen during the time

of open circuit voltage (before reduction). The transition time, τ , was taken at a potential of 0.40 V. An average of at least two readings as reported for the transition time. All potentials reported are referred to a normal hydrogen electrode.

RESULTS AND DISCUSSION

In our earlier study of the formation of surface oxides on smooth platinum in 2 *N* sulphuric acid⁸, we presented evidence for, and postulated the existence of the following surface oxides at the indicated approximate potentials:



Finally, at potentials greater than 1.90 V, the number of oxygen atoms per platinum atom decreased to one to form a *tight* PtO structure with unusual properties.

Effect of low concentration (up to 10^{-3} M) of Cl^- on smooth platinum

The electrode was oxidized at the lowest practical constant current to set potentials at low concentrations of chloride ion. Oxidation current varied but was of the order of $33 \mu\text{A}/\text{cm}^2$ up to 1.6 V and as high as $28 \text{ mA}/\text{cm}^2$ to reach potentials of 2.6 V. The electrode was reduced by the standard procedure and a plot of $\log \mu\text{C}$ for reduction *vs.* oxidation potential is shown in Fig. 2. No major change in surface oxide formation up to concentrations of 10^{-3} M HCl is indicated from our observations. There is, however, a small decrease in the number of coulombs required for reduction, up to an oxidation potential of about 1.44 V which probably results from incomplete surface oxide formation due to coverage by chloride ion¹³. Above 1.44 V, where oxidation of

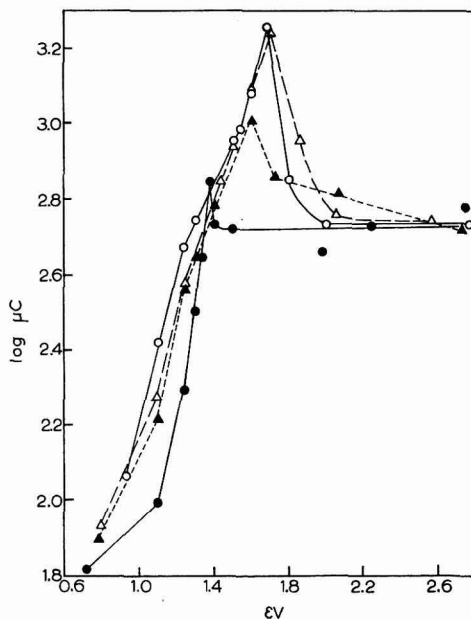


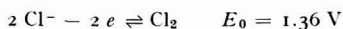
Fig. 2. Plot of $\log \mu\text{C}$ required to reduce the smooth shielded platinum electrode *vs.* the potential to which the electrode was oxidized at constant current in 2 *N* H_2SO_4 containing various concentrations of HCl: \circ , 0.0 *M* HCl; \triangle , 10^{-3} *M* HCl; \blacktriangle , 10^{-2} *M* HCl; \bullet , 10^{-1} *M* HCl.

water occurs, the number of coulombs necessary for reduction is equal to that necessary for reduction after oxidation in pure 2 *N* H₂SO₄. This would indicate that chloride ion in low concentrations does not block the platinum surface at higher potentials.

LLOPIS AND SANCHO⁴ have also noted an oxidation of the platinum electrode during anodic charging at low concentration of Cl⁻ (10⁻² *M* NaCl in 1 *N* H₂SO₄).

Effect of dilute concentration (up to 10⁻¹ M) of Cl⁻ on smooth platinum

Definite changes in surface oxide formation are observed as the concentration of HCl exceeds 10⁻² *M*. The oxidation potential at which the highest number of coulombs for reduction is observed, shifts from 1.68 V (for pure 2 *N* H₂SO₄ and 10⁻³ *M* HCl), to 1.60 V and 1.38 V when the concentration of HCl is 10⁻² *M* and 10⁻¹ *M*, respectively. The trend, under these conditions, is toward



The maximum number of millicoulombs for reduction on smooth platinum is 1.85, corresponding to the formation of Pt(O)₄ in pure 2 *N* H₂SO₄ or 10⁻³ *M* HCl in 2 *N* H₂SO₄. A decrease in the maximum number of millicoulombs to 1.02 (corresponding to the formation of Pt(O)₂) and 0.71 (corresponding to the formation of an oxide between Pt(OH)₂ and Pt(O)₂) was observed in 10⁻² *M* HCl and 10⁻¹ *M* HCl, in 2 *N* H₂SO₄, respectively. This shows that oxygen is no longer held on the Pt(O)₂ surface at a concentration of HCl of 10⁻² *M*, and at a concentration of 10⁻¹ *M*, even the formation of Pt(O)₂ is not complete. BREITER AND WEININGER⁷ oxidized under somewhat different conditions in 1 *N* H₂SO₄ to 1.6 V and then transferred to a 0.2 *N* HCl solution in 0.1 *M* NaCl and found 0.65 mC/cm² to be necessary for cathodic charging in the latter solution. While we have reported evidence for higher (more oxygen) surface oxides in 2 *N* H₂SO₄, a surface oxide, formed at about 1.38 V, corresponding to about 0.7 mC/cm² (our results) would seem to be the highest quasi-stable (of the order of 10 min⁷) surface oxide in the presence of 0.1 *N* HCl.

Inhibition of oxygen adsorption, at platinum electrodes, in the presence of Cl⁻ (4 · 10⁻¹ *M*), has been observed by ERSHLER¹⁴, for alternating current charging curves (1/100th of a sec). HICKLING¹⁵ found a similar effect with 10⁻¹ *M* Cl⁻ in 1 *N* H₂SO₄, and a fast-rise anodic sweep. Anode potential rises sharply to that of chlorine evolution though this potential is higher than that ordinarily encountered for commencement of adsorption of oxygen on the platinum surface.

The change in shape of the curves of Fig. 2 on changing from the very low chloride concentrations through 0.01 *M* HCl (see curve 3) is commensurate with less oxygen being attached to the electrode. At 0.1 *M* HCl concentration, it seems unlikely that the surface species responsible for the two-electron change above 1.4 V in cathodic reduction^{6,8} is the tight relatively unreactive PtO that has been observed before. Probably, at oxidation potentials a little above the chloride discharge potential, the major species is a surface chloride⁵ or incipient chloride especially since oxygen is not readily sorbed on the platinum surface at >0.1 *M* chloride concentration.

Effect of current density

MÜLLER¹ observed that current density, as well as chloride ion concentration, determine the potential when chloride ion is oxidized at a smooth platinum electrode. Later, GLASSTONE AND HICKLING² also reviewed studies in this connection and pro-

posed that hydrogen peroxide decomposition was responsible for a break at a potential of about 1.95 V, well above the reversible discharge potential of chloride ion. The situation and its practical importance is best illustrated by reference to chronopotentiometric curves 1, 2 and 3 of Fig. 3. It is seen that a low current density,

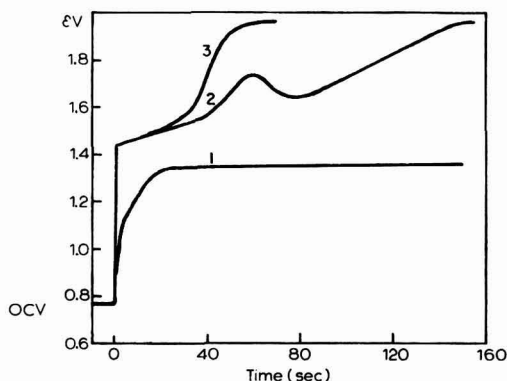


Fig. 3. Plot of potential *vs.* time at the smooth shielded platinum anode when 0.1 *M* HCl was oxidized in 2 *N* H₂SO₄ and constant current density was varied: 1, 33 μA/cm²; 2, 3.48 mA/cm²; 3, 3.99 mA/cm².

33 μA/cm², the potential at the electrode builds up slowly and levels at the chloride ion discharge potential. At a higher current density, 3.99 mA/cm², the potential rises to well over the reversible chloride discharge potential and gives an irreversible chronopotentiometric curve which we plan to discuss in the future. At an intermediate current density, a somewhat more complicated curve is observed, curve 2. The three curves may be interpreted as follows, as a result of our discussion here and elsewhere⁸. In curve 1, a surface platinum oxide layer builds up until the chloride-discharge potential region is reached and chloride ion is discharged reversibly¹⁶. In curve 3, the rapid change in potential results in little surface oxygen adsorption, and discharge of chloride ion at the platinum surface does not take place reversibly. However, it is diffusion-controlled, and one observes an irreversible chronopotentiometric wave¹⁶. Curve 2 is probably complicated by the intermediate formation of mixed oxide-chloride film⁵ in the range of 1.7 V.

It is to be noted that HICKLING¹⁵ did not observe the irreversible chronopotentiometric wave with a fast-rise relatively high current pulse, 10 mA/cm², but a tendency to discharge at the reversible chloride ion potential. However, he also heated his electrodes to redness before using and made no provision for pre-reducing any oxide which might have been present.

Open-circuit potential, (O.C.V.), on smooth platinum

The O.C.V. (of the previously reduced electrode) of 0.93 V, in aqueous 2 *N* H₂SO₄, decreased as the concentration of chloride ion increased after a complete series of oxidations and reductions had been performed. A value of 0.72 V was observed at

0.1 *N* HCl concentration. The number of microcoulombs for reduction from O.C.V. (attained after standing 5 min) decreased from 115.4 in 2 *N* H₂SO₄ to 66.0 when the concentration of HCl was increased to 10⁻¹ *M*.

The decrease of O.C.V. may show the possible formation of platinum chlorides such as^{4,5}



However, the decrease in the number of coulombs for reduction indicates that the platinum chlorides are not formed to any great extent at O.C.V. as compared to Pt(OH)₂. Since Cl⁻ is adsorbed on the platinum surface, the decrease of coulombs for reduction at higher Cl⁻ concentrations appears to be due to blocking of potential oxidation sites.

Effect of chloride ion on molded platinum-black electrodes

The procedure was essentially the same as that used for studying oxide formation on smooth platinum surfaces. Oxidation current was 21.0 mA/cm² up to 1.65 V and about 86.5 mA/cm² for higher potentials. In our earlier work⁸, we have presented

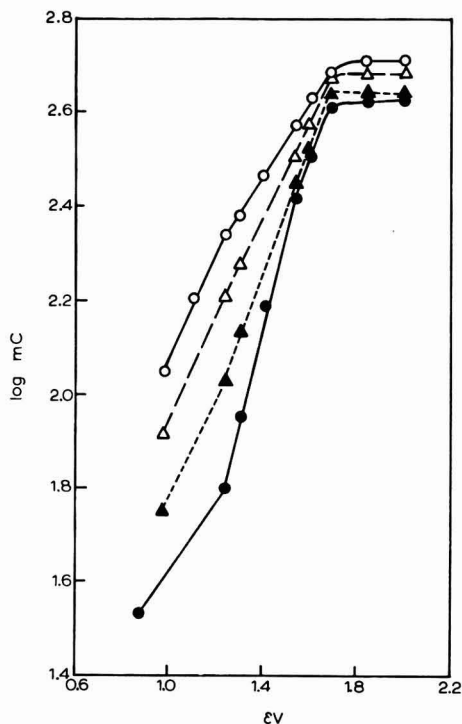
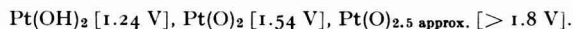


Fig. 4. Plot of log mC required to reduce a molded platinum black electrode vs. the potential to which the electrode was oxidized at constant current in 2 *N* H₂SO₄ containing various concentrations of HCl: ○, 0.0 *M* HCl; △, 10⁻³ *M* HCl; ▲, 10⁻² *M* HCl; ●, 10⁻¹ *M* HCl.

evidence for formation of the following surface oxides in 2 *N* H₂SO₄ at the indicated potentials:



For this work, the logarithm of the number of millicoulombs necessary for reduction at several chloride concentrations is plotted against oxidation potential in Fig. 4. From Fig. 4, it appears that the overall behavior with dilute concentrations of HCl up to 0.1 *M* is similar, except that oxides are formed to a lesser extent as the concentration of chloride ion is increased.

The number of coulombs used in reduction decreases much more readily at lower potentials (< 1.4 V) as the concentration of HCl is increased. Therefore, it is in electrochemical studies at these lower potentials that chloride ion influence may be greatest. The nature of the surface species formed at higher potentials in 0.1 *N* chloride solution is still open to question.

Surface area and activity of platinum-black electrodes

It has been shown⁸ that the electrochemically active surface area of platinum-black can be determined from a comparison of the number of coulombs measured for reduction of the platinum-black to that measured for smooth platinum, when both electrodes are oxidized to 1.24 V *vs.* N.H.E. A decrease in electrochemically active surface area from 4.44 m²/g in aqueous 2 *N* H₂SO₄, to 1.28 m²/g with 0.1 *N* HCl present, was observed. The results are shown in Table 1.

TABLE 1

ELECTROCHEMICALLY ACTIVE SURFACE AREA OF A MOLDED PLATINUM-BLACK ELECTRODE^a WITH DIFFERENT CONCENTRATIONS OF HCl IN 2 *N* H₂SO₄

	0.0 <i>M</i> HCl	10 ⁻⁴ <i>M</i> HCl	10 ⁻³ <i>M</i> HCl	10 ⁻² <i>M</i> HCl	10 ⁻¹ <i>M</i> HCl
Surface area m ² /g of platinum	4.44	4.24	3.28	2.10	1.28
No. of mC ^b reqd. for reduction when the electrode (0.462 cm ²) was oxidized to 1.24 V	219.0	209.2	162.0	107.0	63.1

^a Wt. of platinum-black = 30.8 mg/cm²

^b No. of mC required for reduction of smooth platinum (1 cm²) in 2 *N* H₂SO₄ when oxidized to 1.24 V was 3.47 × 10⁻¹.

Since *E*₀ for chloride ion discharge is 1.36 V, this cannot account for loss of surface activity at lower potentials. Formation of a surface compound such as Pt(Cl)₂ seems unlikely since coulombs for reduction decrease with increasing chloride ion concentration. PETERS AND LINGANE⁵ have also noted a decrease in apparent surface area for bright platinum electrodes in 1 *N* hydrochloric acid. It is clear from comparing coulometric data for oxidation and reduction at several chloride concentrations as shown in Table 2, that dissolution⁷ of surface platinum is not significantly responsible for the decrease in apparent surface area up to 0.1 *N* Cl⁻. It is evident that less surface is oxidized during the oxidation at higher chloride concentrations and there is no decrease in the number of coulombs for reduction because of dissolution of surface.

TABLE 2
EFFECT OF CHLORIDE ION ON MOLDED PLATINUM-BLACK SURFACE OXIDES

Potential to which the electrode was oxidized (V vs. N.H.E.)	mC for oxidation and reduction in 2 N H ₂ SO ₄ with:					
	0.0 M HCl		10 ⁻² M HCl		10 ⁻¹ M HCl	
	Ox.	Red.	Ox.	Red.	Ox.	Red.
O.C.V.	0	112 (0.98 V)	0	56 (0.96 V)	0	34 (0.88 V)
1.24	97	219	66	107	84	63
1.30	126	241	109	137	124	89
1.54	272	374	272	282	384	262

Current for oxidation and reduction was 9.72 mA for 0.462 cm² of geometric area of the electrode.

Adsorption of chloride ion at potential discharge sites most likely accounts for the apparent decrease in surface area on platinum-black. ANSON¹⁷ recently studied oxidation of ethylenediamine-tetraacetocobalt(II) in acidic solution in the presence of Br⁻ and found oxidation at 0.64 V (well below the oxidation potential in the absence of Br⁻) while platinum surface oxide is not formed except at a higher potential. This effect was attributed to adsorbed halide ion and a positive effect on the electron transfer reaction. In our own experience, we have found that the poisoning effect of high concentrations of chloride ion may be removed by soaking the electrode in question in water for several days, which is consistent with an adsorption effect.

It is evident from the change in open-circuit potential as indicated in Table 2 that the surface of the platinum-black electrode is changed in the presence of Cl⁻. Differences in the surface after oxidation are also evident from the curves of Fig. 5. In Fig. 5A, potential decay curves for platinum-black and bright platinum electrodes after oxidation in 2 N H₂SO₄ are seen to be more or less exponential. Decay curves are also shown in Fig. 5B for a platinum black electrode. Behavior is similar to that in Fig. 5A until oxidation above 1.4 V. The change in the decay curve is apparently due to reduction of liberated Cl₂ adsorbed on the catalytic platinum black surface.

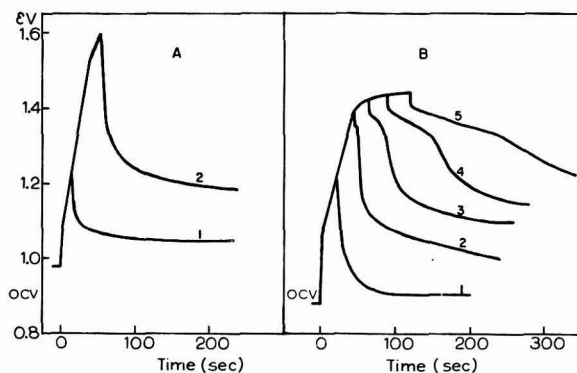


Fig. 5. Plot of potential vs. time at a molded platinum black electrode (0.462 cm²), oxidized (rising part of the curves) at 9.70 mA and then placed on open circuit (declining part of the curves) in: A, 2 N H₂SO₄; B, 2 N H₂SO₄ with 5 × 10⁻¹ M HCl.

This behavior is not observed with bright platinum. If the solution is stirred, the potential falls quickly to its stationary value due to diffusion of chlorine into the bulk of solution.

SUMMARY

Surface oxide formation in the presence of small concentrations of HCl has been studied in 2 *N* H₂SO₄ by anodic oxidation and cathodic stripping on bright platinum and molded platinum black-polytetrafluoroethylene electrodes. At the lowest concentrations, < 10⁻³ *M*, the principal effect at potentials less than 1.4 V appears to result from halide ion surface adsorption which prevents formation of the amount of surface oxide ordinarily observed. On platinum-black, the adsorption effect is considerable and results in significant decrease in electrochemically determined surface area at 1.24 V, based on surface oxide formation. As the concentration of HCl is increased to 10⁻¹ *M*, the sequence of surface oxide formation on bright platinum is changed and higher oxides (higher oxygen concentration at the surface) are not observed. Oxygen tends not to be held on the electrode surface. Chloride ion discharge potential is affected by current density and surface oxide formation on bright platinum electrodes.

REFERENCES

- 1 E. MÜLLER, *Z. Elektrochem.*, 6 (1900) 573; 8 (1902) 425.
- 2 S. GLASSTONE AND A. HICKLING, *J. Chem. Soc.*, (1934) 10.
- 3 J. LLOPIS AND M. VÁZQUEZ, *Electrochim. Acta*, 8 (1963) 163.
- 4 J. LLOPIS AND A. SANCHO, *J. Electrochem. Soc.*, 108 (1961) 720.
- 5 D. G. PETERS AND J. J. LINGANE, *J. Electroanal. Chem.*, 4 (1962) 193.
- 6 F. C. ANSON AND J. J. LINGANE, *J. Am. Chem. Soc.*, 79 (1957) 4901.
- 7 M. W. BREITER AND J. L. WEININGER, *J. Electrochem. Soc.*, 109 (1962) 1135.
- 8 J. S. MAYELL AND S. H. LANGER, *J. Electrochem. Soc.*, in press.
- 9 J. E. HARRAR, *Anal. Chem.*, 35 (1963) 893.
- 10 R. G. HALDEMAN, W. P. COLMAN, S. H. LANGER AND W. A. BARBER, *Thin Fuel Cell Electrodes*, paper presented at 145th American Chemical Society Meeting, New York, September 8-13th, 1963.
- 11 S. H. LANGER AND R. G. HALDEMAN, *Science*, 142 (1963) 225.
- 12 A. J. BARD, *Anal. Chem.*, 33 (1961) 11.
- 13 B. ERSHLER, Thesis, Moscow, 1941.
- 14 B. ERSHLER, *Discussions Faraday Soc.*, 1 (1947) 269.
- 15 A. HICKLING, *Trans. Faraday Soc.*, 41 (1945) 333.
- 16 G. A. TEDORADSE, *Zh. Fiz. Khim.*, SSSR., 33 (1959) 129.
- 17 F. C. ANSON, *J. Electrochem. Soc.*, 110 (1963) 436.

THE ANODIC DISSOLUTION AND PASSIVATION OF SMOOTH PLATINUM

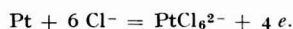
I. ANOMALOUS RESULTS FROM THE RADIOTRACER TECHNIQUE

T. DICKINSON, R. C. IRWIN* AND W. F. K. WYNNE-JONES

Physical Chemistry Department, University of Newcastle upon Tyne (England)

(Received January 29th, 1964)

A platinum anode dissolves in concentrated hydrochloric acid solutions. Experiments¹ over a limited range of conditions have shown that the amount of platinum dissolved is equivalent to that calculated from the quantity of electricity passed, assuming the process is



In the present work similar quantitative experiments were to be made over a wider range of conditions. A method for measuring the amount of platinum in solution, more sensitive than the gravimetric technique used previously, was required and a radiotracer technique was chosen.

Platinum made radioactive by neutron irradiation was used as anode material. Six radioactive isotopes are known to be formed in the irradiation. Three of these emit only γ -radiation, the others (^{197}Pt , $t_{1/2} = 20$ h; ^{199}Pt , $t_{1/2} = 31$ min; and ^{199}Au , $t_{1/2} = 3.15$ day) emit β -radiation also. The ^{199}Au is produced by the decay of ^{199}Pt . The activity of ^{197}Pt and ^{199}Au obtained was 17 mC/g and 18 mC/g respectively. The amounts of the other isotopes produced are unknown. A Geiger-Müller counter for estimating the β -activity of isotopes (γ -counting efficiency less than 1%) was available and the quantity of platinum dissolved was determined by measuring the β -activity of the resulting solutions.

The activity measurements always indicated a greater amount of platinum in solution than that calculated from the quantity of electricity passed; the amounts sometimes differed by a factor of several hundred. However a colorimetric method of analysis showed these two amounts to be equivalent² so that the results obtained using the radiotracer technique must be anomalous. The work reported in this paper is an investigation into the origin of this error, and of the methods for removing it.

EXPERIMENTAL

The anode was a 20-cm length of 0.07-cm diameter "Spectrographically Standardized" platinum wire (Johnson, Matthey and Co. Ltd.) coiled into a small spiral. It was

* Present address: *Department of Chemistry, Australian National University, Canberra, A.C.T., Australia.*

cleaned with carbon tetrachloride and alcohol, placed in a silica container, and irradiated for 1 week at a flux of 10^{12} neutrons $\text{cm}^{-2} \text{sec}^{-1}$. The electrode was then polarized in deoxygenated 3.6 M hydrochloric acid initially at 0.0 V for one min to reduce surface oxide and then at 0.85 V for 2.5 min to remove the first few layers of metal. One of a series of constant potentials was then applied. The amount of platinum dissolved at each of these potentials was calculated from the quantity of electricity passed, assuming that the metal dissolves as the tetravalent ion. Details of the electrolytic cell and the solution preparation are given elsewhere². All potentials quoted are relative to the saturated calomel electrode.

The anolyte and washings obtained after the application of each potential were made up to 15 ml and their β -activity was measured using a 20th Century Electronics Tube, Type M6. The random error of counting was about 2%. After completion of the electrochemical experiments, a known weight of the wire electrode was dissolved to prepare a standard solution with approximately the same activity as the samples. The amount of platinum in the sample solutions was determined by relating their activity to that of the standard, measured at about the same time. These measurements were normally completed within 36 h of the end of the irradiation.

In a number of instances, gold was precipitated from the standard and some sample solutions by the method of BEAMISH *et al.*³ a little auric chloride being added to the solutions to act as carrier.

Some irradiated platinum coils were heated before use. They were maintained in a nitrogen atmosphere at 950° and quenched in triple-distilled water.

The γ -ray spectra were obtained with concentrated solutions, using a single-channel pulse-amplitude analyser with the channel width at about 1 V.

RESULTS AND DISCUSSION

Representative values of the ratio of the weight of platinum determined by the activity measurements, to that calculated from the quantity of electricity passed are given for a range of potentials in column three of Table 1. In the absence of any anomaly, the value of this ratio is 1.0 ± 0.1 at all potentials².

TABLE 1

Potential (S.C.E.)	Dissolution rate of untreated Pt ($\mu\text{A cm}^{-2}$)	Ratio = $\frac{\text{wt. Pt. from activity}}{\text{wt. Pt. from coulombs}}$					
		No treatment	After Au pptn	After $2\frac{1}{2}$ h 950°	After polarising at 0.85 V for		After chemical etch
					55 min	120 min	
0.65	0.5	600(1)		13			
0.70	1.4	400(1)		2.7			1.5
0.75	4	140(2)		2.1			1.3
0.80	12	40(5)		1.3			1.08
0.85	33	20(15)		1.2	5	2.2	0.92
0.90	69	5(30)	1.1	1.2			1.04
0.925	48	3(23)	1.1	1.05			

The figures in parenthesis in the third column indicate the number of monolayers of platinum dissolved, calculated from the quantity of electricity passed.

Since the radiotracer determination was made by comparing the activity of the

sample solutions with that of a standard, the results indicate that the former solutions have a higher β -activity in relation to their platinum content than the standard solution. This could result from the presence in the platinum of a relatively small number of radioactive foreign atoms concentrated at those areas of the metal which dissolve most readily *e.g.*, grain boundaries^{4,5}. It is also possible that these atoms could be uniformly distributed through the metal but dissolved preferentially, a significant surface concentration being maintained by grain-boundary diffusion. The results require that both these mechanisms are operative. Evidence for the diffusion mechanism is provided by the γ -ray spectra (see later), but this mechanism cannot give a satisfactory quantitative explanation for the variation of the ratio with potential and it must be assumed that at less positive potentials the metal is removed predominantly from impurity-rich areas.

Gold is a likely impurity in platinum and is also produced by the decay of radioactive platinum. The ratio was close to unity when this element was precipitated from both the sample and standard solutions (see Table 1). However other impurities could be precipitated with the gold so that the origin of the error is not shown by these results. A considerable reduction in the error was also produced by heating and quenching the metal before the electrochemical experiments. This treatment should reduce the grain-boundary concentration of impurities⁴. It probably also increases the grain size and hence reduces the total rate of grain-boundary diffusion. Similarly, etching the surface by either prolonged electrolysis or boiling in a mixture of concentrated hydrochloric and nitric acids caused a decrease in the ratio. This treatment will remove the accessible impurity-rich regions and will also increase the dissolution rate (10 times after the chemical etch) so decreasing the relative rate of diffusion.

γ -ray spectroscopy was employed to determine the nature of the radioactive impurity. A spectrum obtained with a sample solution is shown in Fig. 1. The prob-

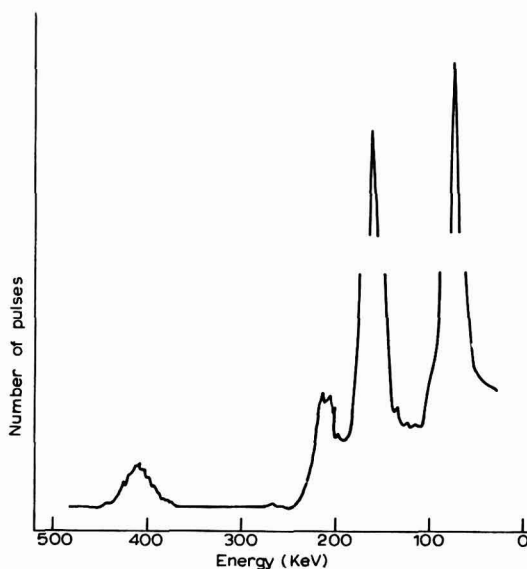


Fig. 1. γ -ray spectrum of sample solution.

able origin of the four main peaks was deduced from the energy levels at which they occur and the half-lives for their decay. Data referring to the spectra of the standard and two sample solutions are reported in Table 2; this gives the origin of the peaks and their heights (approximately proportional to their areas) with respect to the peak at 75 keV.

TABLE 2

Solution employed	Relative heights of peaks at			
	75 keV	159 keV	208 keV	411 keV
Standard	10	3.5	0.5	0
Sample at 0.70 V 4.5 h	10	8.0	1.3	0.5
Sample at 0.85 V 50 min	10	10.3	1.5	0.3
Probable origin of peaks	Pt, (Au,Hg) X-rays	¹⁹⁹ Au	¹⁹⁹ Au	¹⁹⁸ Au

The spectra from both sample solutions show a peak at 411 keV associated with ¹⁹⁸Au which is not observed with the standard solution. This isotope emits β particles (half-life, 2.7 day) and part of the observed error may be attributed to its disproportionate concentration in the sample solutions. The heights of both of the peaks corresponding to ¹⁹⁹Au (relative to the X-ray peak) are greater in the samples than in the standard solution. Since the X-ray peak is produced mainly by the platinum isotopes the sample solutions must contain more ¹⁹⁹Au in relation to their platinum content than the standard solution. This would also contribute to the error.

The ¹⁹⁸Au will be formed after neutron capture by ¹⁹⁷Au, the naturally occurring isotope of gold which must be present as an impurity in the platinum. The ¹⁹⁹Au results from the radioactive decay of ¹⁹⁹Pt. Since gold dissolves more rapidly than platinum in hydrochloric acid⁶ its preferential solution is to be expected. A non-uniform distribution of ¹⁹⁸Au is likely but not of ¹⁹⁹Au so that grain-boundary diffusion of the latter must occur.

The magnitude of the error will be determined by both the difference between the ratio of the activities of the platinum and gold isotopes in the sample and standard solutions and the efficiency with which these activities are measured. The latter is dependent on the extent of β -particle absorption by the solution, which is related to the energy of the β -radiation involved⁷. As shown in Table 3 the maximum energy of

TABLE 3

Isotope	Maximum energy of β -emission (keV)	Capture-cross-section area of parent
¹⁹⁹ Au	300	4
¹⁹⁸ Au	960	100
¹⁹⁷ Pt	650	1

β -emission from ¹⁹⁸Au is considerably higher than that from ¹⁹⁷Pt and ¹⁹⁹Au so that its activity will be counted with appreciably higher efficiency. Moreover the capture-cross section area of its parent isotope (¹⁹⁷Au) is relatively large (Table 3) so that small amounts of ¹⁹⁷Au could give rise to substantial errors in the activity measurements.

The difference in the counting efficiency for ^{197}Pt and ^{199}Au will tend to counteract the difference in their relative activities in the sample and standard solutions.

This work shows that the radio-tracer technique attempted here is likely to be accurate only if the radioisotopes are separated before the activity measurements are made or the analysis is based on the area under the characteristic peak of the γ -ray spectrum. Even the latter procedure may not be free from error, for isotopes of possible impurities give γ -rays of comparable energy to those emitted by radioactive platinum so that the corresponding peaks might not be separated from one another. In particular, about 8% of the γ -radiation of ^{199}Au is emitted at 0.05 Mev⁸, and the resultant peak in the γ -ray spectrum is likely to be incorporated in the peak due to platinum. The error from such a source might be important when the concentration of ^{199}Au in solution is comparatively large. LOSSEW *et al.*⁹ have recently reported the use of this method in platinum analysis but they did not establish its reliability.

ACKNOWLEDGEMENT

We wish to thank Mr. G. R. MARTIN, University of Durham, for assistance in recording and interpreting the γ -ray spectra, and Messrs. Albright and Wilson Ltd., for a maintenance award to R.C.I.

SUMMARY

Radioactive platinum was employed in a study of the electrochemical dissolution of smooth platinum and the amount of metal dissolving was determined by activity measurements. Correlation of the measurements of radioactivity with the coulometric measurements was found to be complicated by the presence of highly radioactive foreign atoms in the platinum. Methods of eliminating this complication are discussed.

REFERENCES

- 1 A. RIUS, J. LLOPIS AND I. M. TORDESILLAS, *Anales Real Soc. Espan. Fis. Quim. (Madrid)*, 48B (1952) 193.
- 2 T. DICKINSON, R. C. IRWIN AND W. F. K. WYNNE-JONES, to be published.
- 3 F. E. BEAMISH, J. J. RUSSELL AND J. SEATH, *Ind. Eng. Chem., Anal. Ed.*, 9 (1937) 174.
- 4 D. MCLEAN, *Grain Boundaries in Metals*, Oxford University Press, London, 1957.
- 5 U. R. EVANS, *The Corrosion and Oxidation of Metals*, Edward Arnold, London, 1960.
- 6 H. GERISCHER, *Angew. Chem.*, 70 (1958) 285.
- 7 G. B. COOK AND J. F. DUNCAN, *Modern Radiochemical Practice*, Oxford University Press, London, 1952.
- 8 D. STROMINGER, J. M. HOLLANDER AND G. T. SEABORG, *Rev. Mod. Phys.*, 30 (1958) 774.
- 9 W. W. LOSSEW, M. A. DEMBROWSKI, A. I. MOLODOW AND W. W. GORODEZKI, *Electrochim. Acta*, 8 (1963) 387.

J. Electroanal. Chem., 7 (1964) 297-301

VOLTAMMETRY OF NICKEL IN MOLTEN LITHIUM FLUORIDE-
SODIUM FLUORIDE-POTASSIUM FLUORIDE

D. L. MANNING

*Analytical Chemistry Division, Oak Ridge National Laboratory,
Oak Ridge, Tennessee (U.S.A.)*

(Received January 25th, 1964)

In this report, studies are presented on anodic stripping voltammetry and rapid scan voltammetry of nickel in molten LiF-NaF-KF (46.5-11.5-42 mole %).

Molten fluoride salt systems are of interest because of their potential use as components of reactor fuels. The possibility of determining impurities such as the corrosion products, iron, nickel, chromium and other electroactive substances, directly in the molten state by electroanalytical methods is very attractive. Previous reports^{1,2} on the voltammetry of iron in molten fluorides have demonstrated that voltammetry is a possible approach to the problem. This paper describes a further application of this electroanalytical method to the determination of nickel which is also a corrosion product associated with molten fluorides.

A controlled-potential polarograph modified to produce rapid scan rates was used to record the anodic stripping curves and the current-voltage curves. A pyrolytic graphite indicator electrode coupled with a platinum quasi-reference electrode comprised the measuring system. A third platinum electrode which was isolated in a separate porous graphite inner compartment served as the counter electrode.

EXPERIMENTAL

The eutectic LiF-NaF-KF (46.5-11.5-42 mole %) was used as the solvent electrolyte. The graphite cell, approximately 2 in. in diameter and 4½ in. long, which contained the melt was enclosed in a quartz jacket to maintain a vacuum or a controlled atmosphere. This cell assembly and the general procedure for handling the molten LiF-NaF-KF and for carrying out the electrochemical measurements have been described previously¹.

An ORNL Model Q-1988 controlled-potential polarograph modified for rapid scan voltammetry², was used to record the current-voltage curves and the anodic stripping curves. The curves were displayed on a Mosely Autograph X-Y recorder Model-3S.

An ORNL Model-2005 controlled-potential coulometric titrator³ was used for the pre-electrolysis of the melt.

The LiF-NaF-KF eutectic, as received, contained approximately 200, 50 and 5 p.p.m. of iron, chromium and nickel, respectively. The melt was pre-electrolyzed

at a controlled potential of -0.8 V *vs.* a platinum quasi-reference electrode to reduce the concentration of these impurities. The cathode was a spectrographic grade graphite rod, 3/16 in. diameter and 2 in. long, and immersed in the melt (40 ml) to a depth of $\sim 5/8$ in. The top of the graphite electrode was screw-fitted to a 1/8 in.-nickel rod to complete the electrode as described previously¹.

The melt was stirred by helium bubbling during the electrolysis period and because of this inefficient mode of stirring, an extended period of time (~ 72 h) was required to reduce the iron level to about 20 p.p.m. and the nickel to ~ 1 p.p.m. Because of the long electrolysis time (low electrolysis current) it was not possible to obtain a meaningful integration of the current-time curve due to the large contribution from the background current. Thus, for practical purposes for removing or lowering the concentration of reducible impurities, the integrator in the controlled-potential coulometric titrator was by-passed while the instrument was used for controlled-potential electrolysis.

Nickel was added to the melt in two ways. For a small amounts (0-20 p.p.m.) a pure nickel anode was oxidized electrolytically. Larger quantities of nickel were added as weighed portions of NiF_2 as follows. With a rapid flow of dry helium through the cell assembly, the nickel anode was removed and a long stem funnel quickly inserted through the 3/16 in. Swagelok fitting to within a few centimeters of the melt. The flow of helium was momentarily interrupted and the weighed NiF_2 rapidly poured through the funnel into the melt. The funnel, with helium flowing, was removed and the electrode re-inserted. The whole operation was performed as rapidly as possible to minimize any contamination of the melt from moisture in the atmosphere.

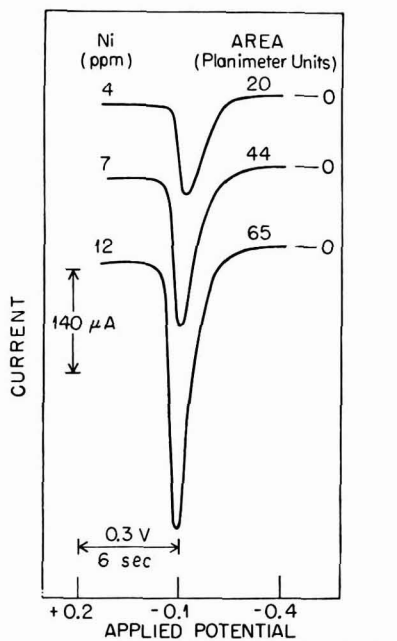
Anodic stripping curves and current-voltage curves for nickel were recorded at a pyrolytic graphite indicator electrode (1/8 in. diam.) sheathed in boron nitride. This type of indicator electrode is described elsewhere².

RESULTS AND DISCUSSION

In anodic stripping voltammetry a metal is deposited on an indicator electrode and then removed anodically under controlled conditions. By controlling such variables as electrode area, potential of the electrode during the plating cycle, plating time and the rate of voltage scan for the dissolution process, the area under the anodic stripping curve is related to the concentration of the metallic ions in the melt. This technique has previously been shown to be much more sensitive than conventional voltammetry^{2,4,5,6}.

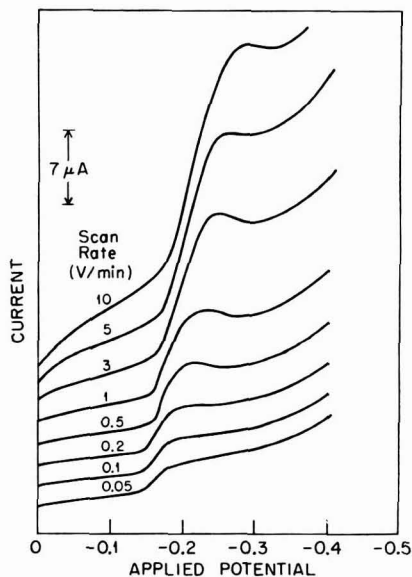
Anodic stripping curves for nickel recorded at a pyrolytic graphite electrode are shown in Fig. 1. A curve was also observed following the controlled-potential electrolysis step prior to adding any nickel back to the melt. On measuring the area under this curve, and by subsequent standard additions of nickel, it was estimated that the residual nickel in the melt following the pre-electrolysis step was of the order of 1 p.p.m. As can be seen from Fig. 1, the stripping curves are well-defined. A plating time of 4 min at a potential of -0.4 V *vs.* a platinum quasi-reference electrode was used for the anodic stripping experiments. The melt was stirred by helium bubbling during the plating and stripping process. Figure 2 shows that a potential of -0.4 V is sufficiently negative to be on the current limiting plateau of the nickel wave. After the plating cycle, the nickel was removed from the electrode by scanning

anodically at a rate of potential change of 3 V/min. The area under the stripping curves was measured with a planimeter. There is slight deviation from linearity in the plots of area (planimeter units) vs. p.p.m. nickel; nevertheless, the analytical utility of these measurements is demonstrated, especially at trace levels of nickel. The reproducibility of the area under the anodic stripping curves from consecutive runs under any one set of conditions is of the order of 5%.



(Volts vs Platinum Quasi-Reference Electrode)

Fig. 1. Anodic stripping curves for nickel from a pyrolytic graphite electrode. Plating time, 4 min; plating potential, -0.4 V; solvent, LiF-NaF-KF; Temp., 500° .



(Volts vs Platinum Quasi-Reference Electrode)

Fig. 2. Effect of scan rate on the current-voltage curves for nickel. Concn. of nickel in the melt, 23 p.p.m.

Current-voltage curves for the reduction of $\text{Ni(II)} \rightarrow \text{Ni(0)}$ at a pyrolytic graphite electrode are shown in Fig. 2. The half-wave potential occurs at approximately -0.2 V vs. the platinum quasi-reference electrode. Generally, the curves are well-defined and exhibit peaks at the faster scan rates which is in agreement with theory⁷ for a diffusion-controlled process. On reverse scans, the stripping curve passed through zero current without inflection, which suggests that the electrode reaction proceeds reversibly.

The limiting current of nickel at different concentrations and rates of voltage scan are tabulated in Table I. Plots of limiting current vs. nickel concentration reveal a linear relationship at the faster scan rates. Reasons for non-linearity at the slower scan rates are not readily apparent; however, convective effects in the vicinity of the electrode may be a contributing factor.

Variation of peak current of nickel with rate of voltage scanning when the tempera-

TABLE 1

VARIATION OF DIFFUSION CURRENT OF NICKEL WITH CONCENTRATION AND RATE OF VOLTAGE SCAN
LiF-NaF-KF (46.5-11.5-42 mole %); Temp., 500°

Ni (p.p.m.)	Current (μA)					
	0.2 ^a	0.5 ^a	1.0 ^a	3.0 ^a	5.0 ^a	10.0 ^a
9	2.3	3.7	4.8	7.4	5.7	8.6
23	3.6	5.7	7.8	11.4	14	19
35	7.1	8.6	11.3	15.7	21.4	30
80	10.7	15	21.4	37.2	43.7	64

^a Scan rate (V/min).

ture of the melt was maintained at 500, 570 and 600° is shown in Fig. 3. From this plot and the equation which relates peak current to scan rate ($i_p = k n^3 A D^{1/2} C v^{1/2}$, where $k = 2.29, 2.19$ and 2.15×10^5 at 500, 570 and 600°, respectively; $v = V/sec$ and n, A, D and C have their usual significance) the diffusion coefficient, D , for nickel was calculated. The values are approximately $1 \times 10^{-6}, 2.7 \times 10^{-6}$ and 4.5×10^{-6} cm²/sec at 500, 570 and 600°, respectively.

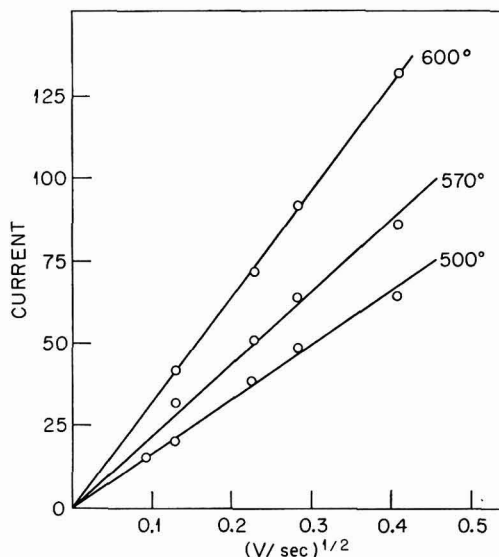


Fig. 3. Effect of temperature on peak current for nickel at different scan rates. Nickel, 80 p.p.m.

To estimate the activation energy (E) of the current limiting process, a plot of $\log D$ vs. $1/T$ was constructed as shown in Fig. 4. From the slope of the line and the relationship

$$\log_{10} D = \frac{-E}{2.3 RT} + \log_{10} A$$

an E -value of approximately 18 kcal was obtained. The value is somewhat higher than the E -values of 5.6 and 10.0 kcal which were reported for the reduction of

Ni(II) \rightarrow Ni(o) in a molten chloride⁸ and nitrate⁹ medium, respectively. This larger value may be partly due to a more complex structure for nickel which probably exists in a molten fluoride environment and to viscosity effects.

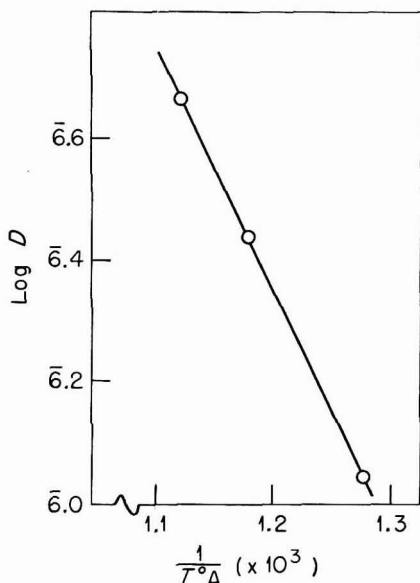


Fig. 4. Plot of $\log D$ vs. $1/T$. Slope of line, -3800 .

SUMMARY

Results are presented on the rapid scan voltammetry and anodic stripping voltammetry of nickel in molten LiF-NaF-KF. The technique of anodic stripping voltammetry is promising as a means of determining trace quantities of nickel directly in the melt; as little as 1 p.p.m. can be detected. The half-wave potential for the reduction of Ni(II) \rightarrow Ni(o) occurs at approximately -0.2 V vs. the platinum quasi-reference electrode. Current-voltage curves were recorded at a pyrolytic graphite indicator electrode at voltage scan rates from 50 mV/min-10 V/min. At the faster scan rates, peak-shaped curves resulted which indicated that the transport process was mainly diffusion-controlled. A diffusion coefficient of $\sim 1 \cdot 10^{-6}$ cm²/sec at 500° was calculated. An activation energy of about 18 kcal/mole was calculated for the current-limiting process which corresponds to the reduction of Ni(II) to the metal.

REFERENCES

- 1 D. L. MANNING, *J. Electroanal. Chem.*, 6 (1963) 227.
- 2 D. L. MANNING AND G. MAMANTOV, *J. Electroanal. Chem.*, 7 (1964) 102
- 3 M. T. KELLEY, H. C. JONES AND D. J. FISHER, *Anal. Chem.*, 31 (1959) 488.
- 4 J. G. NIKELLY AND W. D. COOKE, *Anal. Chem.*, 29 (1957) 933.
- 5 E. S. JACOBS, *Anal. Chem.*, 35 (1963) 2112.
- 6 S. P. PERONE, *Anal. Chem.*, 35 (1963) 2091.
- 7 P. DELAHAY, *New Instrumental Methods in Electrochemistry*, Interscience Publishers, Inc., New York, 1954, pp. 115-146.
- 8 E. D. BLACK AND T. DE VRIES, *Anal. Chem.*, 27 (1955) 906.
- 9 M. STEINBERG AND N. H. NACHTRIEB, *J. Am. Chem. Soc.*, 72 (1950) 3558.

TRACE ANALYSIS BY ANODIC STRIPPING VOLTAMMETRY

II. THE METHOD OF MEDIUM EXCHANGE

M. ARIEL, U. EISNER* AND S. GOTTESFELD

*Laboratory of Analytical Chemistry, Department of Chemistry,
TECHNION - Israel Institute of Technology, Haifa (Israel)*

(Received January 16th, 1964)

INTRODUCTION

In the course of an investigation of the application of anodic stripping voltammetry methods to the analysis of complex materials¹, the usefulness of these methods has been fully demonstrated; it is, unfortunately, frequently limited by interferences inherent in the sample composition. The method of Medium Exchange, briefly mentioned as a qualitative¹ and quantitative^{2,3} approach, often provides an effective solution to the removal of three important sources of interference.

(i) The presence of two, or more, amalgam-forming metal ions, deposited simultaneously in the hanging mercury drop electrode (HMDE), and having similar oxidation potentials in the medium employed for deposition; because of the inevitable overlapping of the oxidation current peaks obtained in the anodic scan, the quantitative interpretation of results is impossible.

(ii) A high residual current, resulting from the presence of some component in the sample solution, may severely distort or obliterate the desired anodic oxidation peak. This interference is particularly serious whenever this residual current has a marked potential dependence, as is the case in the presence of relatively high concentrations of hydrogen ions, or of ionic species having multiple oxidation states; their reduction or oxidation currents are superimposed in the stripping voltammogram.

(iii) For metals having relatively positive oxidation potentials, the proximity of their oxidation current peaks to the mercury oxidation current constitutes a serious interference.

The Medium Exchange method, described below, has been successfully applied in situations where these interferences were present. The amalgam-forming metal ion or ions are electrodeposited in the HMDE; at the end of this pre-electrolysis, the stripping process is carried out into a different medium, chosen according to the interference present. The new medium must, therefore, provide adequate separation of the oxidation current peaks of the deposited metals from one another and/or from the mercury oxidation current, and must not contain significant concentrations of interfering ionic species. While the last requirement is easily satisfied, some ingenuity is frequently demanded for the choice of a satisfactory resolving medium.

* Part of a D.Sc. thesis which will be presented by U.E. to the Senate of the Technion.

EXPERIMENTAL

The electrolysis cell, scanning and recording apparatus and the general experimental procedure employed have already been described¹. During the pre-electrolysis step, another lower part of the cell is filled with the appropriate new medium and de-aerated; at the end of the desired deposition period, the stirring is stopped, the lower parts of the cell are quickly exchanged (transfer is effected in less than 10 sec), the solution stirred very briefly (5 sec), allowed to rest for 30 sec and scanned anodically as usual. During the transfer the electrodes remain connected to the voltage source; where desired, the starting potential of the voltage scan is adjusted to a value different from the electrolysis potential.

Whenever the new medium absorbs atmospheric oxygen rapidly (*e.g.*, alcoholic solutions), so that the amount absorbed during the transfer step interferes with the subsequent determination, the new medium must be de-aerated for an additional short period after the transfer. In these cases great care must be taken to ensure the purity of the new medium (in ordinary cases, analytical grade reagents are entirely satisfactory).

RESULTS AND DISCUSSION

The following may serve to illustrate the application of the Medium Exchange method:

A. The determination of copper in Dead Sea Brine (DSB)

The presence of trace amounts of cupric ions in DSB has been proved¹; the method employed is unsuitable for the quantitative determination of copper because of the long electrolysis periods required. Shorter electrolysis periods may be employed, coupled with rapid voltage scans. In the case of copper, however, the oxidation potential of which in DSB is -0.3 V *vs.* S.C.E., the oxidation current peak merges with the oxidation current of mercury (anodic dissolution of mercury starts very early in this highly concentrated halide medium). Figures 1 and 2 show the difference between the stripping voltgrams obtained at the slow and rapid rates of voltage scan respectively.

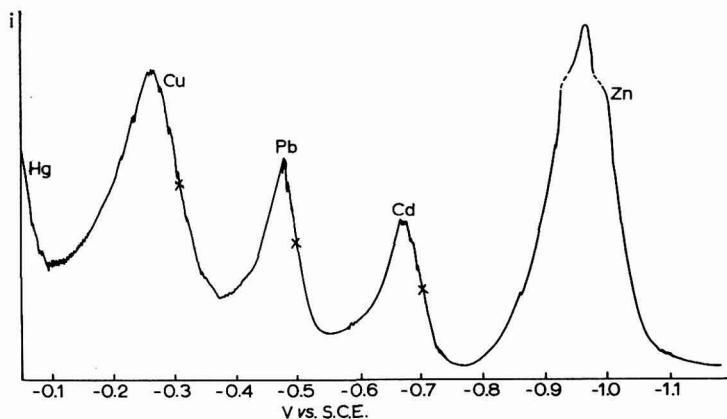


Fig. 1. Amalgam-forming trace metals present in Dead Sea brine. Scanning and recording instrument, Type E Electrochemograph; initial and final potentials, -1.3 and -0.1 V *vs.* S.C.E. respectively; pre-electrolysis period, 80 min.

This problem was solved as follows:

- (a) pre-electrolysis of DSB at -0.48 V vs. S.C.E. for 10–15 min;
- (b) Medium Exchange, to a medium offering adequate resolution of the copper oxidation current peak from the mercury oxidation current;
- (c) rapid anodic voltage scan.

At -0.48 V vs. S.C.E., no lead is deposited from DSB; as this is the nearest metal to copper in the voltagram (Fig. 1), no amalgam-forming metal except copper will be

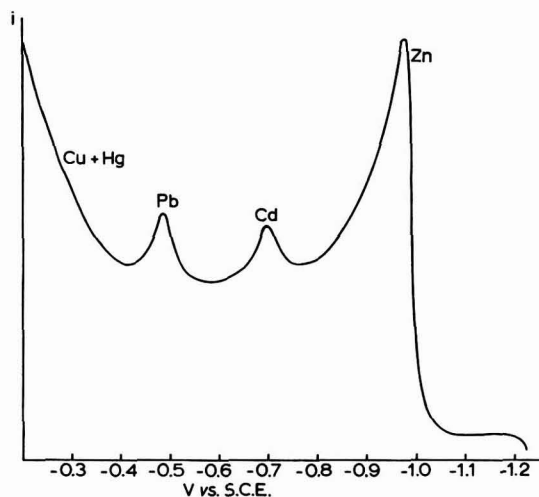


Fig. 2. Amalgam-forming trace metals present in Dead Sea brine. Scanning instrument, rapid voltage scan apparatus; scan rate, 220 mV/sec; initial and final potentials, -1.3 and -0.1 V vs. S.C.E. respectively; recording instrument, DuMont Low Frequency Oscilloscope Type-403; pre-electrolysis period, 7 min.

TABLE I

COMPARISON OF HALF-PEAK POTENTIALS OBTAINED BY ANODIC STRIPPING OF COPPER INTO DIFFERENT MEDIA AND POLAROGRAPHIC HALF-WAVE POTENTIALS^{4,5}

Medium	Half-peak potential (V vs. S.C.E.)	Polarographic half-wave potential (V vs. S.C.E.)
0.2 M EDTA	-0.22	-0.39
0.1 M EDTA, 2 M sodium acetate	no peak	-0.39
0.2 M EDTA, pH 7	-0.24	-0.41
0.2 M ammonium carbonate, 0.01% EDTA	-0.34	—
2% acetyl acetone, 85% ethanol, 0.07 M potassium nitrate	-0.26	-0.26
4% acetyl acetone, 85% ethanol, 0.07 M potassium nitrate	-0.27	-0.27
0.5 M ammonium hydroxide, 0.5 M, ammonium chloride	-0.48	-0.48
0.05 M thiourea, 0.1 M potassium nitrate	-0.51	-0.49
0.1 M thiourea, 0.1 M potassium nitrate	-0.54	-0.54
0.2 M thiourea, 0.1 M potassium nitrate	-0.65	—
1 M sodium hydroxide	-0.45	-0.45

deposited. The choice of the new medium may, therefore, be made solely on the basis of providing adequate copper-mercury resolution.

Inspection of available polarographic data^{4,5}, displayed in Table 1, narrowed the choice to three main groups of media:

- (1) Inorganic bases.
- (2) Organic bases.
- (3) Other inorganic and organic complex-forming reagents.

(1) Although inorganic bases offer good resolution (Table 1), they may not be employed in this case, since they produce interfering precipitates with some of the macro constituents of DSB which are carried over by the liquid film adhering to the mercury drop during the DSB-new medium transfer (DSB contains high concentrations of calcium and magnesium ions).

(2) Organic bases, such as ethylenediamine and triethanolamine in aqueous, inorganic electrolyte containing solutions, were tried and discarded due to the early oxidation of mercury in these media and the resulting base-line distortion.

(3) Other complex-forming reagents often have the same detrimental effect on the base line; Fig. 3 illustrates this for thiourea.

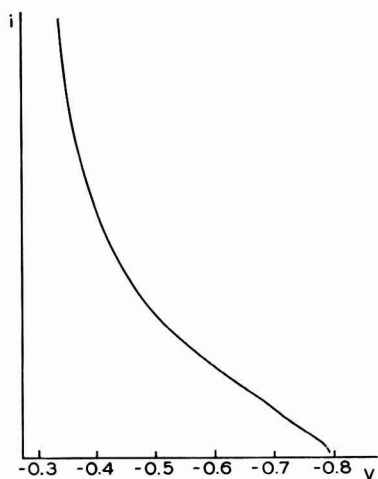


Fig. 3. Base-line distortion in thiourea; scan rate, 220 mV/sec.

In the course of these experiments it was again shown how misleading classical polarographic half-wave potential data may become when applied to the oxidation processes occurring in rapid scan anodic stripping¹. A typical instance is provided by EDTA solutions, which, according to polarographic data⁴, offer good copper-mercury resolution at a number of pH values; in anodic stripping, the copper peak merges with the mercury oxidation current (Fig. 4). These media are obviously unsuitable for the determination of copper by rapid scan anodic stripping voltammetry.

Acetyl acetone solution (containing 2-4% acetyl acetone, 85% ethanol and approx. 0.07 M KNO₃) seemed promising, since its base-line, after thorough de-aeration, was flat in the region where the copper peak was expected (Fig. 5). Unfortunately, the

rapid re-absorption of oxygen by this solution during the transfer step causes the base-line to slope irreproducibly. Although, by extremely careful handling, DSB copper determinations may be effected with this medium, the experimental difficulties involved make it unattractive.

The best medium for the copper determination was 0.5 *M* ammonium hydroxide–0.5 *M* ammonium chloride, neglected at first because the lead and copper oxidation

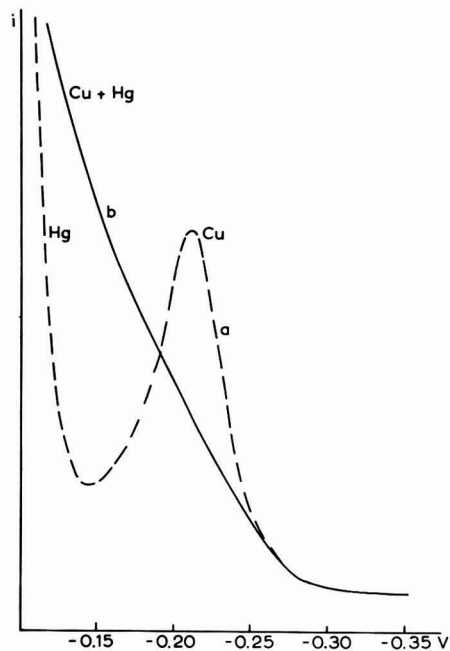


Fig. 4. Anodic stripping voltammogram of copper into 0.2 *M* EDTA, pH 7, after electrodeposition into the HMDE: (a), slow scan rate, 3 mV/sec; (b), rapid scan rate, 220 mV/sec.

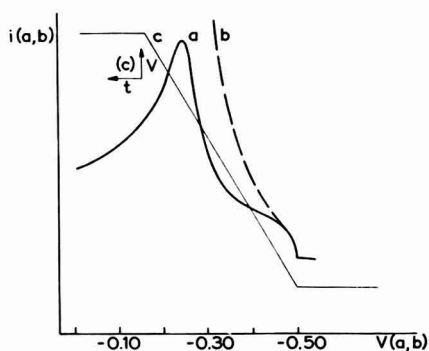


Fig. 5. Anodic stripping voltammogram of copper into 2% acetyl acetone, 85% ethanol, 0.07 *M* potassium nitrate after electrodeposition into the HMDE: (a), thoroughly de-aerated solution; (b), same as (a), after 10 sec exposure to atmosphere; (c), linear voltage scan applied. Rapid scan rate, 220mV/sec; recording instrument, Tektronix type-502 Dual-Beam Oscilloscope.

potentials in this solution are very close (Table 1). Since, however, at the deposition potential of -0.48 V vs. S.C.E. practically no lead is deposited from DSB, there will be no interference of lead during the stripping process. Before the transfer, the potential of the HMDE is shifted to -0.6 V; the anodic scan is carried out from -0.6 – -0.2 V. Figures 6 and 7 demonstrate the effectiveness of this Medium Exchange. Figure 6 shows the results obtained by stripping into DSB, while Fig. 7 shows the stripping voltammogram obtained after transfer to ammonium hydroxide–ammonium chloride, compared to the base-line in that medium alone.

The amount of copper in DSB, found by this method (through standard addition) is 4.5×10^{-8} *M*, with a standard deviation of 15%.

B. The determination of copper in the presence of manganese in triethanolamine solutions

In a proposed new approach to the determination of copper in steels and iron by anodic stripping voltammetry⁶, the electrodeposition of copper into the HMDE is

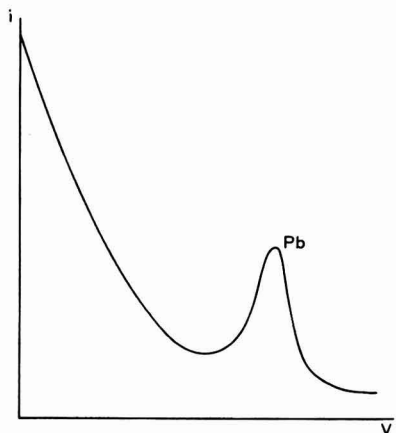


Fig. 6. Anodic stripping voltammogram of lead and copper in DSB. Rapid scan rate, 220 mV/sec.

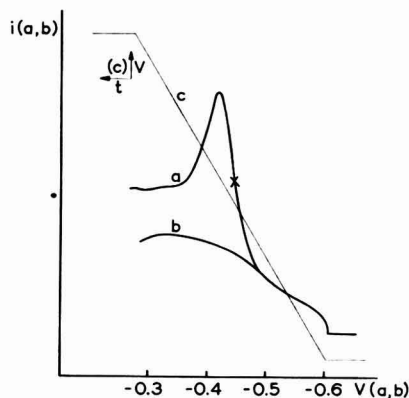


Fig. 7. Anodic stripping of copper in DSB, after electrodeposition into the HMDE from DSB, and Medium Exchange into 0.5 *M* ammonium chloride solution: (a), copper stripping voltammogram; (b), base line in ammonium hydroxide-ammonium chloride solution; (c), linear voltage scan applied. Rapid scan rate, 220 mV/sec; recording instrument, Tektronix Type-502 Dual-Beam Oscilloscope.

Fig. 6. and Fig. 7. Effectiveness of Medium Exchange.

effected from a 0.1 *M* NaOH–0.3 *M* triethanolamine solution, containing the dissolved steel sample. Copper concentration may range from $1 \cdot 10^6$ – $5 \cdot 10^6$ *M* and its oxidation potential in this medium is -0.46 V vs. S.C.E. If, after electrodeposition, the determination of copper is attempted by anodic redissolution (stripping) into the original solution, manganese interferes.

Manganese is a common component of steels, its concentration is usually far higher than that of copper; in the sample solution it is found in the Mn^{2+} oxidation state. During the anodic linear potential scan required for the stripping of copper, an oxidation current peak corresponding to $Mn^{2+} \rightarrow Mn^{3+}$ oxidation (at -0.4 to -0.6 V vs. S.C.E.) is obtained. Mn^{2+} may be pre-oxidized to Mn^{3+} by bubbling oxygen through the solution before the electrodeposition; this, however, does not provide a solution to the problem, since the Mn^{3+} then present distorts the current–voltage curve as it is reduced in the same potential range. This interference becomes noticeable with Mn^{2+} concentrations above $2 \cdot 10^{-5}$ *M* and attains the order of the copper peak at concentrations of 10^{-4} *M* Mn^{2+} approximately (Fig. 8). Since the ratio of manganese and copper in many steels is of the order of 100 : 1, the concentrations of Mn^{2+} resulting from the dissolution of these steel samples will be sufficiently high to interfere seriously with the copper determination.

This problem is easily solved by the method of Medium Exchange. After electrodeposition of copper into the HMDE, a “pure” solution of 0.1 *M* NaOH–0.3 *M* triethanolamine is substituted for the original steel sample solution, and copper stripped into it. The copper peak obtained in this way is free of all distortion. Ten successive medium transfers were carried out into the same “pure” solution; the copper peaks obtained were reproducible and the base line (determined by carrying out a linear potential

scan from -0.70 V to -0.30 V *vs.* S.C.E., after the tenth transfer) was found completely undistorted. This proves that carry-over of components from the original sample solution to the "pure" solution is entirely negligible.

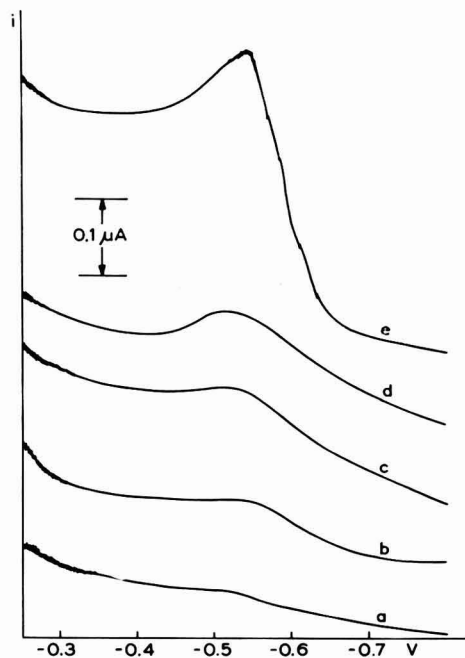


Fig. 8. Current-voltage curve (base-line) distortion due to the presence of manganese in 0.1 M sodium hydroxide- 0.3 M triethanolamine solution: (a), $3 \cdot 10^{-6}$ M Mn^{2+} ; (b), 10^{-5} M Mn^{2+} ; (c), $2 \cdot 10^{-5}$ M Mn^{2+} ; (d), $3 \cdot 10^{-5}$ M Mn^{2+} ; (e), 10^{-4} M Mn^{2+} . Slow scan rate 3 mV/sec; initial and final potentials, -0.7 V and -0.2 V *vs.* S.C.E. respectively.

C. The determination of copper in the presence of bismuth

Copper and bismuth are simultaneously electrodeposited into the HMDE from alkaline triethanolamine solutions; Fig. 9 shows the overlapping of the oxidation current peaks obtained subsequently. For the determination of copper, a resolving medium exchange, after electrodeposition, is essential. 1 M potassium thiocyanate solution was found suitable; in this medium the copper oxidation potential is -0.60 V *vs.* S.C.E., while that of bismuth, -0.25 V *vs.* S.C.E. approx., causes the bismuth and mercury oxidation currents to merge. Copper oxidation current peaks, obtained from 10^{-5} M Cu^{2+} solutions (electrodeposited from 1 M NaOH- 0.3 M triethanolamine; stripped into 1 M KCNS), in the presence of equal concentrations of bismuth ions, were of the same height as those obtained from solutions containing copper only (within the limits of experimental error).

D. Reproducibility of the method

In order to assess the possibly detrimental influence of the additional step of medium exchange on the precision of the method, results obtained by anodic stripping voltammetry with and without medium exchange were compared.

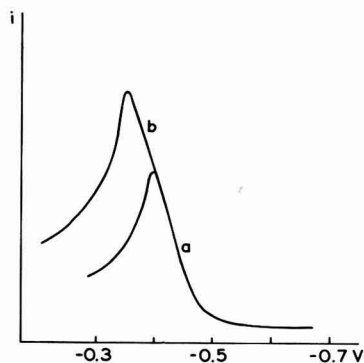


Fig. 9. Anodic stripping voltammograms in 0.1 *M* sodium hydroxide–0.3 *M* triethanolamine: (a), copper only; (b), copper in the presence of an equal amount of bismuth. Slow scan rate, 3 mV/sec.

Lead and cadmium were determined from the following media:

(a) without Medium Exchange:

1. Pb^{2+} 10^{-6} *M*, KCl 1 *M*
2. Cd^{2+} 10^{-7} *M*, KCl 1 *M*

(b) with Medium Exchange:

electrodeposition from:

1. Pb^{2+} 10^{-6} *M*, KCl 1 *M*, HCl 1 *M*
2. Cd^{2+} 10^{-7} *M*, KCl 1 *M*

stripping into:

1. and 2. KCl 1 *M*.

Results obtained by methods (a) and (b) were of comparable precision (3–5% standard deviation). Similar experiments, carried out with various copper and tin solutions, confirmed that the introduction of the Medium Exchange step does not affect the reliability of the method.

SUMMARY

The method of medium exchange, consisting of electrodeposition of an amalgam-forming metal or metals in the hanging mercury drop electrode, followed by a stripping process into a suitable, different medium, is described and its effectiveness in overcoming various sources of interference, common in complex materials, proved. Since the precision of results obtained through the introduction of this additional step into anodic stripping voltammetry methods is comparable to that obtained in regular anodic stripping determinations, the method affords a significant extension of the applicability of anodic stripping voltammetry to trace analysis.

REFERENCES

- 1 M. ARIEL AND U. EISNER, *J. Electroanal. Chem.*, 5 (1963) 362.
- 2 S. L. PHILLIPS AND I. SHAIN, *Anal. Chem.*, 34 (1962) 262.
- 3 M. ARIEL, U. EISNER AND S. GOTTESFELD, XIXth International Congress of Pure and Applied Chemistry, London 1963.
- 4 L. MEITES, *Polarographic Techniques*, Interscience Publishers, Inc., New York, 1955, pp. 261–264.
- 5 T. A. KRYUKOVA, S. I. SINYAKOVA AND T. V. AREFYEVA, *Polarograficheski Analiz*, G. Ch. I, Moscow, 1959, pp. 687–691.
- 6 M. ARIEL AND S. GOTTESFELD, to be published.

VOLTAMMETRIC DETERMINATION OF CARBON MONOXIDE AT GOLD ELECTRODES

JULIAN L. ROBERTS, JR. AND DONALD T. SAWYER

Department of Chemistry, University of California, Riverside, California (U.S.A.)

(Received January 6th, 1964)

* see Correction. *J. Electroanal. Chem.*, 9 (1965) 172

Although there are a number of analytical methods for the determination of carbon monoxide (including colorimetric, gas chromatographic, titrimetric, and gas absorption methods¹⁻⁷), the direct electroanalytical determination of this gas has not been reported previously. An indirect polarographic procedure is available which is based on the reduction of the iodine released by the reaction of carbon monoxide with I_2O_5 ⁸. Considerable interest in the electrochemistry of carbon monoxide has developed because of potential fuel cell applications. Most of these fundamental studies have been concerned with the oxidation of carbon monoxide at platinum electrodes in aqueous solutions^{8,9}. For such conditions the anodic current is not diffusion-controlled, but is complicated by adsorption of carbon monoxide on the platinum surface.

During the course of a general investigation of the electrochemistry of carbon monoxide at various metal electrodes a voltammetric method for determining carbon monoxide at gold electrodes has been developed. By using an aqueous alkaline solution and a properly activated gold electrode, a diffusion-controlled oxidation occurs which is not complicated by adsorption.

EXPERIMENTAL

Voltammetric measurements were made with a versatile instrument constructed from Philbrick operational amplifiers. The design of this instrument and the details of its performance have been discussed by DEFORD¹⁰. All measurements were made using a three-electrode circuit to eliminate IR corrections. Voltages are reported vs. the saturated calomel electrode (S.C.E.).

The electrolytic cell was prepared from a 200-ml. tall-form beaker fitted with a rubber stopper. The latter was drilled to accommodate the gold working electrode, a Leeds and Northrup saturated calomel electrode, a platinum gauze counter-electrode, and two glass tubes for bubbling gas into the solution and over the solution surface. All samples were introduced by bubbling the gas sample through the solution until saturation was attained; the gas was swept over the surface during the electrolytic sweep of the unstirred solution. The cell was immersed in a water bath maintained at $25.00 \pm 0.02^\circ$.

The working electrode was prepared with reagent-grade gold in two different forms

to give a wide range of electrode area. A foil electrode was made by welding a $1 \times 1 \times 0.01$ cm piece of gold foil to a length of 0.6 mm-diameter gold wire and sealing this into thick-walled polyethylene tubing such that approximately 0.6 cm of wire above the foil was left exposed. A bead micro-electrode was made by melting the end of a length of 0.6 mm-diameter gold wire, such that a 1.5 mm-diameter bead was formed on the end of the wire. The other end of the wire was then sealed into polyethylene tubing so that the bead plus approximately 2 mm of wire were left exposed. Fresh surfaces were obtained on the gold electrodes by anodizing them at 3 V *vs.* platinum for 15 min in a solution containing 3 *F* HClO₄, 0.03 *F* HCl, and 3 *F* acetic acid. The areas of the working electrodes were determined with the Sand equation¹¹ by chronopotentiometric reduction of known concentrations of K₃Fe(CN)₆ in 0.5 *F* KCl and using a diffusion coefficient for Fe(CN)₆³⁻ of 7.67×10^{-6} cm²/sec. The area of the foil electrode was found to be 2.42 cm² and for the bead micro-electrode, 0.141 cm²; these areas were both about 8–10% larger than the geometric areas.

Carbon monoxide (99.9% pure) and mixtures of carbon monoxide–pre-purified nitrogen containing 3.03, 10.0 and 29.46% CO by volume were obtained from the Matheson Co. The gases were passed through a train of washing towers containing in sequence, concentrated H₂SO₄, 10% NaOH, and distilled water, before being introduced into the electrolysis cell. All other materials were reagent grade. The supporting electrolyte for all measurements was 0.01 *F* NaOH plus 0.1 *F* K₂SO₄.

RESULTS AND DISCUSSION

The oxidation of carbon monoxide at gold electrodes is dependent upon the composition of the electrolyte solution. In acidic solutions the electrode reaction is complicated by a rate-controlling process involving adsorption of CO on the electrode surface. This is similar to the behavior in general of carbon monoxide at platinum surfaces^{8,9}. In 1 *F* NaOH the anodic wave is partially obscured by a competing electrode reaction. Thus, the most satisfactory supporting electrolyte from an analytical standpoint is 0.01 *F* NaOH in 0.1 *F* K₂SO₄.

To obtain useful analytical data the gold electrode must be properly activated. The current–voltage response for an inactive electrode is shown by curve A in Fig. 1. By anodizing a gold electrode for at least 10 min in a solution containing 0.03 *F* HCl, 3 *F* HClO₄, and 3 *F* acetic acid, a new surface is obtained which is easily activated for the diffusion-controlled oxidation of carbon monoxide. Activation is accomplished by placing the resurfaced electrode in a solution containing carbon monoxide and the supporting electrolyte (0.01 *F* NaOH plus 0.1 *F* K₂SO₄), and applying a potential to the electrode which is cycled 3 or 4 times between -0.8 and $+1.0$ V *vs.* S.C.E. using a scan rate of 0.1 V/sec. With such an activated electrode the current–voltage response indicated by curve B in Fig. 1 is obtained for the oxidation of carbon monoxide.

A systematic sequence of operations has been found desirable for making analytical measurements with an activated electrode. After the CO-containing gas sample is bubbled into the supporting electrolyte solution the voltage is scanned at 0.1 V/sec. without stirring from -0.8 – $+1.0$ V. While additional sample gas is bubbled through the solution the voltage is held at $+1.0$ V for 10–20 sec and then switched to -0.8 V for 30 sec. Finally the solution is allowed to become quiescent for 30 sec while sweeping sample gas over the surface and then the current–voltage sweep is recorded from -0.8 – $+1.0$ V at a scan rate of 0.1 V/sec. Figure 2 indicates peak current, i_p ,

as a function of percentage by volume of CO in gas mixtures for two different electrodes.

Chronopotentiometric measurements have been used to establish that the oxidation of CO at gold electrodes is irreversible. For such systems DELAHAY¹¹ has derived an expression for the peak current, i_p , for voltage scans of irreversible reactions whose

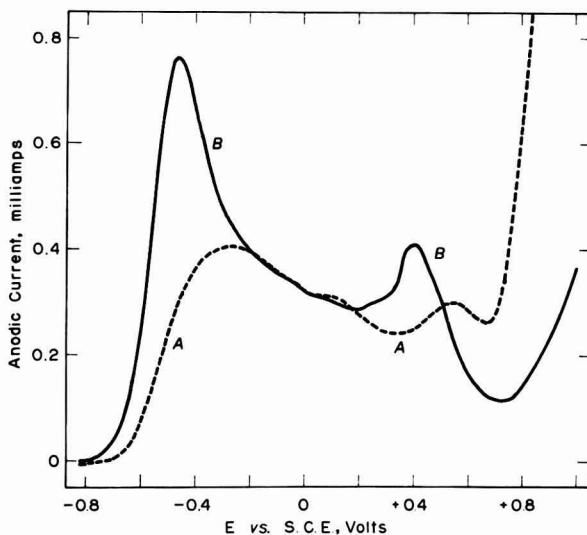


Fig. 1. Voltammetric oxidation of carbon monoxide at a gold electrode: curve A, an inactive electrode; curve B, an activated electrode. Scan rate, 0.05 V/sec; supporting electrolyte, 0.01 *F* NaOH in 0.1 *F* K₂SO₄; solution saturated with 100% CO ($\sim 10^{-3}$ *M*); electrode area, 2.42 cm².

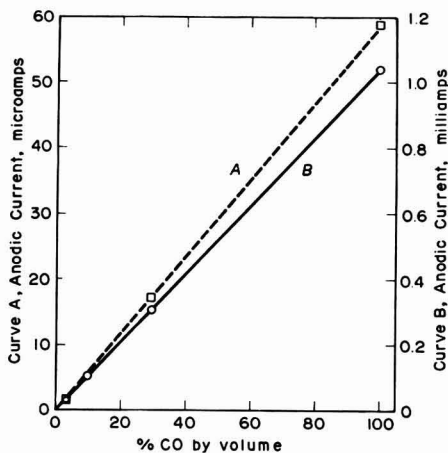


Fig. 2. Anodic peak current vs. % CO by volume in CO-N₂ mixtures: curve A, bead electrode, area 0.141 cm²; curve B, foil electrode, area 2.42 cm². Scan rate, 0.1 V/sec; supporting electrolyte, 0.01 *F* NaOH in 0.1 *F* K₂SO₄. The measured currents were corrected for residual currents which were 1.8 and 6.8 μ A, respectively, for the bead electrode and the foil electrode.

current is limited by semi-infinite linear diffusion. For an irreversible anodic reaction the expression becomes

$$i_p = 3.01 \times 10^5 n [n_a(1 - \alpha)]^{1/2} AD^{1/2} C v^{1/2} \quad (1)$$

where v is the scan rate in V/sec. Data for the oxidation of CO at an active gold electrode using various scan rates are given in Table 1. A plot of the logarithm of peak currents *vs.* the logarithm of the scan rate gives a linear slope for both electrodes with a value between 0.46 and 0.48. Thus, the electrode reaction is definitely diffusion-controlled and adsorption is not the limiting process.

TABLE 1

PEAK CURRENT AS A FUNCTION OF SCAN RATE; ACTIVATED ELECTRODE IN 0.01 *F* NaOH PLUS 0.1 *F* H₂SO₄ SUPPORTING ELECTROLYTE

Scan rate (V/sec)	i_p Bead electrode	(μA) Foil electrode
0.10	58.7	1037
0.05	41.2	770
0.02	27.7	505
0.01	19.4	368

The activity of the pre-conditioned electrode is subject to a number of factors which must be noted if reproducible and meaningful analyses are to be obtained. The active state of the electrode apparently can be preserved indefinitely (in the absence of poisoning agents) if the voltage-scan sequence is continuously repeated. The initial scan potential is not critical and can be varied between -1.0 and -0.8 V. On the other hand the scan must be taken up to $+1.0$ V. Otherwise the peak currents on successive scans will decrease and the current-potential curve will gradually change from the state shown by curve B to that of curve A in Fig. 1. If the electrode is held at -0.8 V for longer than the suggested 30 sec (*i.e.*, for 2-60 min), then the current-voltage curve will approximate to curve A of Fig. 1. However, one or two scans from -0.8 to $+1.0$ V will restore the electrode activity. Alternatively the electrode can be held at $+1.0$ V for 10-20 min; this will give an active surface and cycling is not necessary. However, after long periods of standing at open circuit (more than 15 h) the electrode must be strongly anodized at 3 V *vs.* a platinum electrode in 0.03 *F* HCl, 3 *F* HClO₄, and 3 *F* acetic acid to obtain a fresh surface before activating by cyclic scans. Finally, rapid scan rates are recommended because they give larger peak currents and require less analysis time.

For maximum accuracy the peak currents must be corrected for the residual current observed for a scan of a nitrogen-saturated solution. When this is done, the reproducibility with a properly conditioned electrode for samples containing 10-100% CO by volume gives an error of less than $\pm 1\%$. The overall accuracy of the method for this concentration range probably gives relative errors of less than $\pm 2\%$. The sample solution must be free of oxidizing substances such as oxygen if meaningful analyses are to be obtained.

ACKNOWLEDGEMENT

This work was supported by the United States Air Force Research and Development Command, Geophysics Research Directorate, under Contract No. AF 19(604)-8347.

SUMMARY

A voltammetric method has been developed for the determination of dissolved carbon monoxide in 0.01 *F* sodium hydroxide solutions. Details of the activation process are discussed as well as effects of various supporting electrolytes. The peak current is diffusion-controlled and is directly proportional to the percentage by volume of carbon monoxide in gas mixtures used to saturate the electrolysis solution. In the concentration range of 10–100% by volume the method gives errors in accuracy of less than $\pm 2\%$.

REFERENCES

- 1 H. HEIDRICH, Ger. Pat. 1, 120,768; *C. A.*, 56, (1962) 10921d.
- 2 J. W. SWINNERTON, V. J. LINNENBOM AND C. H. CHEEK, *Anal. Chem.*, 34 (1962) 483.
- 3 J. V. A. NOVAK, *Chem. Listy*, 49 (1955) 277.
- 4 S. MUSUMECI AND S. GURRIERI, *Boll. Sedute Accad. Gioenia Sci. Nat. Catania*, 5 (1959) 255.
- 5 L. W. WINKLER, *Z. Anal. Chem.*, 97 (1934) 18; 100 (1935) 321.
- 6 W. M. MACNEVIN AND W. N. CARSON, JR., *J. Am. Chem. Soc.*, 72 (1950) 42.
- 7 R. STEWART AND D. G. EVANS, *Anal. Chem.*, 35 (1963) 1315.
- 8 R. MUNSON, *J. Phys. Chem.*, 66 (1962) 727.
- 9 S. GILMAN, *J. Phys. Chem.*, 67 (1963) 1898.
- 10 D. D. DEFORD, private communication, presented at the 133rd American Chemical Society Meeting, San Francisco, California, 1958.
- 11 P. DELAHAY, *New Instrumental Methods in Electrochemistry*, Interscience Publishers, Inc., New York, N.Y., 1954.

LINEAR POTENTIOMETRIC TITRATIONS

PIETRO LANZA AND ILEANA MAZZEI

Istituto Chimico "G. Ciamician", Università, Bologna (Italy)

(Received December 30th, 1963)

INTRODUCTION

Such is the precision attained by modern instruments for pH-measurements that many available models permit this measurement to be made with an instrumental error which is negligible with respect to the uncertainty which is implicit in the operational definition of pH. In any case it should be borne in mind that it is impossible to give an exact practical definition of pH which is theoretically significant and unobjectionable from a thermodynamical point of view¹. The absolute values of the conventional international standards themselves are defined with an accuracy of ± 0.02 pH-units².

Many modern precision instruments, owing to the development of a.c. amplification techniques, permit the exact evaluation of differences of ± 0.01 pH-units by direct reading and of ± 0.001 pH-units by compensation reading.

The sensitivity of such instruments encourages us to consider again with some interest, the possibility of evaluating the hydrogen ion activity (a_{H^+}) from pH-measurements with sufficient precision to find useful applications.

Potentiometric acid-base titration curves, for instance, are obtained in a simpler form, analogous to amperometric curves, by plotting the a_{H^+} value against the volume of the titrant, instead of the measured pH value. Here a_{H^+} is taken as $\text{antilog}(-\text{pH}) = 10^{-\text{pH}}$ irrespective of any precise thermodynamical meaning. It is proportional to the hydrogen ion concentration, $[H^+]$, at constant ionic strength, and changes linearly with the volume of the added titrant, when, the equivalent point (E.P.) having been passed, the free acid or base is present in sufficient excess. The limits and the practical possibilities of such a form of graphical plotting are shown in Fig. 1.

Figure 1 represents a series of titration curves of 100 ml of 0.01 *N* salts of acids of different strength, when titrated with 0.1 *N* HCl solution and corrected for the dilution effect. The chemical reaction is a displacement reaction of a weak acid from its salt: $A^- + H^+ \rightarrow HA$. The $\text{p}k_a$ indicated is the $\text{p}k_a$ of the weak acid, which is conjugate to the base to be titrated.

The group of curves is limited by the two straight lines *a* and *b*, passing through the origin and the E.P. respectively.

The straight line *a* represents the addition of 0.1 *N* strong acid to 100 ml of pure water (titration of an extremely weak base). The straight line *b* represents the titration

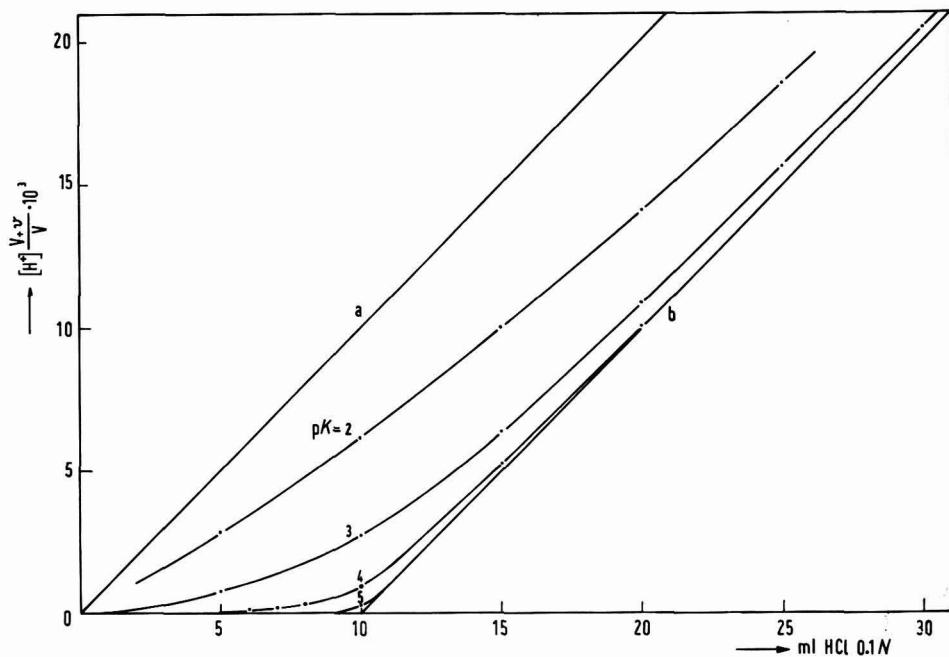


Fig. 1. Titration curves for bases of different strength.

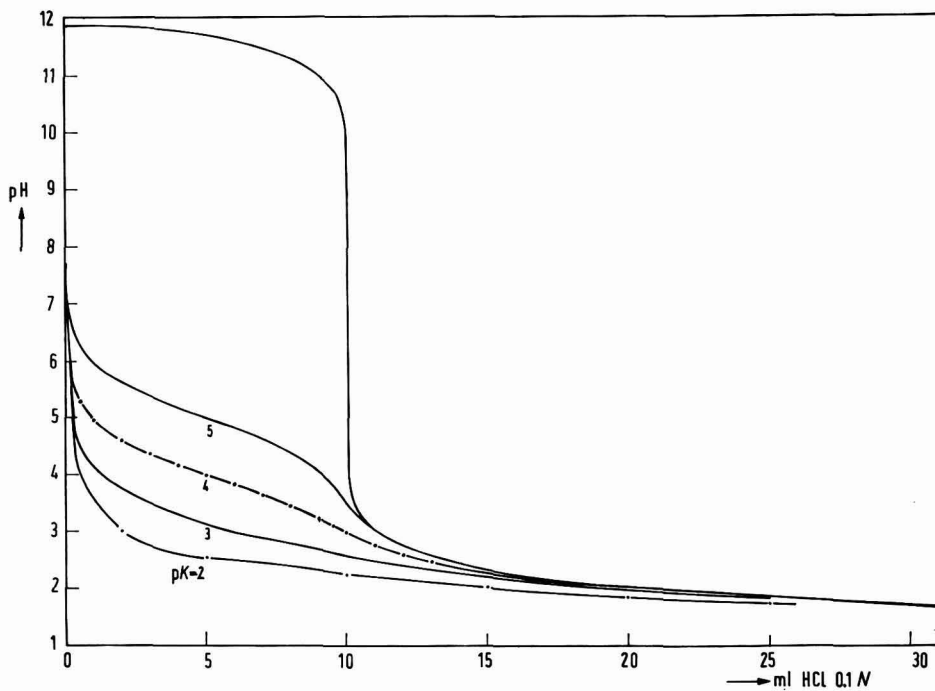


Fig. 2. Conventional representation of potentiometric titration curves.

of a strong base (or of a salt of an extremely weak acid with a strong base). The E.P. is found by extrapolation of the linear part of the curve to intersect the axis of the abscissae.

Using a sufficient excess of titrant in the indicated concentration range, the method is useful for titrations of bases having pK_b values ~ 10 (salts of acids with $pK_a \sim 4$).

In Fig. 2, the same titrations are represented as conventional pH-volume curves. It is evident that with a $pK_a = 5$ ($pK_b = 9$) the E.P. is not determinable with certainty; the conventional graphical method is made uncertain by the asymmetry of the curve at the inflection point and even the geometrical construction of the derivative function fails in practice to define the E.P. with greater precision.

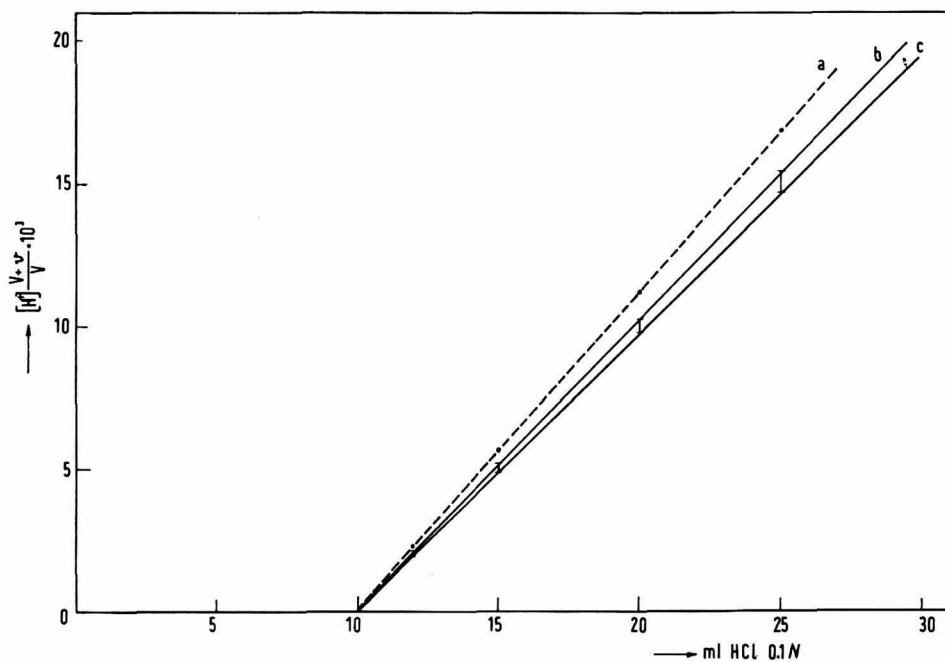


Fig. 3. The influence of errors in pH-measurement and in calibration of the pH-meter on the linear diagrams. (a), error in the pH-meter calibration of -0.05 pH-units; (b) and (c), error in the pH-measurement of ± 0.01 pH-units.

The influence of errors in pH-measurement and in calibration of the pH-meter, on the linear diagrams is represented in Fig. 3. The straight lines *b* and *c* define the angle in which the a_{H^+} values are included, when the uncertainty of the pH-measurement is limited to ± 0.01 unit. The dotted straight line *a* represents the calculated a_{H^+} values, when all the pH-meter readings are displaced by -0.05 pH-units from the true value.

The diagrams show, and it is obviously possible to deduce from the properties of logarithms, that a calibration error or the insertion of a constant diffusion potential in the measuring cell, have no influence on the position of the intersection of the

straight line with the axis of the abscissae. The latter conclusion is of importance, because it allows the equation $pOH = 14 - pH$ in calculations of the titration in the alkaline region to be valid for every temperature and value of the ionic strength of the solution; *i.e.*, it is possible to keep the ionic product of the water constant under different experimental conditions, and to attribute to it arbitrarily the value $pK_w = 14$, without affecting the determination of the E.P.

It is obvious that the considerations, the diagrams and the conclusions, that hitherto have been treated in terms of a_{H^+} or $[H^+]$, can be extended to the values a_{OH^-} or $[OH^-]$.

In alkaline region titrations, it may be convenient, to plot, in a general way $\text{antilog}(pH) = 10^{pH}$, as a function of the volume of the titrant, without any consideration concerning the concentrations or the activities of the H^+ or OH^- ions, but only with the exclusive meaning of a simple mathematical artifice to attain linearity of the potentiometric titration curves.

EXPERIMENTAL

0.1 N solutions of acids, bases or salts to be titrated were prepared by dissolving the necessary amount of the material, exactly weighed, in 0.1 N KCl solution.

10 ml, or less, of these solutions was diluted to 100 ml with 0.2 N KCl solution and titrated with 0.2 N HCl or NaOH. In this way, the ionic strength was kept practically constant during the titration.

The pH-measurements were made with a precision pH-meter (Electrofact, Type 53 A) and a glass-electrode (Metrohm, Type EA121UX), with a low alkaline error. Standard buffers, *i.e.*, phosphate-, phthalate-, and borax-buffers prepared as described in the N.B.S.¹, were used for calibration.

The compounds which have been chosen as examples, are collected in Table 1.

TABLE 1

	pK_a	pK_b
$HCOO^- + H^+ \rightarrow HCOOH$	3.77	<u>10.23</u>
$CH_3COO^- + H^+ \rightarrow CH_3COOH$	4.76	<u>9.24</u>
$C_6H_5NH_2 + H^+ \rightarrow C_6H_5NH_3^+$	4.65	<u>9.35</u>
$C_6H_5OH + OH^- \rightarrow C_6H_5O^- + H_2O$	<u>9.95</u>	
$NH_3^+CH_2(CH_2)_3CHCOO^- + OH^- \rightarrow$	2.18	
$\begin{array}{c} \\ NH_2 \end{array}$	8.95	
$\rightarrow NH_2CH_2(CH_2)_3CHCOO^- + H_2O$	<u>10.53</u>	
(lysine)		
$NH_2CNH(CH_2)_2CHCOO^- + OH^- \rightarrow$	2.01	
$\begin{array}{c} \\ NH \end{array} \quad \begin{array}{c} \\ NH_3^+ \end{array}$	<u>9.04</u>	
$\rightarrow NH_2CNH(CH_2)_2CHCOO^- + H_2O$	<u>12.48</u>	
$\begin{array}{c} \\ NH \end{array} \quad \begin{array}{c} \\ NH_2 \end{array}$		
(arginine)		
$NH_3^+(CH_2)_4CH_2COOH + OH^- \rightarrow$	<u>4.37</u>	
$\rightarrow NH_3^+(CH_2)_4CH_2COO^- + H_2O$	<u>10.80</u>	
(ϵ -amino-caproic acid)		

The aminoacids were used as hydrochlorides and the bases HCOO^- and CH_3COO^- as sodium salts.

In the table are tabulated the acid dissociation constants (pK_a). For the bases, the pK_a are referred to the conjugated acid. For the polybasic acids all the constants are tabulated, those concerning the course of the titration are underlined. For the three bases the pK_b also are tabulated.

RESULTS

In the following diagrams the linear titration curves are compared with the conventional curves. It is evident from Fig. 4 that the E.P. in the titration of HCOO^-

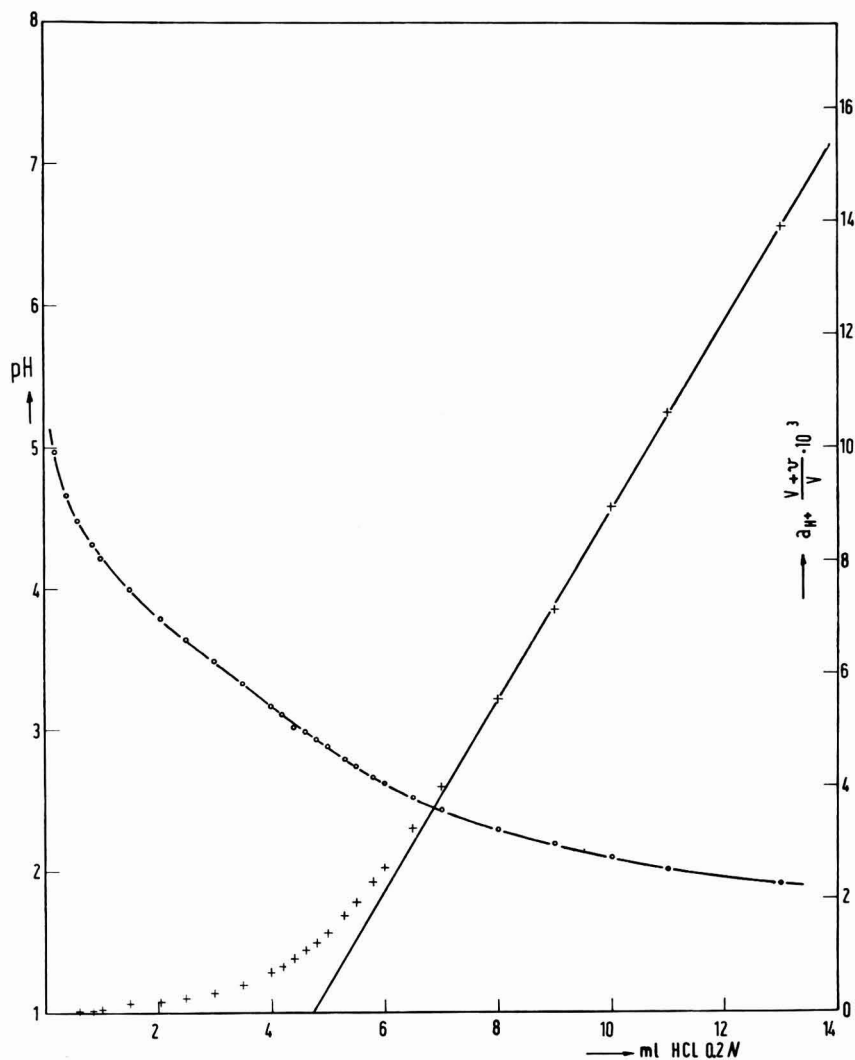


Fig. 4. Conventional and linear titration curves of the base HCOO^- .

base ($pK_b = 10.23$) is again clearly definable with the linear diagram but not at all in the conventional representation.

Aniline can be exactly titrated in water with HCl.

In the titration of the ϵ -amino group of lysine ($pK_a = 10.53$), the strength of the acid is insufficient to give an inflection in the conventional curve. In this case the linear diagram permits only an approximate determination of E.P.; for as already stated above, acids with $pK_a > 10$ or bases whose conjugate acid has a $pK_a < 4$, cannot be titrated using this method.

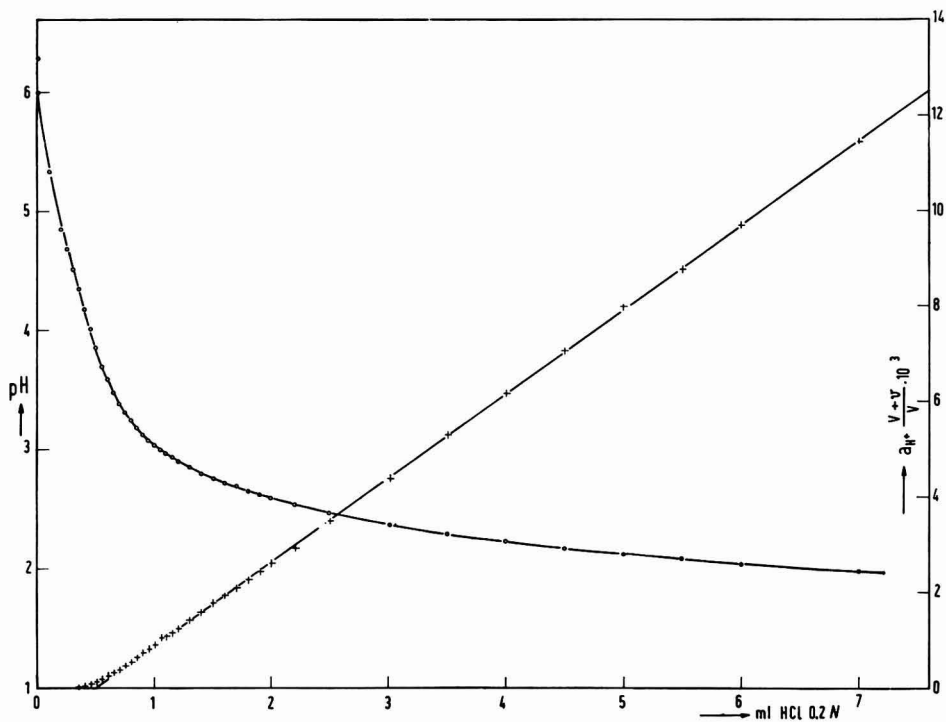


Fig. 5. Conventional and linear titration curves of the base CH_3COO^- .

In Fig. 5 a titration of a dilute CH_3COONa solution is represented. The E.P. can be determined exactly even if in the conventional curve no utilizable inflection is evident.

Another useful application is the titration of ϵ -amino caproic acid in water, with a slight excess of HCl. The usual potentiometric curve presents a first very indefinite E.P. due to excess of HCl and a second E.P. due to the carboxyl of ϵ -amino caproic acid. In the linear diagram the first E.P. is precisely defined. The amount of ϵ -amino caproic acid is calculated from the difference of two E.P., the second of which is satisfactorily determined by the conventional diagram (Fig. 6).

For easy comparison, the results obtained with the two methods are tabulated in the Table 2.

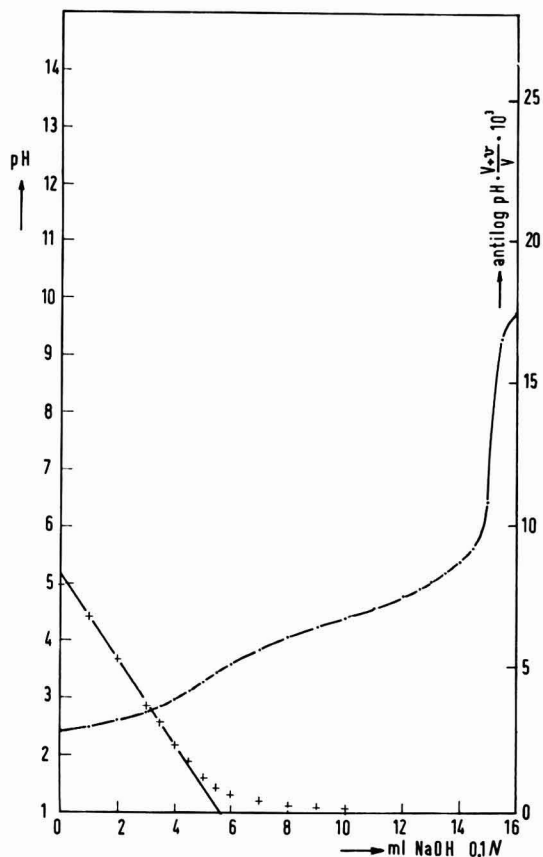
Fig. 6. Conventional and linear titration curves of ϵ -amino caproic acid.

TABLE 2

Compounds	Concn. (mole l^{-1})	Quantity (g)	% Found	
			conventional titrn.	linear titrn.
HCOONa	$1 \cdot 10^{-2}$	0.06802	not determ.	95.00
HCOONa	$5 \cdot 10^{-3}$	0.03401	not determ.	92.00
CH ₃ COONa	$1 \cdot 10^{-2}$	0.1360	103.09	98.09
CH ₃ COONa	$5 \cdot 10^{-3}$	0.06794	96.14	98.15
CH ₃ COONa	$1 \cdot 10^{-3}$	0.01360	not determ.	100.07
Lysine · HCl	$1 \cdot 10^{-2}$	0.1794	not determ.	88.07
Lysine · HCl	$5 \cdot 10^{-3}$	0.0897	not determ.	88.57
Arginine	$1 \cdot 10^{-2}$	0.2096	99.52	100.52
Arginine	$5 \cdot 10^{-3}$	0.1048	102.52	102.52
C ₆ H ₅ OH	$1 \cdot 10^{-2}$	0.0928	not determ.	102.48
C ₆ H ₅ OH	$5 \cdot 10^{-3}$	0.04638	not determ.	101.47
C ₆ H ₅ NH ₂ · HCl	$1 \cdot 10^{-2}$	0.1292	105.34	99.69
C ₆ H ₅ NH ₂ · HCl	$5 \cdot 10^{-3}$	0.06462	103.06	103.06

SUMMARY

A method for graphical representation of potentiometric titration curves is proposed. It permits determination of the end-point even if the conventional potentiometric curve, pH–volume, fails to define exactly an inflection point.

The limits and the possibilities of the method are discussed and some examples of practical applications are illustrated.

REFERENCES

- 1 R. G. BATES, *Electrometric pH-determinations*, J. Wiley, New York, 1954.
- 2 V. GOLD, *pH Measurements*, Methuen, London, 1956, p. 37.

J. Electroanal. Chem., 7 (1964) 320–327

THE POLAROGRAPHIC DIFFUSION COEFFICIENT OF CADMIUM ION IN
0.1 M POTASSIUM CHLORIDE

DANIEL J. MACERO* AND CHARLES L. RULFS

Department of Chemistry, University of Michigan, Ann Arbor, Michigan (U.S.A.)

(Received January 7th 1964)

In connection with the determination of polarographic diffusion coefficients by a modified Cottrell technique³ it was considered necessary to re-determine independently the diffusion coefficient of cadmium ion in 0.1 M KCl. The method chosen was one first employed by GRAHAM¹ since this technique would allow an absolute determination of the diffusion coefficient.

EXPERIMENTAL

The experimental equipment consisted of a cylindrical tube closed at one end and filled with a solution containing the substance in question. This was carefully submerged below the level of a large outer reservoir of liquid initially containing none of the substance. Diffusion then takes place from the inner solution into the outer reservoir. The diffusion was terminated at the end of two or three days and an analysis of the outer solution made, to determine the amount of substance diffused out of the inner tube.

A glass vial 3.59 cm in length and with an internal diameter of 1.43 cm was used as the diffusion cell. The open end was ground with carborundum to give a flat edge. The diffusion cell was attached to a glass rod which could slide smoothly through a length of glass tubing inserted in a rubber stopper cover.

A known volume of temperature-equilibrated 0.1 M KCl solution was pipetted into a clean, dry 100-ml beaker and the diffusion cell filled with a 2.39 mM solution of cadmium chloride dissolved in the same KCl solution. The open end of the diffusion cell was kept above the level of the outer potassium chloride solution while the entire apparatus was allowed to equilibrate with the constant temperature bath. The temperature was kept constant at $25.00 \pm 0.05^\circ$ and the entire system insulated against vibration. After approximately one hour, the diffusion cell was slowly and carefully lowered into the potassium chloride solution. Diffusion was allowed to take place from 1-3 days, after which time the cell was carefully removed, the outer KCl solution stirred and a sample of this removed for analysis. The analytical measurements were made polarographically with a Fisher Eledropode. The galvanometer scale and shunts of the eledropode had been previously calibrated. Three trials were made.

* Department of Chemistry, Syracuse University, Syracuse, New York 13210, U.S.A.

RESULTS AND DISCUSSION

If the volume of the outer KCl solution is sufficiently large, the concentration of cadmium ion at the open end of the diffusion cell may be considered equal to zero. This system then corresponds to that of linear diffusion out of a cylinder, and can be described by the following relationship²:

$$\Delta m = 2AC_0(Dt/\pi)^{1/2}$$

where Δm is the number of moles of cadmium ion which have diffused into the outer KCl solution in time, t (sec); C_0 (moles/cm³) is the initial concentration of cadmium ion in the diffusion cell; A (cm²), the cross-sectional area of the cell and D (cm²/sec), the diffusion coefficient. The values obtained for the diffusion coefficient are listed in Table I.

TABLE I
DIFFUSION COEFFICIENT OF CADMIUM

<i>Trial</i>	Δm (moles · 10 ⁶)	<i>t</i> (sec · 10 ⁻⁵)	<i>D</i> (cm ² /sec · 10 ⁵)
1	6.28	2.96	0.772
2	4.89	1.76	0.785
3	3.55	0.869	0.837

These D -values are approximately 10% greater than the value at infinite dilution of 0.720×10^{-5} cm²/sec calculated from the Nernst relation and experimental values obtained by other investigators^{4,5,6} for this ion. This large discrepancy suggests that the transport of cadmium from the inner diffusion cell to the outer solution may involve some initial mixing in addition to diffusion. Most of the mixing probably occurs when the inner cell is first submerged below the level of the outer solution.

The equation predicts that, in the absence of any initial mixing, a plot of Δm

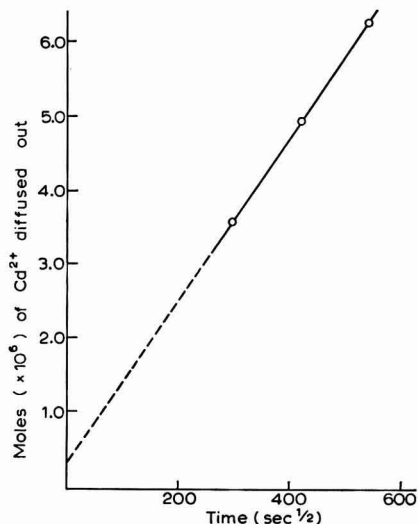


Fig. 1. Linear relation between Δm and $t^{1/2}$.

against $t^{\frac{1}{2}}$ should yield a straight line which passes through the origin at zero time. A slight amount of mixing is unavoidable in such boundary formations; however, this would result in the curve intersecting the Δm axis at zero time. Assuming that the same amount of substance is transported out of the diffusion cell each time it is submerged, then the intercept on the Δm axis should correspond to the amount of cadmium ion transported across the boundary solely by initial mixing. Such a plot is shown in Fig. 1. The observed linearity of Δm with $t^{\frac{1}{2}}$ supports the assumption that substantially the same amount of substance was lost initially in all three trials. This corresponds to 0.31×10^{-6} moles of Cd^{2+} . Using this value, the number of moles of cadmium transported by diffusion alone was determined and a new value for D calculated. These are shown in Table 2.

TABLE 2
DIFFUSION COEFFICIENT VALUES OBTAINED AFTER CORRECTION FOR INITIAL MIXING

Trial	$m(\text{uncorr.})$ (moles $\cdot 10^6$)	$m(\text{corr.})$ (moles $\cdot 10^6$)	$D(\text{corr.})$ ($\text{cm}^2/\text{sec} \cdot 10^5$)
1	6.28	5.97	0.696
2	4.89	4.58	0.688
3	3.55	3.24	0.694

The agreement between the three individual D -values is considerably improved and the average value of 0.693×10^{-5} cm^2/sec is more in accord with values previously reported. Table 3 lists the D -values obtained for cadmium ion by other investigators using a variety of methods.

TABLE 3
DIFFUSION COEFFICIENT VALUES FOR Cd^{2+} IN 0.1 M KCl AT 25° OBTAINED BY DIFFERENT INVESTIGATORS

D ($\text{cm}^2/\text{sec} \cdot 10^5$)	Method	Investigator
0.693	Graham	D. J. MACERO
0.700	Diaphragm cell	C. L. RULFS ⁵
0.717	Cottrell Method	M. VON STACKELBERG, <i>et al.</i> ⁶
0.720	Chronopotentiometry	C. N. REILLEY, <i>et al.</i> ⁴

The value $0.700 \pm 0.013 \times 10^{-5}$ cm^2/sec which represents a weighted average of the diffusion coefficient values listed in Table 3, was selected as the best available value for the diffusion coefficient of cadmium ion in 0.1 M KCl at 25°.

SUMMARY

The diffusion coefficient of cadmium ion in 0.1 M potassium chloride at 25° was determined by an absolute method. Straight calculations using the equation derived by JOST yielded values which were too high when compared to the infinite dilution value of 0.720×10^{-5} cm^2/sec . A correction for initial mixing was made which yielded

more reasonable values for D . The value of $0.70_0 \times 10^{-5} \text{ cm}^2/\text{sec}$ which represents a weighted average of the diffusion coefficient values obtained in this and other investigations was selected as the best available value for the diffusion coefficient of cadmium ion in 0.1 M KCl at 25° .

REFERENCES

- 1 T. GRAHAM, *Phil. Trans. Roy. Soc., London*, 1861, 138–224.
- 2 W. JOST, *Diffusion in Solids, Liquids and Gases*, Academic Press, New York, N.Y., 1952, p. 41.
- 3 D. J. MACERO AND C. L. RULFS, *J. Am. Chem. Soc.*, 81 (1959) 2942.
- 4 C. N. REILLEY, G. W. EVERETT AND R. H. JOHNS, *Anal. Chem.*, 27 (1955) 483–491.
- 5 C. L. RULFS, *J. Am. Chem. Soc.*, 76 (1954) 2071.
- 6 M. VON STACKELBERG, M. PILGRAM AND V. TOOME, *Z. Elektrochem.*, 57 (1953) 342.

J. Electroanal. Chem., 7 (1964) 328–331

Preliminary Note

A substitution-inert metal complex as an indicator in a.c. polarographic titrations; a new type of metal indicator

It has been found, in the course of the polarographic studies of chromium(III) complexes, that reduction waves of some chromium(III) complexes decrease in height by the addition of ethylenediaminetetraacetate (EDTA) and at the same time a new wave due to the reduction of chromium(III)-EDTA complex appears*. More recently, AMEMIYA AND HIRATA¹ reported on an apparently reversible type of square-wave polarographic wave of chromium alum obtained in the supporting electrolyte solution containing EDTA. These phenomena suggested to us the development of an alternating current (a.c.) polarographic titration using a new type of metal indicator, *i.e.*, a substitution-inert metal complex. In this note, an example of the titration, where a nickel nitrate solution is titrated with an EDTA solution using hexamminechromium(III) chloride as indicator, is presented.

The preparation and the standardization of the nickel nitrate and the EDTA solution were carried out as described previously^{2,3}. The errors in the standardization of both solutions were considered to be less than 1%. A.c. polarograms were recorded with a Yanagimoto Galvarecorder Y-GR 2 at 25°. Potentials in this paper are referred to the saturated calomel electrode (S.C.E.).

In Fig. 1 is shown the change in a.c. polarograms of 1.00 mM nickel nitrate and 1.00 mM hexamminechromium(III) chloride with the addition of EDTA. The sup-

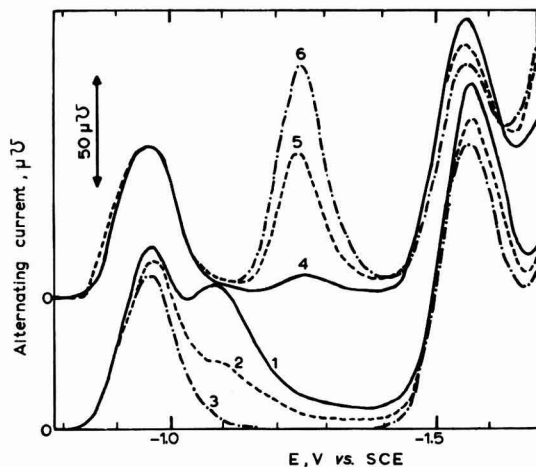


Fig. 1. A.c. polarographic waves of 1.00 mM nickel nitrate and 1.00 mM hexamminechromium(III) chloride, in 25 ml of the supporting electrolyte solution (pH 5.46) containing 0.1 M acetate buffer and 0.1 M ammonium chloride, with the addition of various amounts of 0.994×10^{-2} M EDTA solution: (1), 0 ml; (2), 1.19 ml; (3), 2.51 ml; (4), 2.62 ml; (5), 2.96 ml; (6), 3.25 ml.

* The details of this phenomenon will be reported elsewhere.

porting electrolyte solution (pH 5.46) contained 0.100 *M* acetate buffer, 0.100 *M* ammonium chloride and 0.005% gelatin. The peaks at -0.97 V and -1.57 V are due to the reduction of hexaminechromium(III) to chromium(II) and chromium(II) to chromium(0), respectively. The peaks of nickel(II) at -1.09 V decrease in height upon the addition of EDTA; at the appropriate amount of EDTA added, the nickel peak vanishes, and a new peak due to the oxidation-reduction of chromium-EDTA complex appears at -1.25 V. This indicates that there is excess of un-complexed EDTA in the solution, the nickel being completely complexed with EDTA.

Plots of the peak current at -1.25 V against the amount of the EDTA solution added are given in Fig. 2. The magnitude of the peak current is corrected for the dilution effect. The end-point of the titration is obtained as an intersection of two straight lines. The experimental end-point, 2.555 ml, determined from Fig. 2, is in agreement with the expected equivalent point of 2.515 ml.

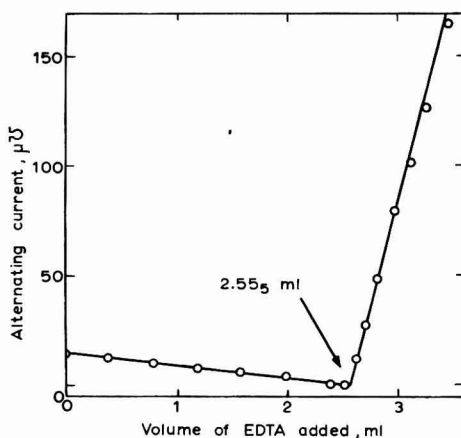


Fig. 2. A.c. polarographic titration curve obtained at -1.25 V vs. S.C.E. with the same solutions as given in Fig. 1.

The use of a substitution-inert metal complex as an indicator has great advantages over the use of conventional metal indicators. In the latter case, the relative apparent stability constant of the EDTA complex of metal ions to be titrated to that of metal ions used as an indicator, and the relative concentration of the metal indicator in the solution to be titrated, affect to a great extent the accuracy in the determination of end-point. The substitution-inert metal complex, on the other hand, does not react with EDTA in the bulk of solution, and consequently, neither of the above factors can be the cause of error in the determination of the end-point of the titration. A variety of applications of the use of this type of metal indicator in amperometric and a.c. polarographic titrations are expected.

*Department of Chemistry,
Faculty of Science,
Tohoku University,
Sendai (Japan)*

NOBUYUKI TANAKA
HIROSHI OGINO

- 1 T. AMEMIYA AND H. HIRATA, *Base solutions for the square-wave polarographic determination of chromium*, paper presented at the Annual Symposium on Polarography, Nagoya, November, 1963.
- 2 N. TANAKA AND H. OGINO, *Bull. Chem. Soc. Japan*, 34 (1961) 1040.
- 3 N. TANAKA, K. KATO AND R. TAMAMUSHI, *Bull. Chem. Soc. Japan*, 31 (1958) 283.
- 4 G. SCHWARZENBACH, *Die komplexometrische Titration*, Ferdinand Enke, Stuttgart, 1957.

Received January 14th, 1964

J. Electroanal. Chem., 7 (1964) 332-334

Book Reviews

The Agar Precipitation Technique and its Application as a Diagnostic and Analytical Tool, by F. PEETOOM, Charles C. Thomas, Springfield, Illinois, and Oliver & Boyd, Edinburgh, 116 pages, 35s.

This book describes a development of the Ouchterlony agar-precipitation technique for the study of antigen-antibody reactions. The immuno-electrophoresis method consists of agar thin-layer electrophoresis of antigens, followed by diffusion of antibody into the gel. With suitable geometry, field strength, etc., the resulting precipitation patterns are often characteristic, and can yield useful diagnostic information concerning abnormal serum conditions. The book contains useful practical information and many hitherto unpublished results on various blood conditions and as such will be useful to diagnostic biochemists and serologists. The book is, however, a very indifferent translation into English. The style is jerky, and many sentences are either ungrammatical or very obscure. For example, the opening sentence is rather fascinating, and one on p. 27 can be unravelled after some guesswork. There are many typographical errors (a temperature on page 9 is given as $\pm 80^{\circ}\text{C}$, for example). The chapters dealing with experimental results record many inconclusive and incompletely analysed experiments. Phrases such as, 'In some cases the line is slightly thickened but in general distinctly weakened', together with phrases such as 'on a few occasions', 'is rarely as great as', 'often lowered', etc., are indicative of the lack of diagnostic precision that the technique gives in many situations. This state of affairs arises partly from biological variability, but a more rigorous approach to much of the data would have been better.

B. A. PETHICA, Unilever Research Laboratory
Port Sunlight, Cheshire

J. Electroanal. Chem., 7 (1964) 334

Physicochemical Hydrodynamics, by V. G. LEVICH, Prentice-Hall, 1962, 700 pages, \$20.00.

It is very pleasant to be able to welcome the publication of the English translation of Professor LEVICH's valuable book. The first edition was published (in Russian) in 1952

J. Electroanal. Chem., 7 (1964) 334-335

and this is a translation of the revised edition of 1959. In the last few years several attempts at the formidable task of translation have foundered. Consequently, it is greatly to the credit of Professor SCRIVEN and *Scripta Technica* that they have succeeded in producing such an excellently clear and readable text. Very few errors have been noted and most of these are likely to be obvious to the reader even without referring to the Russian text, e.g., page 3, first line 'not' is omitted; page 10, the last line refers to rot v not to the velocity; page 308, line 8, 'regeneration' should be 'reduction'; page 560, in the sentence below equation (110.18) the phrase 'number of cations transferred' should read 'transport number of the cations'.

Professor LEVICH's book is concerned with the region between physics, chemistry and engineering which is accurately described by this title. Most of the important subjects covered are those in which he has made outstanding contributions leading to his world-wide reputation, and the book provides ample evidence of his skill as a theoretician with the gift of physical insight.

The book begins with a summary of the theory of hydrodynamics on which the rest of the book is based. Electrochemists who have not access to the original papers in *Acta Physicochimica* will be particularly glad to have the full discussion of the rotating disc electrode. They will also, no doubt, find much to interest them in the chapter on irreversible electrolytic processes, electrophoresis, the precipitation of disperse systems in flowing media and the theory of polarography (especially of the polarographic maximum). In the first of these the more experimentally inclined reader may find it helpful to start with the comparison with experiment beginning on page 301, rather with the theoretical treatment which logically precedes it. Much of the material in these chapters is closely related to the remaining chapters on heat transfer, motion induced by capillarity and waves on liquid surfaces so that the whole book is of great interest to the theoretical electrochemist.

The book is well produced with clear type and only the occasional misprint. Most of the equations (and there is a great number) have been photocopied from the original so that no errors have been introduced here. Like the original, the translation has no index, but there is a detailed contents list. The price is very much more reasonable than some other translations of less importance.

ROGER PARSONS, University of Bristol

J. Electroanal. Chem., 7 (1964) 334-335

Errata

RICHARD P. BUCK, *J. Electroanal. Chem.*, 5 (1963) 295-314

The treatment given in the paper HALF-WAVE POTENTIALS FOR REVERSIBLE PROCESSES WITH PRIOR KINETIC COMPLEXITY (April issue, 1963) was erroneously stated (page 295) to be applicable to the reduction of unsaturated dibasic acids. These reductions, while showing kinetic complexity, are clearly irreversible* and require a modification of the stated theory.

Typographical errors include:

Page 296, line 10: read primarily for specifically.

Equations (2a), (2b), (2c): read ∂x^2 for $\partial \cdot x^2$.

Equations (7e), (7f): read ∂x for ∂X .

Equation (8b): read C_0 for C_Y .

Page 304, line 6: KOUTECKÝ^{23,28}.

Equation (63a), (63c): read (x,t) .

Equation (67): i omitted on the left of the = sign.

Equation (72): first brace reads

$$\left[\frac{i_{\infty} + \left[1 + \frac{K}{C_x^p} \right] \theta'(i_a) a}{i + \left[1 + \frac{K}{C_x^p} \right] \theta'} \right]$$

Page 308, paragraph 2, line 2: A plot of $E_{\frac{1}{2}}$ vs. $\log C_x$ for case I is shown in Fig. 1. The reversible curve -----

Page 312, (91) missing.

Page 313, line 1: read D_{ϕ}' for D_{ψ} ;

line 6: LINGANE⁴⁸;

(95) omitted; first ln term read $f_M K D_{M(Hg)}^{\frac{1}{2}} / f_{M(Hg)} D_p^{\frac{1}{2}}$

* R. P. BUCK, *Anal. Chem.*, 35, #12 (1963) 1853.

CONTENTS

Original papers

- Chemical kinetics in electrochemical processes. Electron transfer between or within multi-component sub-systems of the type: $A_1 \rightleftharpoons A_2$, $A_2 \rightleftharpoons A_3$, $A_3 \rightleftharpoons A_1$
J. W. ASHLEY, JR. AND C. N. REILLEY (Chapel Hill, N.C., U.S.A.) 253
- The catalytic polarographic current of a metal complex
II. The nickel(II)-*o*-phenylenediamine system
H. B. MARK, JR. (Ann Arbor, Mich., U.S.A.) 276
- Effect of dilute chloride ion on platinum electrodes
J. S. MAYELL AND S. H. LANGER (Stamford, Conn., U.S.A.) 288
- The anodic dissolution and passivation of smooth platinum
I. Anomalous results from the radiotracer technique
T. DICKINSON, R. C. IRWIN AND W. F. K. WYNNE-JONES (Newcastle upon Tyne, England) 297
- Voltammetry of nickel in molten lithium fluoride-sodium fluoride-potassium fluoride
D. L. MANNING (Oak Ridge, Tenn., U.S.A.) 302
- Trace analysis by anodic stripping voltammetry
II. The method of medium exchange
M. ARIEL, U. EISNER AND S. GOTTESFELD (Haifa, Israel). 307
- Voltammetric determination of carbon monoxide at gold electrodes
J. L. ROBERTS, JR. AND D. T. SAWYER (Riverside, Calif., U.S.A.) 315
- Linear potentiometric titrations
P. LANZA AND I. MAZZEI (Bologna, Italy) 320
- The polarographic diffusion coefficient of cadmium ion in 0.1 *M* potassium chloride
D. J. MACERO AND C. L. RULFS (Ann Arbor, Mich., U.S.A.) 328
- Preliminary note*
- A substitution-inert metal complex as an indicator in a.c. polarographic titrations; a new type of metal indicator
N. TANAKA AND H. OGINO (Sendai, Japan). 332
- Book reviews* 334
- Errata*. 336

All rights reserved

ELSEVIER PUBLISHING COMPANY, AMSTERDAM

Printed in The Netherlands by

NEDERLANDSE BOEKDRUK INRICHTING N.V., 'S-HERTOGENBOSCH

Elsevier books for the laboratory. . . .

HANDBOOK OF LABORATORY DISTILLATION

by ERICH KRELL

edited by E.C. LUMB

Contents.

1. Introduction. 2. A review of the history of laboratory distillation. 3. Standardization and data on concentrations. 4. Physical fundamentals of the separation process. 5. Separating processes. 6. Selective separating processes. 7. Constructional materials and apparatus. 8. Automatic devices; measuring and control equipment. 9. Arrangement of a distillation laboratory; starting up distillation. Glossary. Appendices I, II and III. Author index. Subject index. List of symbols. Nomograms.

x + 561 pages, 77 tables, 440 illustrations, 1963, 100s.

PHYSICO-CHEMICAL CONSTANTS OF PURE ORGANIC COMPOUNDS

by J. TIMMERMANS

Volume 2

The second volume is the fruit of the extraordinary research effort in fundamental organic chemistry in the years 1951–1961, in which definitive analytical studies provided new improved data comparable in value with the entire body of physico-chemical determinations carried out up to 1950. It maintains the mode of presentation and subdivision of volume 1.

Contents.

1. Hydrocarbons. 2. Halogenated derivatives. 3. Oxygenated derivatives of the aliphatic series. 4. Oxygenated derivatives of the aromatic series. 5. Oxygenated derivatives of polymethylenes. 6. Heterocyclic oxygen compounds. 7. Sugars. 8. Mixed oxyhalogenated derivatives. 9. Nitrogen derivatives of the aliphatic series. 10. Nitrogen derivatives of the cyclic series. 11. Oxygen and nitrogen derivatives. 12. Mixed halogen-nitrogen derivatives. 13. Sulphur derivatives. 14. Derivatives with other elements. References. Index.

Approx. 450 pages, 430 literature references, 1964, 120s.

Volume 1 is still available

The first volume brings together a large body of data on pure organic compounds published up to 1950.

viii + 694 pages, 1315 literature references, 1950, 102s.



ELSEVIER PUBLISHING COMPANY

AMSTERDAM

LONDON

NEW YORK